# INVESTIGATION OF ACOUSTIC EMISSION WAVE GUIDE SYSTEMS FOR DETECTING SLOPE INSTABILITY

**Anna Kousteni**

A thesis submitted in partial fulfillment of the
requirements of the Nottingham Trent University
for the degree of Doctor of Philosophy.

March 2002

**Investigation of Acoustic Emission Wave Guide Systems for Detecting Slope Instability**

**Anna Kousteni**

## Abstract

This thesis presents results of a study of the acoustic emission (AE) monitoring technique for detecting slope deformations. Laboratory studies carried out at Nottingham Trent University to develop and assess an acoustic emission monitoring system, including data processing and interpretation criteria, are described. Due to the low energy of soil generated AE and their high attenuation as they propagate through soil, a key element of the system is the wave guide used to transmit signals from depth within the deforming soil body to the sensor at ground level. This investigation is centred on assessing the performance of 'active' wave guides. A steel tube is located in a pre-drilled borehole with granular surround. Deformation of the host soil results in deformation of the wave guide/backfill system and generation of AE. Interpretation requires information on the location of generated AE along the length of the wave guide and on the relationship between AE and ground deformation rates.

Each component of the wave guide system has been investigated to assess its influence on the generated and transmitted signal (i.e. wave guide diameter, connection type, sensor attachment details and backfill soil grading). The main findings from the study are: a) soil generated AE signals can be generated and transmitted by an active wave guide; b) high attenuation and signal dispersion can result from poor connections between wave guide lengths and this reduces the sensitivity of the system; c) AE levels emitted due to bending of the steel wave guide are negligible and need not be considered; d) the source of AE along the wave guide can be located using only one transducer by identifying different velocity signal wave modes (Lamb waves) that travel through thin walled pipes; e) sand backfill soil is responsive to faster deformation rates than gravel and AE amplitude increases with displacement; f) gravel backfill generates detectable AE even under extremely slow rate of deformation ($10^{-4}$mm/min) and AE increases with displacement but with constant amplitude. This research demonstrates the ability of active wave guides to generate AE in response to very slow ground deformation rates, and hence its potential to provide an early warning of slope instability.

# Acknowledgement

This thesis wouldn't have been completed without the considerable attention and assistance received from numerous valued individuals.

I would like to thank my supervisors Dr. N.Dixon, Dr. R.Hill and Dr V.Krylov, for their instructions, support and assistance. My utmost appreciation goes to Neil Dixon for his continuous support and encouragement that I received during the last most difficult months of my research.

Respect to all my friends and colleagues who enlightened and encouraged me during my time as a researcher by sharing similar difficulties and challenges that every research project brings.

I would like to express my gratitude to my family for their continuous support and encouragement throughout my academic career, an act that played a major part in what I have accomplished in life so far.

At this stage I would like to share with the reader an old Greek saying that kept my strength and spirit high in those difficult moments during my research.

"Knowledge is a treasure and action is its own key".

"Η γνωση ειναι θησαυρος και η πραξη το κλειδι του "

## Glossary

**Active wave guide system:** Wave guide surrounded by granular soil

**Attenuation :** Loss of acoustic energy measured in dB per propagation length (dB/m)

**Backfill :** Soil surrounding the wave guide

**Bulk waves:** Waves propagating through solids

**Decibel (dB):** Unit of measuring the intensity of sound

**Event:** Captured specified number of AE data when signal exceeded the threshold level

**Fast Fourier Transform (FFT) :** Fourier equation transforming signal from time domain to frequency domain.

**Lamb waves**: Waves propagating through plates and cylinders

**Piezoelectric transducer:** Sensor housing crystal that transforms the mechanical pressure or tension to electric charge(Volts).

**Rayleigh waves:** Surface waves propagating along the surface of solids.

**Threshold:** Voltage level using for capturing AE event when was exceeded

**Wave guide:** Steel tube section used to guide the AE signal to the sensor

**Wave guide system:** Wave guide surrounded by backfill.

# CONTENTS

# Chapter 1-Introduction

## 1.1 Introduction

"If a landslide comes as a surprise to the eyewitness, it would be more accurate to say that the observers failed to detect the phenomena which preceded the slide" (Terzaghi, 1950). The implication is that the smallest possible movements should be measured at the earliest possible time. Small movements of a soil mass prior to failure are not easy to detect and interpret, so the value of information that can be obtained using surface survey markers or inclinometer tubes can be limited (Shuster et al. 1978).
Therefore, there is a need of an instrumentation system which:

i) is sensitive to small deformations;
ii) can detect changes in the rate of movement;
iii) provide information about the location of sliding surface; and
iv) monitor the slope continuously using portable field equipment.

Such a system could provide an early warning of slope instability.

Acoustic emission (AE) monitoring techniques have the potential to meet the above requirements. Acoustic emission is a non-invasive technique, which since the 1970's has been increasingly employed to monitor the stability of soil bodies. The main body of research into AE applications for soil assessment has been carried out in the USA (e.g. Koerner *et al.* 1981), Japan (e.g.Chichibu *et al.* 1989, Nakajima *et al.* 1991) and more recently at Nottingham Trent University (Dixon *et al.* 1997). When any material is stressed, it generates micro-seismic activity at locations of local instability. The associated stress waves propagate from the source of instability through the surrounding material and can be detected by suitable high sensitivity transducers. This is the main principle of the AE monitoring technique, which enables the detection of the occurrence of distress in soil before the development of significant movements thus providing an early warning of instability.

Although field and laboratory investigations conducted in the past proved the qualitative status of the AE technique, there is a need for additional research to improve its quantitative status. The present research project aims to quantify the AE response from a deforming soil system moving at very slow rates where other monitoring systems may not be sensitive enough, and hence to develop a more reliable early warning system for detecting slope instability.

Detecting rock and slope instability by using AE testing has been proved to be a successful application since the late 1930's (Hardy 1989). Field (Hardy 1994) and laboratory studies (Koerner *et al.* 1981) indicate that the AE monitoring technique can provide an Engineer with an early indication that small deformations are taking place during progressive failure. However, the quantitative assessment of AE needs to be developed and improved so it can be used commercially as a reliable monitoring technique.

This research was focused on carrying out laboratory studies on various instrumentation design wave guide systems in order to provide a detail understanding of soil and wave guide AE response. The factors, which control instrumentation design, were investigated and suggestions for improvement made. The AE response of two types of backfill soil, sand and gravel, has been studied. In this study it was found that it is possible to obtain the slip surface location (i.e. source location) by studying the difference in the arrival time of different wave modes. Sensitivity of the AE monitoring system was tested under extremely slow soil strain rates and it was found that is able to detect strains as slow as 0.0001mm per minute. The AE response of sand and gravel backfill soils were investigated and compared.

## 1.2 Slope movement types and processes/rates

Landslides are commonly regarded as one of the most predictable of geological hazards, however, many people are killed each year by landslides. In China and Peru, tens of thousands of deaths have resulted from single landslides. Annual property damage from landslides world-wide is estimated in the tens of billions of dollars, with more than $1.5 billion in annual losses in the USA alone. Globally, landslides cause 1000s of deaths and

injuries, each year (CEOS org. website). A monitoring system that can detect small pre-failure slope movement can provide a timely warning to people in down slope areas.

It is clear that the identification and classification of landslide types requires the consideration of many factors. Among the factors used for identification are: type of movement, kind of material, rate of movement, geometry of the area of failure and the resulting deposits, causes, degree of disruption of the displaced mass, geographic location and state of activity.

Type of movement are divided into five main groups:

1. Falls
2. Topples
3. Slides
4. Spreads
5. Flows

Complex slope movement include combination of two or more of the other five types.

Materials are divided into two classes:

1. Rock
2. Engineering soil
   a) Debris
   b) Earth

Rate of movement scale

In Figure 1.1 a rate of movement scale is illustrated. These have been regarded as primary definitions by Shuster *et al.*(1978).

## 1.3 Available slope monitoring techniques

A large variety on slope monitoring instrumentation exists in the market and is available to geotechnical engineers. Surface methods for measuring the development of cracks, subsidence and uplift include repeated surveying using conventional techniques, installation of various instruments to measure movements directly, and tiltmeters to record changes in slope inclination near cracks and areas of greatest vertical movements. Subsurface methods include installation of inclinometers to record the

profile of the casing. This should ideally pass through the slip surface. Conventional slope monitoring instrumentations are listed below including a brief discussion on their applications, advantages and limitations.

**a) Soil strain meter**

Applications of the soil strain meter include: monitoring tension cracks in earth structures and monitoring horizontal strain in embankment dams.

The soil strain meter employs a potentiometer and a rod mounted between two anchors to monitor horizontal movements of the surrounding soil. These components are linked together so that movement of one anchor relative to the other causes a change in the output of the potentiometer. The initial reading of the strain meter is used as a datum. Subsequent readings are compared to the datum to calculate the magnitude, rate, and acceleration of movement.

Strain meters are usually installed in series along the axis of anticipated deformation. Strain meters may also be arranged in arrays or in groups with different alignments. A gauge length of 3 to 6 meters is typical, but will vary according to the expected magnitude of movement and the type of structure being monitored.

Advantages

The advantages on using strain meters are:

Easy installation: The strain meter is designed for easy assembly, easy extension of gauge lengths, and easy adjustment.

Manual or Automatic Readout: Strain meters can be read manually with a portable indicator or can be connected to a data logger for unattended readings.

**b) Rod Extensometers**

The rod extensometer monitors changes in the distance between one or more downhole anchors and a reference head at the borehole collar. Typical applications include:

- Monitoring settlement in foundations.
- Monitoring subsidence above tunnels and mines.

- Monitoring heave in excavations.
- Monitoring the stability of tunnels and other underground openings.
- Monitoring deformation in abutments and walls.

Components of a rod extensometer include anchors, rods with protective tubing, and a reference head. The anchors, with rods attached, are installed downhole. The rods span the distance between the anchors and the reference head, which is installed at the borehole collar. Measurements are obtained at the reference head with a sensor or a depth micrometer, either of which measures the distance between the top (near) end of the rod and a reference surface.

A change of slope displacement, is found by comparing the current measurement to the initial measurement, indicates that movement has occurred. Movement may be referenced to a downhole anchor that is installed in stable ground or to the reference head, which can be surveyed. The resulting displacement data can be used to determine the zone, rate, and acceleration of movements, or to calculate strain.

Advantages

The advantage of this system is that it can be automated, (real-time or continuous monitoring) and can be read remotely. It can be used in any orientation. The rod extensometer can monitor up to six points along the borehole.

Limitations

However, the number of monitored points is limited by the size of the borehole, the type of anchor used, the diameter of the rods, and the amount of tubing required for grouting and activating anchors. The measurement range is limited between 50 to 100 mm.

**c) Vertical Inclinometers**

Inclinometer applications are:

- Monitoring slopes and landslides to detect zones of movement and establish whether movement is constant, accelerating, or responding to remedial measures.

- Monitoring diaphragm walls and sheet piles to check that deflections are within design limits, that struts and anchors are performing as expected, and that adjacent buildings are not affected by ground movements.
- Monitoring dams, dam abutments, and upstream slopes for movement during and after impoundment.
- Monitoring the effects of tunnelling operations to ensure that adjacent structures are not damaged by ground movements.

Inclinometer casing is installed in a borehole that passes through suspected zones of movement. Inclinometer casing can also be embedded in fill, buried in a trench, cast into concrete, or attached to a structure. Important features include the diameter of the casing, the coupling mechanism, groove precision and straightness, and the strength of the casing.

Inclinometer casing is a special purpose, grooved pipe that:

a) Provides access for the inclinometer probe, allowing it to obtain subsurface measurements;
b) Controls the orientation of the inclinometer probe;
c) Deforms with the adjacent ground or structure.

The inclinometer probe, control cable, pulley assembly, and readout are used to survey the casing. During a survey, the probe is drawn upwards from the bottom of the casing to the top, halted in its travel at half-meter intervals for tilt measurements. The first survey establishes the initial profile of the casing. Subsequent surveys reveal changes in the profile if ground movement occurs. The inclination of the probe body is measured by two force-balanced servo-accelerometers. One accelerometer measures tilt in the plane of the inclinometer wheels, which track the longitudinal grooves of the casing. The other accelerometer measures tilt in the plane perpendicular to the wheels. Inclination measurements are converted to lateral deviations. By comparing data from current and initial surveys, changes in the lateral deviations will indicate ground movements.

Advantages

Inclinometers can provide high resolution displacement profile of cumulative changes at each measurement interval. Displacement profiles are useful for determining the magnitude, depth, direction, and rate of ground movement.

Possible problems and disadvantages

In borehole installations, the annular space around the casing is usually backfilled with grout. The grouting process can generate pressures high enough to cause the casing to collapse.

If the casing joints are not sealed properly grout can enter the casing and can cause blockages, unreliable tracking, and damage to the wheels of the inclinometer probe.
When the inclinometer probe is drawn upwards through casing deformed by ground movement, its wheels are forced against the sides of the guide grooves. Unless the grooves are designed to facilitate tracking through curvatures of the casing, the wheels may jump out of the groove. If this occurs, repeatable positioning of the probe is nearly impossible and the reliability of the data suffers.

Requires an engineer on the site to obtain each survey reading. Strings of in place inclinometers can be installed in a casing and read continuously. Reading can be transmitted for remote monitoring applications. The main disadvantage with this system is its high cost.

## 1.4 Acoustic Emission monitoring system

Acoustic emission monitoring is a subsurface non-invasive technique. Its applications are:

- monitoring slopes and landslides to detect zones of movement ;
- monitoring ceiling stability in tunnels and mines to give an early warning indication of instability; and
- monitoring seepage and ground water movement in embankments and dams.

The principle components of an AE monitoring system are: AE sensor, wave guide and the analogue to digital conversion board where the recorded noise from the sensor can be processed and accessed by the engineer. There are different types of sensors that can be used: geophones, accelerometers and piezoelectric transducers. Wave guides are used to guide the signal from the source to the sensor with minimum attenuation.
Wave guide is installed in a borehole that passes through suspected zones of movement or in some cases is driven into the soil. The sensors are attached to the wave guide and detect AE from small deformations of the material surrounding the wave guide.

Advantage

The main advantage of this system is its high sensitivity that can provide an early warning of catastrophic failure. It does not necessarily require repeatable surveying to establish trends of behaviour. It can be used to provide real time continuous monitoring. Is not expensive to use and can record information from multiple boreholes at the same time. The above AE monitoring system is suitable for monitoring slide and flow types of movement of both rock and soil material. The main advantage of the AE monitoring system is its sensitivity. It can be used to detect even creep types of movement.

Limitations

At present AE can provide qualitative but not quantitative results. Its high sensitivity can became a disadvantage when background noise interferes with the signal from the deforming ground. The purpose of this study is to overcome the above limitations by

carrying out an investigation of the measuring system and AE response of deforming soil.

## 1.5 Aims and Objectives

The aims of the current research are:

(i) To develop and improve the design of AE monitoring systems.

(ii) To produce a reliable early warning system of slope instability.

The objectives of this work are:

1. examine various designs of AE wave guide systems (i.e. construction and installation procedures) ;
2. investigate AE signals generated by the deformation of granular soil backfill at a range of strain rates;
3. investigate the use of wave guides to locate the source of an AE signal below ground level; and
4. develop data processing and interpretation techniques, which can be used for continuous monitoring of a potential unstable slope.

Acoustic emission monitoring of slopes involves the measurement of just one parameter: the output AE signal voltage (which is detected by sensors). The input signal (generated by the source) is unknown. The characteristics and nature of the source, including the amount of movement, the rate of displacement and the location of the source are not known. In the past, researchers have related the AE response to the amount of displacement of a slope, which was measured using nearby inclinometers (e.g. Chichibu *et al.* 1989), or they have modified the inclinometer casing so it can be used as a wave guide to monitor both AE and displacements (Kavanagh 1997). However, the AE signal could not be quantified and compared between studies because the conditions of each field test were different. To be more specific, the factors, which have varied in previous studies, have included.

- the geological stratum at each site.

- different monitoring components (e.g. AE sensor, amplifier, type of wave guide) and method of wave guide installation including types of backfill material. Backfill is used when a drilled borehole accommodates the wave guide in order to improve the contact conditions between the host soil and the wave guide.

It is also worth emphasising that AE monitoring of slope instability started 50 years ago, and to date the case studies conducted are not adequate to allow clear quantitative conclusions to be made.

In contrast to field studies, laboratory studies could provide useful results by enabling repeated testing under controlled and hence reproducible conditions.

## 1.6 Contribution to knowledge

An investigation of the parameters that influence the AE signal has been carried out in a laboratory study. The results of these investigations provide a better understanding of the AE signal behaviour and contribute to knowledge in the following areas.

- Optimisation of wave guide design following comparison of different types of wave guide systems (i.e. connection type, tube diameter, sensor attachment arrangement).
- Develop a method for estimating the source of generated AE events by using a single sensor.
- Demonstration of the sensitivity of AE monitoring via detection of AE from two granular backfill soils deformed under controlled slow rates of strain. It should be noted that no previous study has carried out at such small strain rates as those used in this research.

## 1.7 Thesis layout

Chapter 2

The literature review provides a summary of field case studies using the AE monitoring system published in the literature. Each study employed different instrumentation components and monitoring strategies. In a number of cases complimentary laboratory

studies were also carried out and reported. This chapter also includes a summary of research that has been carried out into locating the AE source.

Chapter 3

This chapter describes the instrumentation components used in this study. (i.e. hardware components and software). The function of each component is discussed along with capabilities and applications. Additional programs used for the interpretation and processing of the captured AE data are presented and discussed.

Chapter 4

The propagating path of the AE signal from its source to the sensor is explained. A brief discussion on the theory of plane and tube wave modes is given. The expected captured wave modes according to the current instrumentation components is explained. Pencil leads break tests are described. They are used to help demonstrate the existence of the different wave modes and to aid development of an AE source location technique.

Chapter 5

Laboratory studies to investigate the effect of different wave guide designs are presented in this chapter. Signal attenuation was quantified along the length of the wave guide and also through connections. Two types of steel tubing connections were investigated: threaded and welded. In additional, the sensor attachment arrangement with the tube was studied.

Chapter 6

The AE response of sand and gravel backfills was studied by using two different experiments. Both experiments attempt to resemble the field condition of borehole accommodating the wave guide surrounded by the backfill soil. During the first experiment the displacement was measured and related to the AE response of the soil. However, the rate of strain was not controlled adequately. Hence the second experiment was designed so the rates of strain could be controlled. The results of these tests are presented and are discussed.

Chapter 7

A summary of the findings and main conclusions are provided in this chapter. Limitations of the experimental work carried out in this research project in representing the failure mechanism of slopes in the field are discussed. Suggestions for future research on the wave guide and backfill and AE processing methods, are given.

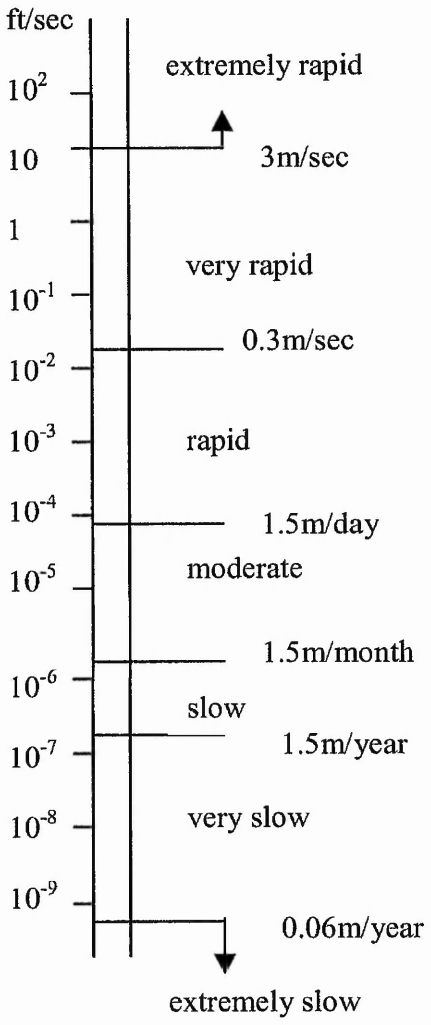


**Converting the velocity into mm/min**

**1. Extremely rapid**
$Vs > 180x10^3$mm/min

**2. Very rapid**
$18x10^3$mm/min $< Vs < 180x10^3$mm/min

**3. Rapid**
1.04 mm/min $< Vs < 18x10^3$ mm/min

**4. Moderate**
0.03 mm/min $< Vs <$ 1.04 mm/min

**5. Slow**
0.0028 mm/min $< Vs <$ 0.03 mm/min

**6. Very slow**
0.000115 mm/min $< Vs <$ 0.0028 mm/min

**7. Extremely slow**
$Vs <$ 0.000115 mm/min

Figure 1.1 Slope movement scale after Shuster *et al.*(1978).

# Chapter 2-Literature Review

## 2.1 Introduction

Since the early 1970s, there has been an accelerating interest in the use of AE techniques. To date, international research related to the geotechnical field application of AE techniques has involved a wide variety of field topics. Historically, AE work began in the mining industry to detect instability of the mine roof, face, or pillar rock, Obert (1941), and Obert and Duvall (1946) in the United States, Hodgson (1943) in Canada and more recently Wood *et al.* (1990). Landslide studies have been described by Yuda *et al.* (1984) and Rouse *et al.* (1991) and highway and railway slope stability by McCauley (1977). Seepage through dams has been investigated by Koerner *et al.* (1979), (1981) and Blystra (1994).

This literature review chapter is divided into four sections. Section 2.2 focuses on previous field applications of AE monitoring for the detection of slope instability, emphasising the sensitivity of the instrumentation at small deformations or when stresses build up in a soil mass prior to failure. Section 2.3 describes studies carried out on instrumentation development, especially on the wave guide design (i.e. material types used, composite, connections and backfill materials). Section 2.4 includes a discussion on various methods carried out in the past for estimating the source location. Finally, section 2.5 includes a discussion of the nature and advantage of using Lamb wave modes to assess waves propagating through thin plates and cylindrical tubes.

## 2.2 Slope stability monitoring studies

Engineers and researchers have been interested in the application of AE monitoring since it can provide an early warning and prediction of slope instability. There is a large number of field studies which clarify this ability of the AE monitoring technique. In this section, a small selection of these studies will be described in detail in order to

demonstrate the application of the technique. Before referring to the field case studies, it is useful to define the purpose of the wave guide and the wave guide systems.

Most commonly, metal wave guides are used which can take the form of steel reinforcing rods, various metal instrumentation pipes, (for example aluminium inclinometer tubes) or construction units (for example tiebacks, anchors, piles or soil reinforcement units). It is possible to drive the wave guide into the host soil providing that the height of the slope is small. For larger slopes it is necessary to install the wave guide in pre-drilled boreholes. This method requires a backfill material which is used to improve the contact between the host soil and wave guide. Depending on the backfill material two possible systems are formed: *Passive* and *Active* wave guides.

In passive systems the annulus around the wave guide has to be backfilled with low AE activity material (i.e. clay), so the installation does not introduce additional sources of AE into the wave guide. Any recorded AE signal is assumed to emanate from the deforming host soil. Driven systems can also be defined as passive since the wave guide is in direct contact with the in-situ material.

Active wave guide systems are installed when the monitoring site consists of cohesive material. As the emission levels generated by cohesive soils are low it is difficult to obtain quality AE data on these sites (Koerner *et al.*1981). Therefore, the annulus is backfilled with granular soils such as sand or gravel which produce high levels of AE when deformed. Although the recorded AE data will not relate directly to the stress state of the host soil, it may be possible to calibrate the system, such that the recorded AE signal can be related to the magnitude of the general ground deformations.

McCauley (1977) described two interesting case studies of slope monitoring using AE.

**i) *Field study in rock without wave-guides.***

A new highway alignment was being constructed in the Kern River Canyon about 48 km east of Bakersfield, California. The new construction was 91 m below the existing

highway. Natural slopes were as steep as 1.2:1 in the differentially weathered granitic rock and a high cut slope was being constructed with a slope 0.6:1. Before the cut was completed, in July of 1973, cracks were noted in the ground and the Transportation Laboratory in Sacramento was requested to evaluate the stability of the slope. Two methods of monitoring were begun. Nails were driven in the pavement on both sides of the cracks and distances between sets of nails were measured regularly, and monitoring with a 6 transducer acoustic emission system was begun. There was a steady increase in noise rate recorded from the transducers during 10th and 15th July. This information was coupled with the measurements taken across cracks in the pavement and it was decided to construct a buttress against the cut slope immediately. The AE levels after the completion of the buttress were lower and remained low, which indicate how effective the corrective action had been.

### *ii) No waveguides transducer lowered into borehole*

In June 1971 monitoring with AE was begun on Thornton Bluffs cliffs which are situated on the western side of San Francisco Peninsula. These cliffs extend from beach level to elevations as high as 150 m and at slope angles varying from 30 to 45 degrees. The material in the cliffs and the slide mass consists of poorly consolidated marine sand, silt and clay of the Merced Formation. The base of the cliffs is subjected to continuing erosion and as the slopes become over-steep, sliding occurs. One such slide that developed affected Lynvale Court and part of the coastal highway. Cracking was evident in the pavement of the court and in three houses adjacent to the court. The displacements across the cracks were measured periodically by monitoring the position of nails driven into the pavement in opposite sites of the crack. The positions of the six AE transducers, which were used for monitoring, are numbered (1-6) in Figure 2.1. Also, three slope indicator holes were drilled and cased, which are designated SI-1, SI-2, SI3 in Figure 2.1.The slope indicator holes were used for AE monitoring by lowering the transducer below water table. In Figure 2.2 the counts per minute recorded in hole SI-3 are plotted. The displacements of the slope indicator hole at a depth of 29 m, and the measurements at the nail point 6, are also plotted. The graph shows that the increase in AE that occurred in mid-December suggested increased activity in the slide a month

before evidence was available from the other types of monitoring. It is interesting to note that although the AE counts were high, the total displacement measured across the cracks and in the slope indicator hole was only about 2.5 cm.

Chichibu *et al.* (1989) monitored an embankment and an unstable slope by using both AE monitoring and traditional field techniques. Sudden slope failure occurred at a road construction area consisting of a material described as "Clayed rock of Kobe Group", which is known in Japan as a slaking material. This failure was caused by the road cutting but it was not anticipated since the displacement stakes installed to monitor deformations indicated little movement (less than 5 mm). Consequently, a 20 m high embankment was constructed to prevent further collapse. At the same time a ground surface displacement meter, borehole inclinometer and AE instrumentation were installed to monitor the stability of the slope. The locations of these installations are shown in Figure 2.3. Note that both the counterweight fill embankment and the slope were monitored.

The AE instrumentation components were a transducer (accelerometer), a preamplifier of 30dB gain, a main amplifier of 40 dB gain and a steel reinforcing bar was used as wave guide. AE ringdown counts were recorded and the average of AE count rate per 10 min was used to examine daily changes of AE activity.

$$\text{Average AE count rate (per 10 min)} = \frac{\text{Total AE counts per day}}{\text{No. of monitoring period}}$$

The vertical and horizontal movements of the embankment were measured by installing a displacement stake 2m away from the driven AE wave guide, see Figure 2.4. The results of the AE monitoring and the displacements of the stake are shown in Figure 2.5. Initially rates of movements and AE rates were high, so it was decided to construct an additional embankment, which was completed on 14-15 November. The AE count rates and the movements were reduced significantly and almost vanished on 19 November. These results show a good correlation between the AE rates and the horizontal movement of the stake.

The natural slope was monitored using a borehole inclinometer, installed 1 m away from the AE wave guide. In this case the wave guide was inserted into a 17 m deep borehole which then was backfilled with mortar to improve the transmission of signals from the surrounding soil, Figure 2.6. At the ground surface a displacement meter was installed which was divided into two parts (A and B) and both displacements were measured separately. The results are illustrated in Figure 2.7 where A, and B refer to ground surface movements. The underground movements were recorded by the inclinometer at a depth of 14.5 m. Significant AE activity was observed during mid-January and continuing over February, while the values of displacements measured were very small during the same period. It was suggested that this could be due to the presence of underground microcracks, which can not be detected by the displacement meter but generate significant AE signals. On 1 March, due to diminishing AE levels near the end of February, it was decided to change the AE monitoring point and a water proofed transducer was lowered down the inclinometer borehole to a depth of 20m. The AE activity was higher than that obtained through the wave guide, and remained so for several days. After 10 days, AE levels decreased to very low levels while displacements underground and at the ground surface (A and B) started increasing. The authors commented that high AE levels occur when high stress is accumulated before the slope failure, while AE levels decrease when large displacements take place releasing the stored energy. However, this could not be the case. The slope was moving when the AE levels were high but the direct measurements of movement only detected movement at a later date.

Results from recent field studies are reported by Dixon *et.al.* (1996) and Kavanagh, (1997). One of the case study areas was located on the north eastern coast of England at Cowden. At this location 20 meters high cliffs are formed of stiff cohesive glacial till. The failure mechanism of the cliffs is by rotational sliding which is triggered by marine erosion of the toe. Twelve steel tubing wave-guides and two inclinometer casings were installed into the coastal cliff section. Figure 2.8 shows the instrumentation array arrangement at November 1993.

Part of the results that were obtained from a monitoring period of almost one year are shown in Figure 2.9 In this figure a comparison of the AE recorded data from 4 different wave-guides is made with displacement rates recorded by inclinometer I1

It can be seen that there is a reduction in AE mean signal value between days 149 and 163 recorded by all wave-guides, which is accompanied by a reduction in the rate of increase of displacement recorded by the inclinometer. The monitoring method wasn't continuous, but based upon periodic site visits and acquisition of AE data. Therefore, it is likely that much deformation-related AE was not captured because no operator was present when it was generated. However, under these conditions the correlation of displacement rates with AE was encouraging, and proved the good qualitative status of the AE monitoring technique. Unfortunately, at this stage, the signal could not be quantified to provide an independent measure of slope instability. The operator was not aware about the amount and the speed of displacement that the slip surface was moving to be able to quantify the AE signal.

One of the wave-guide design parameters was backfill type. Wave-guides 1, 5 (WG1, WG5) and 12 (WG12) were backfilled with sand, wave-guides 2, 6 (WG2, WG6) with gravel and the rest of them (WG3, WG4, and form WG7 to WG11), with grout. The grout backfill produced the least AE, gravel appeared to be the next active and the sand backfill clearly produced the highest levels of AE (Figure 2.9). The poor response of gravel backfilled wave-guides was a result of the gravel particles requiring greater displacements of the host soil to cause them slip. In addition, slippage would occur over a shorter period of time, but AE would be of much greater amplitude than for sand particles.

## 2.3 Investigations on Wave Guides

### 2.3.1 Wave guide advantages

Monitoring soils by using acoustic emission (AE) techniques, has a major disadvantage namely *attenuation*. The attenuation of AE energy in soils is highly frequency

dependent. This attenuation was evaluated for sands and clays by Koerner *et al.* (1981). Koerner used a box filled with soil, two AE sensors placed at different locations and an AE source. Various types of sand and clays were tested in the box. As the signal from the source sequential passes by the two sensors, both sensed signals were monitored on a dual-channel oscilloscope. The attenuation coefficient ($\alpha$) was calculated by using the output signal amplitudes.

$$\alpha = \frac{20}{x} \log \frac{A_1}{A_2} \qquad (2.1)$$

where

$\alpha$ = attenuation coefficient in dB/distance

x = distance between the two sensors

$A_1$ = amplitude of first sensor output wave, and

$A_2$ = amplitude of second sensor output wave

It was found that the attenuation coefficient in dry sands varies from 0.09 dB/cm at 500 Hz to 10 dB/cm at 16 kHz, and for a clayey silt varies from 1.9 dB/cm in the dry state to 1.0 dB/cm near saturation, both values at a frequency of about 1.0 kHz. This can be seen in Figure 2.10 along with typical ranges for attenuation coefficients of rock and coal and of iron and steel. It is obvious, from Figure 2.10, that steel has three to four orders of magnitude lower attenuation than soils. This relatively low attenuation characteristic of metal is the reason for using a metal wave guide when monitoring soil, thus reducing signal strength losses.

The effect of the wave guide on acoustic emission monitoring was assessed by Lord *et al.* (1982). Tests were carried out with and without a wave guide. The signal loss from the AE source to the pickup transducer consisted of propagation loss in the soil from the source to the wave guide, coupling loss into the wave guide and the soil covering loss in the wave guide up to the transducer. The sum of these losses are equal to the detection limit of a typical AE wave guide.

$$DL = CL + (SCL)z + \alpha_s r \qquad (2.2)$$

where :

DL : detection limit

CL : coupling loss

SCL : soil covering loss per distance

$\alpha_s$ : propagating loss in the soil per distance

r : distance of AE source from the wave guide

z :vertical distance between AE source to the sensor (depth)

By solving the equation (2.2) with respect to r, the radius of a cone is obtained

$$r = \frac{DL - CL - (SCL)z}{\alpha_s} \qquad (2.3)$$

Considering values DL = 60dB, CL = 15dB, SCL = 1dB/m, and $\alpha_s$ = 60dB/m the equation (2.3) becomes r = 0.75-0.017z. At the ground surface where z = 0 , r = 0.75m , and when r = 0, z = 45m. This describes a cone of 0.75m radius base and a depth of 45m. The volume of the cone, which represents the approximate volume of soil monitored, is equal $26m^3$.

Without a wave guide the volume of the monitored soil is equal to 0.88 $m^3$ which is the volume of a hemisphere with the same radius as the previous cone base (0.75 m). A schematic presentation is given in Figure 2.11. As a conclusion, the use of a wave guide results in an increase in both of sensed soil volume and depth, which makes the use of a wave guide beneficial.

Hardy (1989) and (1992) discusses the use of wave guides to monitor rock. He found that wave guides not only provide a path of low attenuation but also acts as a transducer. The part of the wave guide which acts both as a collector of AE emissions and as a source is defined by the author as an Acoustic Antennae.

### 2.3.2 Development of wave guide design

The earliest study on wave guides was carried out by Koerner and Lord (1975). In this study two different sized (0.32 cm and 1.27 cm in diameter) metal rods were used to investigated the influence of wave guide on acoustic emission response. As it can be seen in Figure 2.12 a standard shaker was fixed at the one end of the wave guide and a pickup system at the other end.

Results showing the influence of various lengths and diameter of steel rod wave guides are illustrated in Figure 2.13;

Koerner drew some conclusions after this study which are listed below.

- Longer wave guides lower the frequency of the first resonant frequency of the system.
- Different diameter rods do not appear to influence the first resonant frequency of the system.
- Different surface conditions (threaded versus smooth) do not appear to affect the location of the first resonance.
- The method of connecting one rod to another does not appear to influence the resonance, so long as such connections are solid and firm in their metal- to-metal contact.

The next stage of Koerner's study was to examine the response of the above wave guide/ accelerometer system when it was surrounded by soil. The wave guides this time were 1.21 m long and 1.27 cm diameter rods surrounded by silty sand soil, and the response was studied at various water content.

The results are summarised in Table 2.1 where it can be seen that the location of the first resonant is slightly altered by the influence of the surrounding medium. The higher density has the effect of maximising the particle contacts on the rod which in turn lowers the amplitude of the first resonance. It was concluded that the influence of the soil is negligible on the detector's frequency response but does reduce its sensitivity to a certain extent.

A similar, but expanded investigation was carried out by Lord *et al.* (1982). The experimental set-up is shown in Figure 2.14. A pulse of about 30 msec duration and of various frequencies was generated and amplified before it reached the accelerometer. The pulse travelled through the 2m long steel bar which was covered with soil and at the other end reached the second accelerometer (same type at both ends). The output pulse was amplified before being displayed on a dual channel oscilloscope. During the course of this study various types of soil were investigated, and the attenuation of the signal travelling in the steel due to the absorption of the surrounding soil was estimated for each soil type.

To quantify the attenuation, or loss due to soil covering, the following formulas were used:

Total Loss (TL)

$$TL = 20\log\left(\frac{V_{out}(air)}{V_{out}(soil)}\right) \qquad (2.4)$$

Insertion Loss (IL)

$$IL = 20\log\left(\frac{V_{in}(air)}{V_{in}(soil)}\right) \qquad (2.5)$$

where : V= voltage

Soil Cover Loss (SCL)

$$SCL = TL - IL \text{ (in dB)} \qquad (2.6)$$

This study showed the following :

- The soil covering loss amounts are in a range of 0-6.0 dB/m for axial drive and pickup depending upon water content and soil type. The soil covering loss varies from 10-17 dB/m for transverse drive and pickup. These values signifying that the transverse waves attenuated more than longitudinal waves.

- Generally, the increase in water content increases the soil covering loss but not by significant amounts.

- It was observed that soil density effects do have an effect on soil cover loss in that higher density has larger attenuation. Additional work is required in this regard.

- Also it was found that the resonant frequency of the rod changed by only 0.05 kHz to 0.1 kHz over the range of frequencies and soil types.

Hardy and Taioli (1989) used wave guides for rock monitoring, and describe the difficulties that they faced and what alternative solutions they found. In order to monitor in a rock mass, as it can be seen in the Figure 2.15 c& d, a hole was drilled into the rock mass and accommodated a steel wave guide rod which was grouted in place. At the outer end of the wave guide a suitable pickup transducer was fixed.

Although the attenuation of the signal propagating through the rock mass can be eliminated by the use of mechanical wave guides the major problem with conventional wave guides is that they are not able to provide information about the AE source location. One solution to this problem was the suggestion of using "dual wave guide"

where a transducer is mounted on both ends, as shown in the Figure 2.16. AE data from both transducers are recorded and by analysing these data using linear source location methods, those regions of the slope where major AE activity is occurring can be located. Laboratory studies described by Hardy & Taioli (1988) on dual straight wave guides indicated source location errors of 3% or less.

Although these results suggest that dual wave guides could be effectively utilised for accurate one dimension source location in rock masses, dual wave guide for monitoring soils is not always used successfully. This is because long wave guides installed into vertical borehole to depths of 30m-40m, provide insufficient control on the bottom transducer e.g. there is uncertainty as to whether it is still in good contact with the wave guide.

*Rock bolts and connections*

Hardy & Taioli (1989) and Hardy (1992) presented studies on using mechanical wave guides and associated rock bolts to monitor mine and tunnel roof stability. Figure 2.17a shows how the monitoring can be carried out. The horizontal wave guide is attached to a series of in-plane rock bolts and suitable transducers are located at the two ends of the wave guide. A concrete model was constructed in order to study the concept in more detail. The concrete block contained a number of holes for mounting mechanical and grouted type rock bolts. Energy leakage of these two different types of wave guide was found to be in different zones as indicated in Figure 2.17b

In most instances it is necessary to connect two or more sections of wave guide together. Experimental work has been carried out to investigate the energy leakage on a variety of wave guide connections. These include welding, brazing, silver soldering and mechanical clamping. The results of this work are listed in Table 2.2 (Hardy *et al. 1992).*

*Improved wave guide for monitoring slope instability in soils*

Nakajima *et al.* (1991) designed a composite wave guide in order to convert the deformation of the rod due to sliding movement into the occurrence frequency of acoustic emissions. Special attention on the design and improvement of this wave guide has been paid to the following two points.

i) Improvement of the acoustic emission material

In Figure 2.18 it can be seen that the wave guide is composed by two pipes, the inner and outer pipe. The inner pipe is a steel pipe in filled with the acoustic emission material, which is a composite material of resin and glass fibre. Nakajima considered these materials the most suitable acoustics emissions materials following a series of tests carried out. Various composite materials were deformed in bending tests and the relationship between acoustic emission and deflections were obtained. An example of the results of a bending test is shown in Figure 2.19

ii) Reducing in the damping factor

In the past, when the wave guide was installed directly in a borehole the amplitude of acoustic emission were significantly damped due to friction on the surface of the wave guide. The structure of the monitoring rod (Figure 2.18) improved the contact conditions between wave guide and borehole, since the outer polyvinyl chloride pipe was in contact with the inner pipe through nylon rings. The acoustic emission was detected by two transducers which were fixed on each end of the inner pipe. Under these contact conditions the damping factor was reduced significantly from 0.84dB/m to 0.07dB/m.

This improved monitoring rod was applied practically to the measurements of the Numamae Landslide at the Shakotan Peninsula in Hokkaido, Japan, monitoring took place more than one year. The monitoring results identified the landslide movement with high sensitivity and reliability. It was found that sliding was generated in response

to seismic oscillations and the seasonal changes of ground water level. Additionally, the depth of the slip surface was determined by means of the AE monitoring rod and this agreed well with the depth found by pipe strain gauge measurements.

## 2.4 Methods used for AE source location

One method that has been already mentioned above in Hardy & Taioli (1988) studies for locating the AE source is by using the Dual transducer system. This method is accurate enough within an error of 3%. However, monitoring deep into the ground for slip surface could be difficult to control the contact conditions between transducer and wave guide. Transducers are the expensive components of the AE instrumentation and is preferable to monitor multiple boreholes with less amount of transducer units if possible. Hence this section discusses, other methods where a source can be located with the use of one transducer unit.

### 2.4.1 Source location using a single transducer unit

Maji *et al.* (1997) carried out laboratory work on steel beams and plates to explore the theory of wave propagation and digital signal processing. To be more precise, the objective of his study was to exploit the Lamb wave propagation for source location.

The AE source location problem has been usually estimated on the basis of the difference in arrival times of the AE event at a number of transducers (at least two transducers for linear source location).

The first stage of this study, an investigation was carried out on the effects of attenuation of longitudinal waves on a thin plate. A thin 1.6mm steel plate was instrumented with two AE transducers, type R15, with a resonant frequency 160 kHz. A known AE source was available from pencil lead breaks at the location marked X in Figure 2.20. Transducer A was stationary while transducer B was placed 30, 60, 90, 120 cm from the transducer A. Comparison between the source location determined from arrival times of the initial longitudinal wave and the known location of the AE source

showed an error which increased with distance. Figure 2.21 shows that the errors in source location increased exponentially with distance between the two transducers. The error (y) is represented by an exponential function

$$y = 0.23e^{0.039x}, \text{ (x = transducer separation)} \qquad (2.7)$$

This error is due to the progressive attenuation of the longitudinal wave, which leads to the transducer picking up other portions of the AE event. This attenuation of the longitudinal waves precludes their use for large scale (more than 1 m distance) source detection.

Taking advantage of the nature of Lamb waves another solution of source location can be achieved, which requires only one transducer. This method involves looking at the separation in time of different frequency Lamb wave modes, in the same AE event. However, this method does not give information about the direction of the source (left or right side of the transducer). If the time interval $\delta t$ between the arrival of the two frequencies, with known velocities $C_1$ and $C_2$, can be determined the distance of the source $\Delta s$ can be found.

$$\Delta s = \frac{\delta t}{(\frac{1}{C_1} - \frac{1}{C_2})} \qquad (2.8)$$

The frequency content of the AE events generated by the pencil lead fracture on a 213 cm span steel section (W8 x 58) was determined by digital fast Fourier transform (FFT). Due to the transducer resonance, peak frequencies were observed at 100, 160, and 240 kHz. However, a FFT of the initial 50 μs of the AE signal, does not include a peak at 240 kHz. Also, it was observed that the 100 kHz frequency dominates, rather than the 160 kHz, in the initial 25 μs of the same signal. The first arrival time is therefore determined by the velocity of the 100 kHz pulse. The 160 and 240 kHz components follow at slower speeds.

A simple experiment was conducted by Maji *et al* (1994) on a 6.3 mm steel plate with AE instrumentation and pencil lead fracture for the simulated AE source for the separation of different Lamb wave modes by frequency domain filtering. Time domain data of two AE events 30.5 cm and 61 cm away from the transducer are shown in Figure 2.22. Comparing these two figures it was clear that the length of the low amplitude wave, prior to the high amplitude wave, in the (b) is twice as long as the wave in (a). Figure 2.23 shows the frequency content corresponding to the (a) AE event. It shows that the dominant frequencies are between 90 to 160 and 200 to 250 kHz. Having this information the parameters of filters are defined, to separate the energy contained near the 100 kHz resonant frequency from the energy contained near the 240 kHz resonant frequency.

The 240 kHz component was extracted by high-pass filtering with a cut-off frequency of 190 kHz and the energy at 100 kHz was extracted by low-pass filtering with a cut-off at 110 kHz to prevent the 160 kHz resonance from passing through. The effect of the high-pass and low-pass filtering is shown in Figure 2.24 (a) and (b) respectively. The initial low amplitude signal is predominantly of higher frequency (above 190 kHz) and arrives about 90 μs. The low frequency wave arrives at 125 μs hence arrives 35 μs later.

The velocities of the low and high amplitude waves were measured using the difference in arrival times at two transducers. These velocities were 5,400 m/s and 3,300m/s for the low amplitude (high frequency wave larger than 190 kHz) and the high amplitude (low frequency wave less than 110 kHz) respectively. Using the values C1 = 5,400 m/s, C2 = 3,300 m/s and $\delta t$ = 35 ms in equation the $\Delta s$ is given 29.7 cm which is close enough to the pragmatic distance of 30.5 cm where the pencil lead was fractured. Hence, Maji proved, that the distance between source and transducer can be determined. The applicability of these findings, was verified on AE events monitored on a real steel I-40 bridge over the Rio Grande in Albuquerque.

### 2.4.2 Cross correlation technique for source location

Another method for AE source location in thin plates has been studied by Ziola *et al.* (1991) using cross-correlation. This method allows the detection of specific phase points in the waveforms so that the same phase point could be determined as the wave arrived at the different transducers.

The difference in arrival times of the acoustic emission wave at the sensors is usually determined by threshold crossing techniques. The extensional wave mode has the advantage of being non-dispersive so it was used successfully on small specimens for source location. However, extensional mode contains higher frequency components than the flexural mode, therefore this method is not effective in larger specimens since high attenuation of the wave mode exists. If the flexural wave mode is to be used since it does not suffer from high attenuation there is the problem of dispersion. The acoustic emission pulse changes shape due to dispersion, which can cause errors on the triggering. These problems of the first threshold crossing method can be eliminated by using cross correlation method.

Cross correlation is defined as the time average of the product of two functions, where one function has been delayed relative to the other.

$$R_{xy}(\tau) = \lim_{T\to\infty} \frac{1}{2T} \int_{-T}^{T} x(t)y(t+\tau)dt \qquad (2.9)$$

In this study, the transducer output was cross-correlated with an input pulse consisting of a cosine wave modulated by a Gaussian pulse in order to locate a single frequency in the output waveform. The modulated cosine is shown on Figure 2.25 and its equation is expressed as:

$$x(t) = e^{-\left[(t-t1)^2/\sigma^2\right]}\cos(\omega_1 t) \qquad (2.10)$$

where: $\omega_1$ the angular frequency

For this particular simulation $\omega_1 = 6.283 \times 10^5$ rad/s ($f_1$ = 100kHz), $t_1$ = 100μs and $\sigma$ = 40 μs. This single frequency component was isolated from each transducer output and then the time difference due to the propagation of this frequency component was used for source location analysis. The Gaussian pulse was chosen since it allowed a gradual tapering of the cosine, therefore narrowing the frequency content of the input signal. The response of a thin plate to an impulse loading was calculated and the displacement function of the flexural mode was:

$$y(r,t) = 2\,[\cos(r^2/4bt)/(r^2/4bt)] \qquad (2.11)$$

where $b^2 = Eh^2/12\rho^2(1-\nu^2)$,

E, is the modulus of elasticity

h, is the plate thickness

ρ, is the density

ν, is the poisson ratio

r, is the distance form source to sensor, and

t, is the time

The two functions were digitally cross-correlated using

$$R_{xy}(r\,\Delta t) = \frac{1}{N-r}\sum_{n=1}^{N-r} x_n y_{n+r} \qquad (2.12)$$

where x is defined in equation (4) and y in equation (5), N is the number of digital samples and r is the lag number, r = 0,1,2,.., m, where m is the maximum lag number and m<N. The total number of points was 2500, and the step Δt was 0.2 μs for the experiment carried out in this study.

An aluminium plate of 7178-T6 was used, with dimensions of 129.9 cm times 182.9 cm and 0.142 cm thick. The material properties of the plate were E = 70 GPa, ρ = 2750

$kg/m^3$ and $\nu = 0.33$. Figure 2.26 illustrates the experimental set-up. The transducers used to detect the wave propagating through the plate were Harisonic G0504 ultrasonic transducers with a resonant frequency of 5 MHz. The outputs from the transducers were amplified 60 dB using Physical Acoustics Corporation 1220A amplifiers, which had been converted from narrow-band to broad-band filtering. The preamplifier filtering used for the high gain/broad-band test was 125-1 MHz. For the conventional AE monitoring approach PACR-15 resonant transducer of 150 kHz was used and narrow-band filters 125-250 kHz.

Pencil lead breaks (PLB) is a method generating short and consistent events. A 2mm long of 0.2mm pencil lead at a constant angle is forced to break on a structure under investigation. PLB are carried out at various locations and distances from the sensor, shown in Figure 2.27. The results of the tests can be seen in Figures 2.28, 2.29, 2.30 and 2.31. The three pencil lead breaks at each position are plotted (+) along with the measured location (x). Both high gain broadband and high gain narrow band (Figure 2.28 and 2.29) shows high resolution since the measurements were based on the non-dispersive extensional mode. The results from the low gain/narrow band test in Figure 2.30 shows high scattering at location 1 to 5 and none of the lead breaks were located at positions 6,7 and 8. These poor results are due to the triggering of the flexural high amplitude mode instead of the extensional mode. The first positive peaks from the cross-correlation method were plotted since the other peaks are due to reflections. The data in Figure 2.31 show the good agreements with the measured values except for two points at location 1 and all points at locations 6 and 7. The reason of this disagreements was not understood. However, the error was quite small compared with the error that was found when a threshold technique was applied to the flexural mode. This is important in large scale structures where due to the high attenuation of the extensional mode only the flexural mode is able to propagate any distance and can be captured. Another advantage of this method is that the time measurement differences are independent of gain or voltage threshold settings.

## 2.5 Discussion

Chichibu *et al.* (1989) field studies results from the embankment showed that the period of AE occurrence approximately coincides with the movement of the embankment. In natural slope, the level of AE count rates were significant increased two months earlier before the ground movements were detected. Kavanagh (1997) field results also indicated that AE monitoring provides early warning of slope instability, while conventional monitoring techniques are unable to detect the pre-failure small displacements. Also comparing the response of backfill material showed that the most promising area of research relates to the use of active wave guide systems with the assessment of AE signal characteristics.

Field and experimental studies to date demonstrate how advantageous and beneficial is the use of wave guides in AE monitoring systems. Although the attenuation of the acoustics emission while travelling along the metal body of the wave guide is very low, energy leakage hence loss in amplitude is still present. This could be due to its connections and the friction along its surface with the borehole.

Connections should be designed carefully to obtain a good contact metal to metal so the wave could travel through without its amplitude being reduced. The best connection method is proved during laboratory tests (Hardy *et al.*, 1992) to be welding. The only disadvantage is its practicality on the site.

Nakajima (1991) showed that is possible to design a more sensitive wave guide by using composite acoustic emission material moulded into steel and reduce the soil covering loss by constructing a double pipe wave guide described above. This wave guide design seemed to be successful when applied to field work

The concept of dual wave guide enables location of the AE source, hence the depth of the slip surface, which in turn gives information about the size of the hazardous slope failure and likely mechanism.

Soils of various densities and moisture content surrounding the wave guide influence the level of emissions being recorded.

Further detailed studies need to be carried out on improving the design of the wave guide in order to produce a reliable and feasible monitoring system, for field work.

Two main characteristics of Lamb waves (i.e. different dispersive modes and their ability to propagate long distances with little attenuation) make their application to the AE monitoring system attractive. The design of a monitoring system which captures a signal consisting of certain Lamb wave modes, will assist the user to locate the AE event source, due to the different velocities with which each mode propagates through the system. The low attenuation characteristics of Lamb waves enables the user to estimate the location of the soil deformations at large depths.

| | *Loose dry soil* | *Dense dry soil* | *10% wc* | *20% wc* | *30% wc* | *Water* | *Air* |
|---|---|---|---|---|---|---|---|
| **Wet density (PCF)** | | | 98 | 106 | 118 | - | - |
| **Dry density (PCF)** | 85 | 91 | 91 | 82 | 90 | - | - |
| **Frequency (Hz)** | 1,630 | 1,670 | 1,840 | 1,730 | 1,690 | 1,632 | 1,630 |
| **Amplitude (v)** | 28 | 15 | 5 | 4 | 11 | 83 | 96 |

**Table 2.1 Influence of Medium Surrounding Wave Guide on Frequency and Amplitude of First Resonance, after Koerner *et al.* (1975)**

| Method of Connection | Percent Amplitude Loss at Connection |
|---|---|
| Welding | 22.2 |
| Brazing | 27.8 |
| Silver Soldering | 38.2 |
| Clamping | 71.3 |
| Clamping w/Solder Pilow | 67.3 |

**Table 2.2 Amplitude Loss at Wave Guide Joints as a Function of Connection Method, after Hardy *et al.* (1992)**

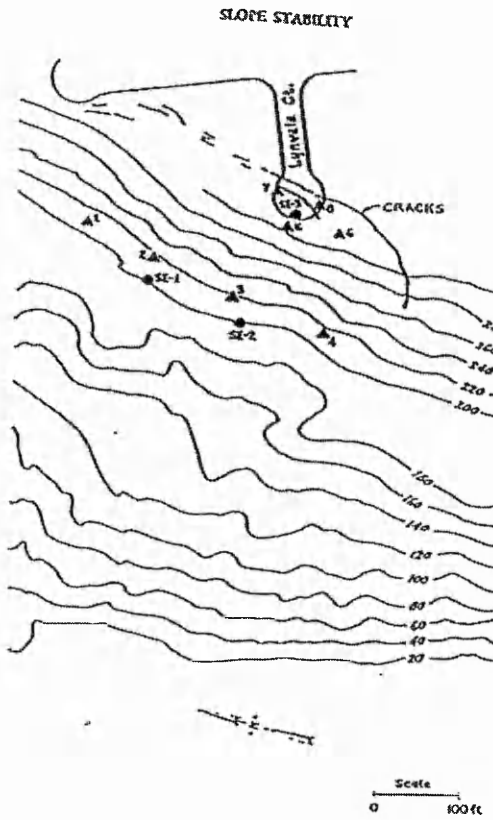


Figure 2.1 Details of Thorton Bluffs field site, McCauley (1977).

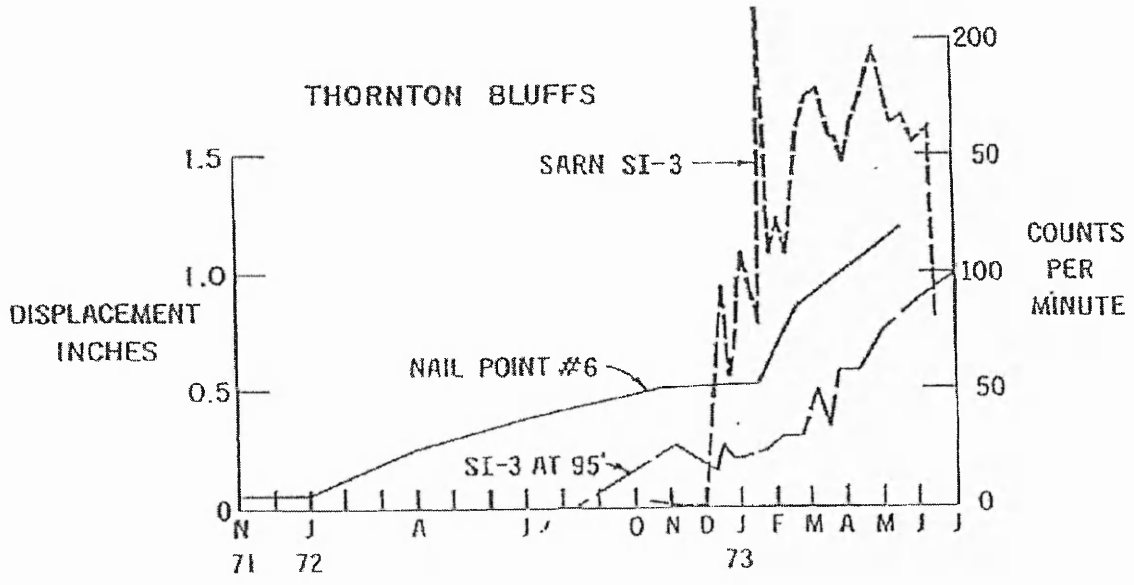


Figure 2.2 Noise rates and displacements at Thornton Bluffs field site, McCauley (1977).

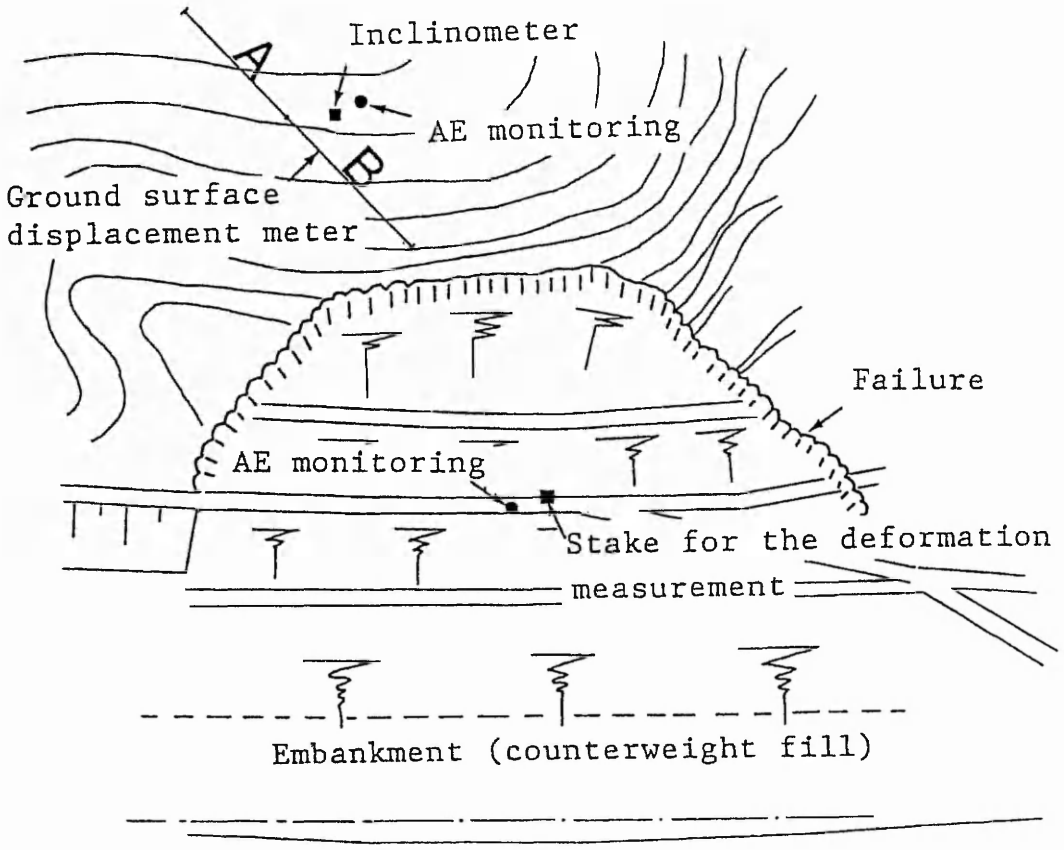


Figure 2.3 Plan view of monitoring site, Chichibu *et al* (1989)

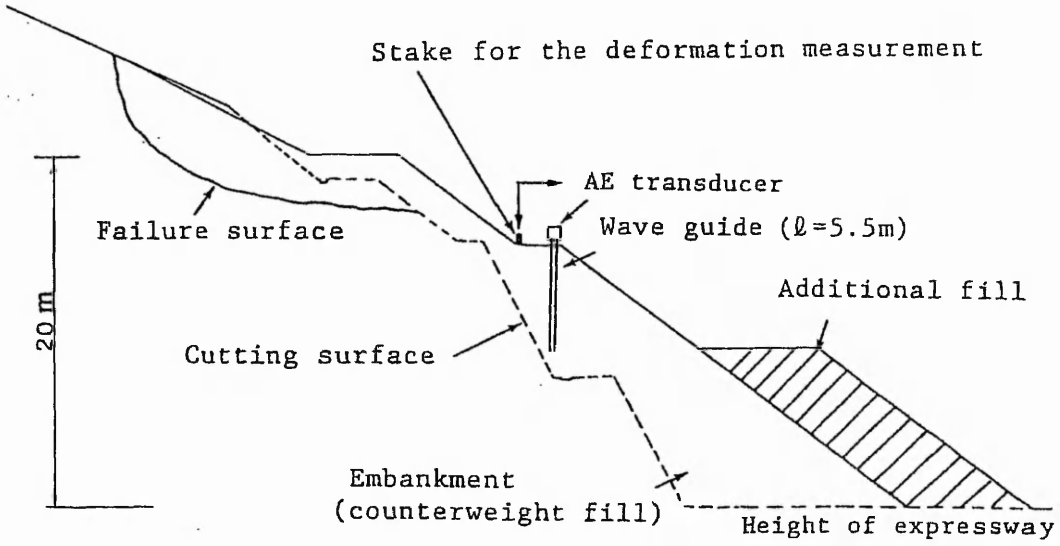


Figure 2.4 Section of the embankment and the cutting slope Chichibu *et al* (1989)

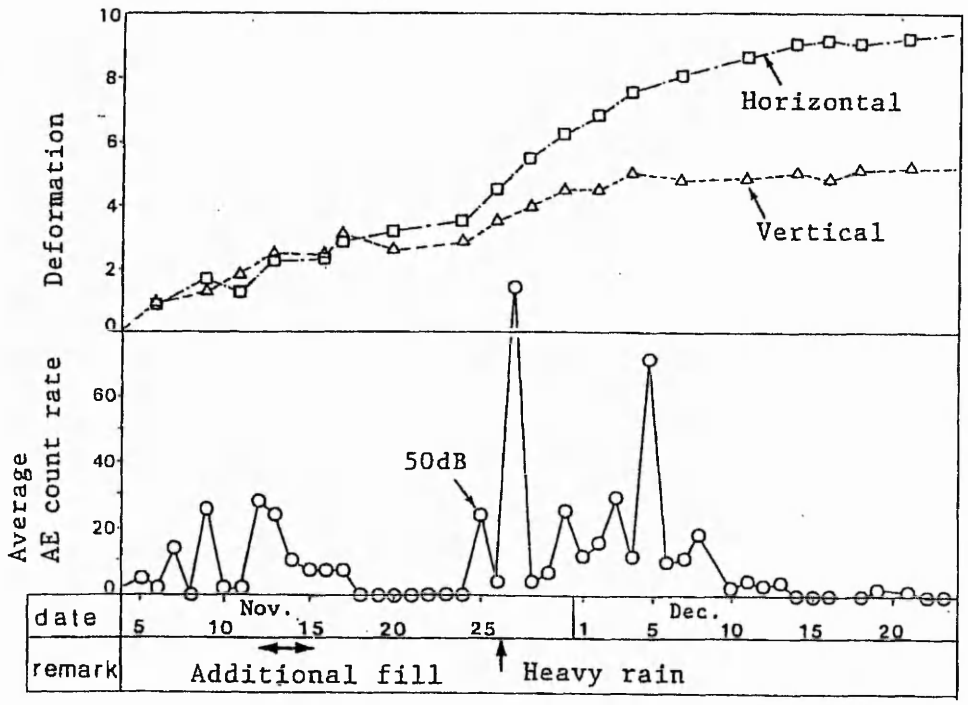


Figure 2.5 Results of monitoring for the embankment. AE counts are per 10 min periods and deformation is measured in cm, Chichibu *et al* (1989)

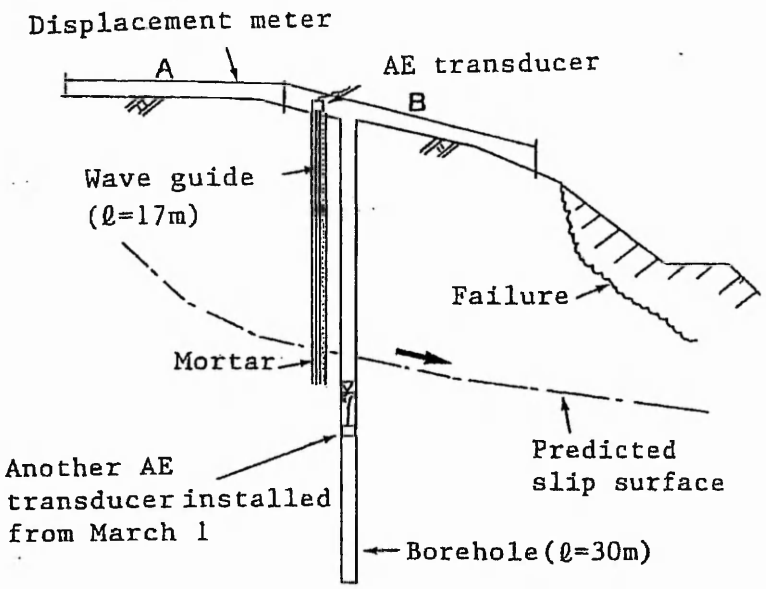


Figure 2.6 Section of the natural slope Chichibu *et al* (1989)

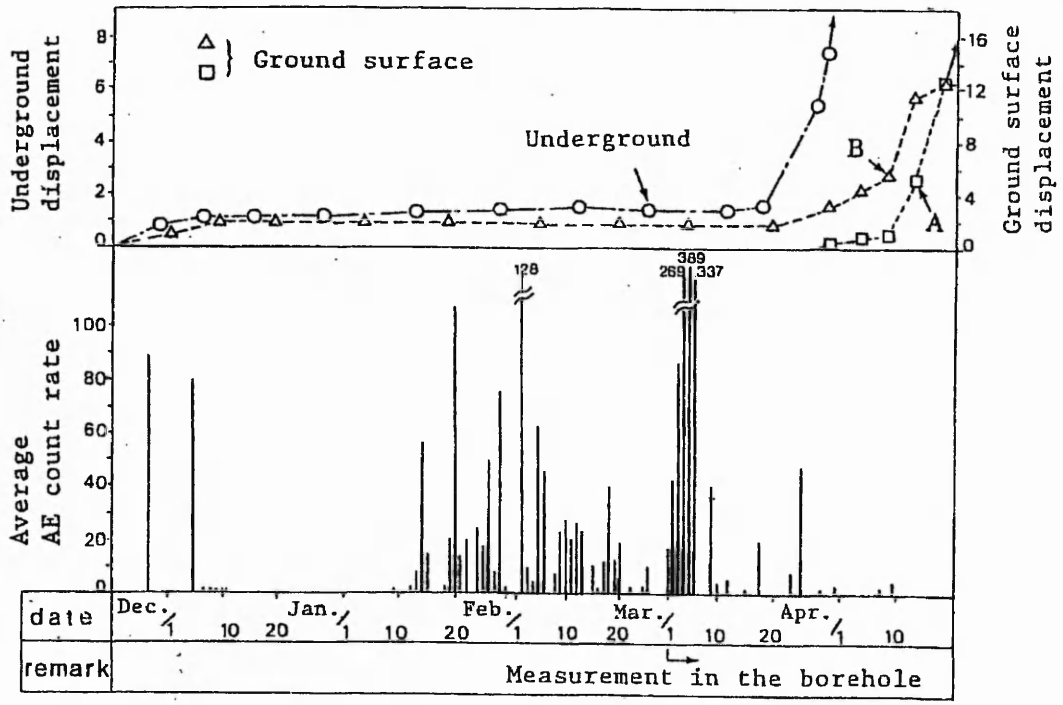


Figure 2.7 Results of monitoring for the natural slope. AE counts are per 10 min periods.Underground displacement is measured in mm while ground surface is in cm, Chichibu *et al* (1989)

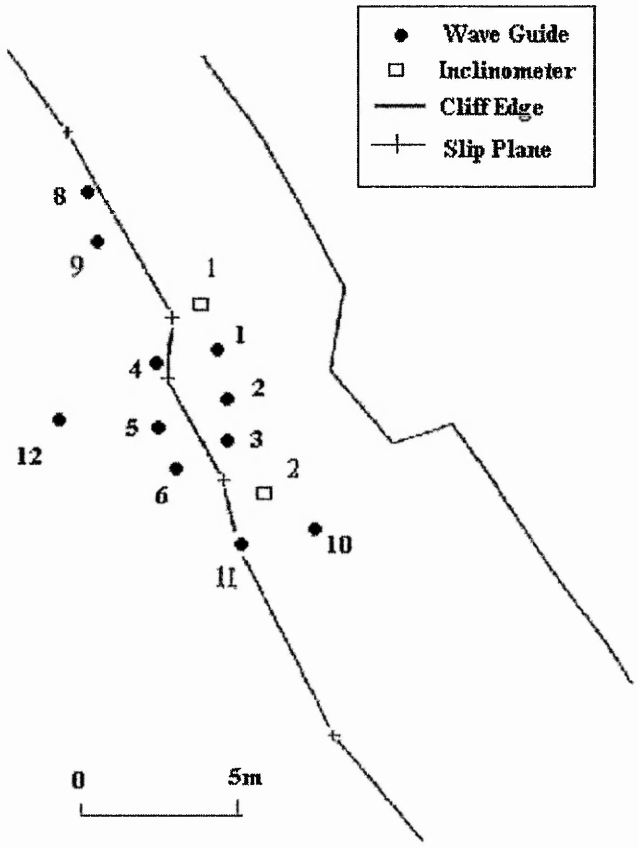


Figure 2.8 Instrumentation array after Kavanagh (1997)

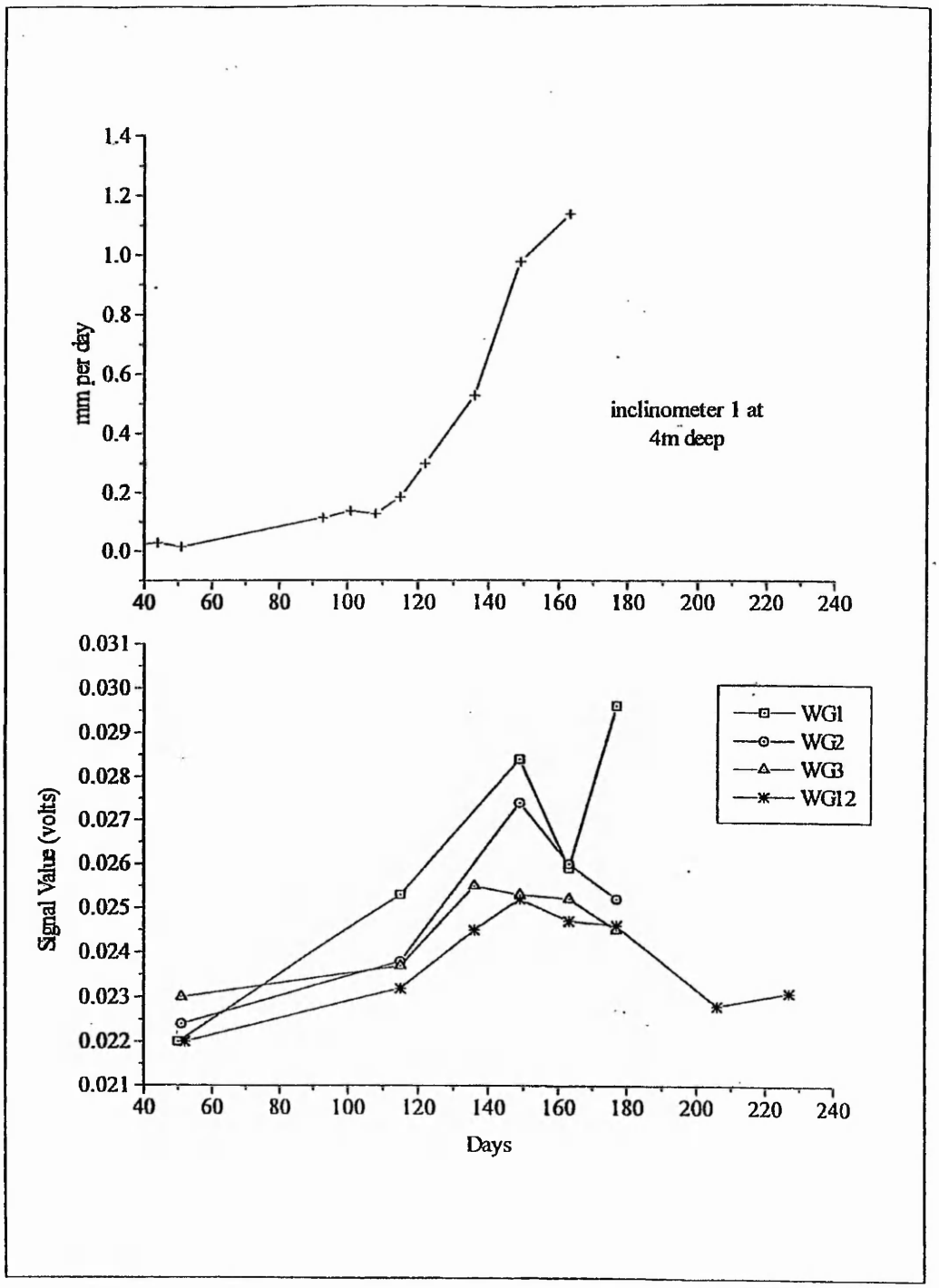


Figure 2.9 AE mean signal value WG's 1,2,3 &12 and displacement rate inclinometer 1, Kavanagh (1997)

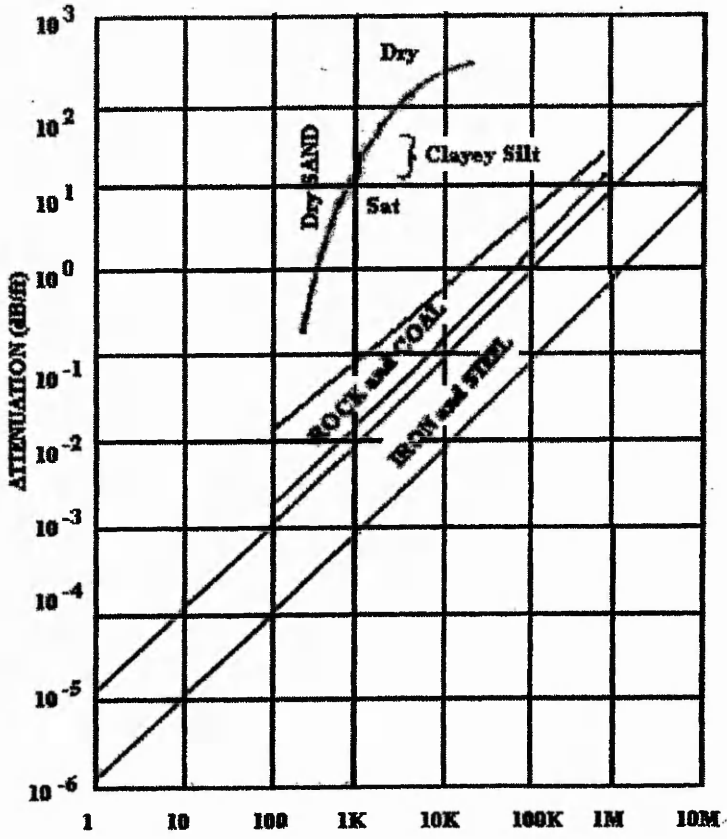


Figure 2.10 Attenuation coefficients of soil rock and iron or steel, after Koernel (1981)

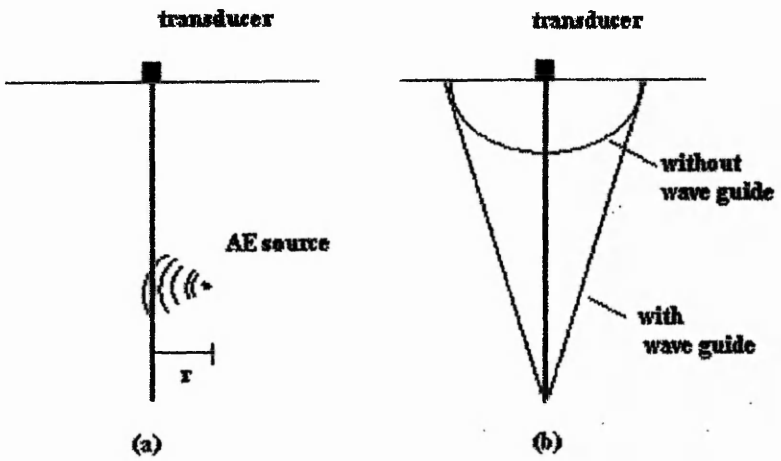


Figure 2.11 Idealised configuration of soil volume sensed by AE methods using steel rod wave guides (a) model of sample problem (b) volume of soil sensed, after Lord *et al* (1982).

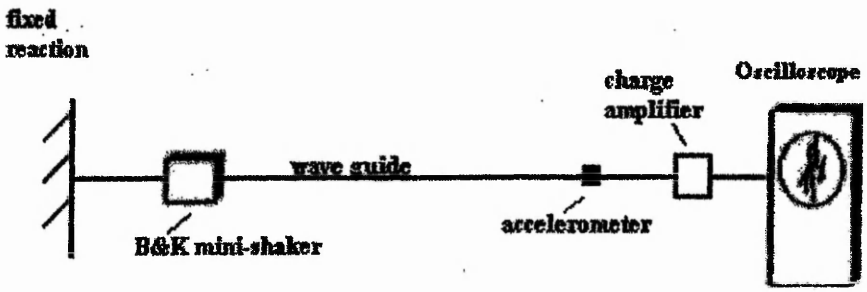


Figure 2.12 Schematic diagram of experimental set-up after Koerner *et al* (1975)

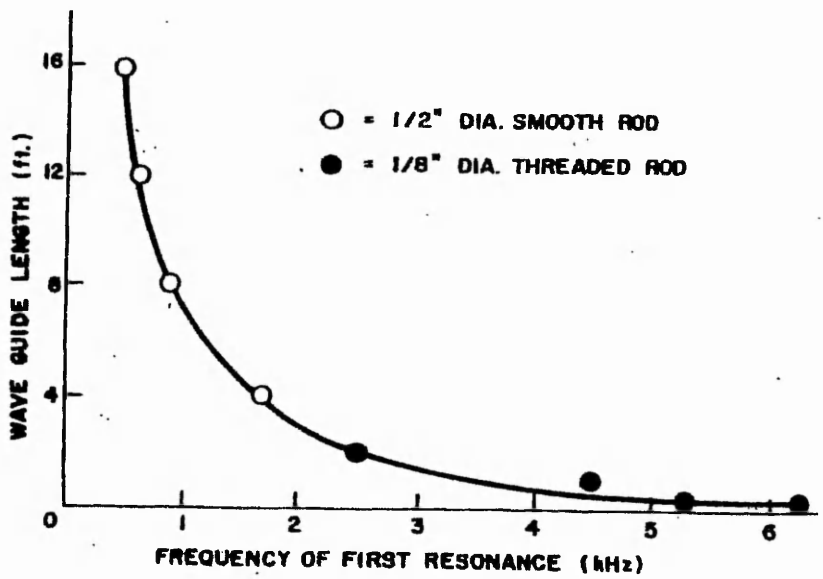


Figure 2.13 Results of the influence of various lengths and diameters of steel rod wave guide on AE response, after Koerner *et al* (1975)

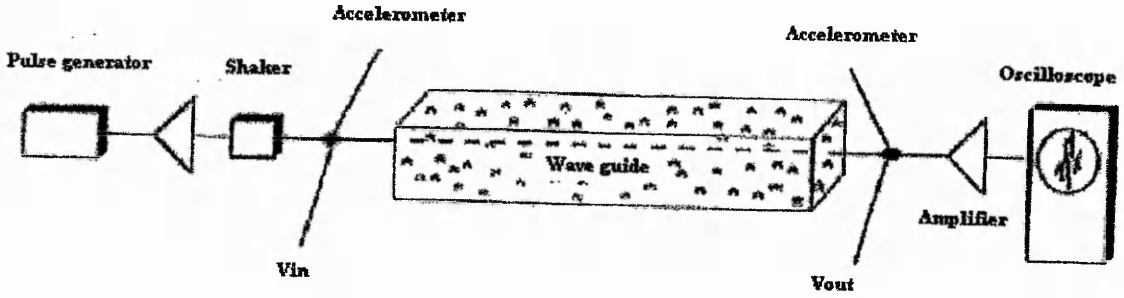


Figure 2.14 Schematic diagram of experimental set-up used to determine soil covering loss in steel rod wave guides, after Lord *et al* (1982).

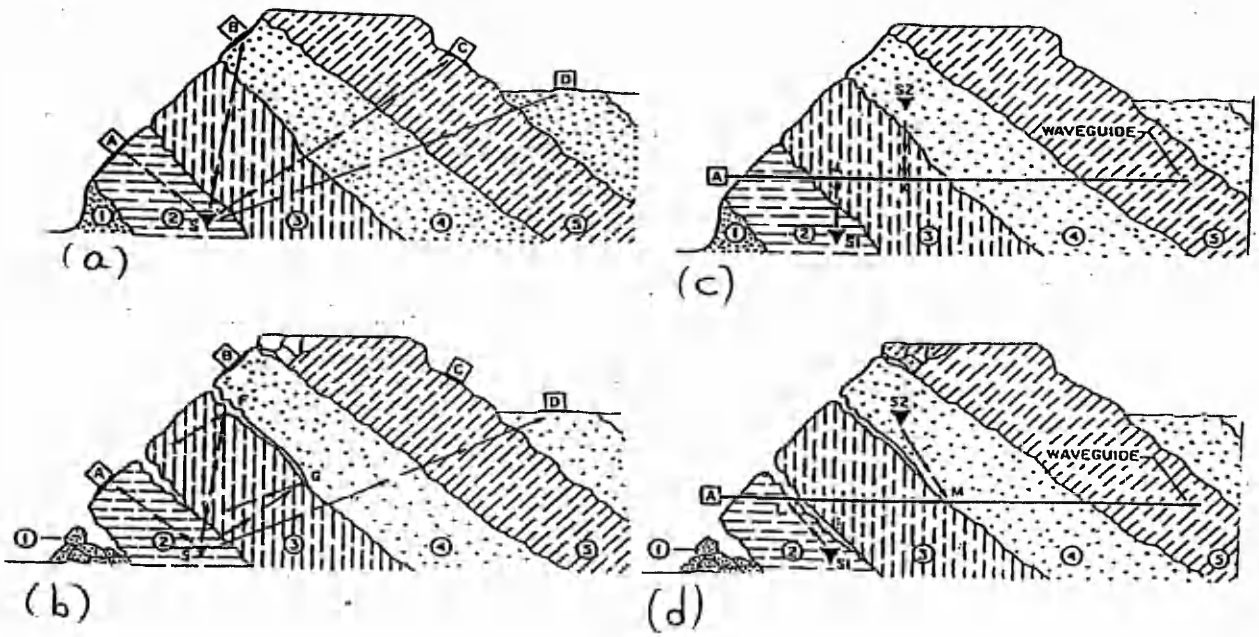


Figure 2.15 Effect of rock mass deterioration on the ability to detect AE activity using surface and mechanical wave guides, after Hardy *et al.*(1989).

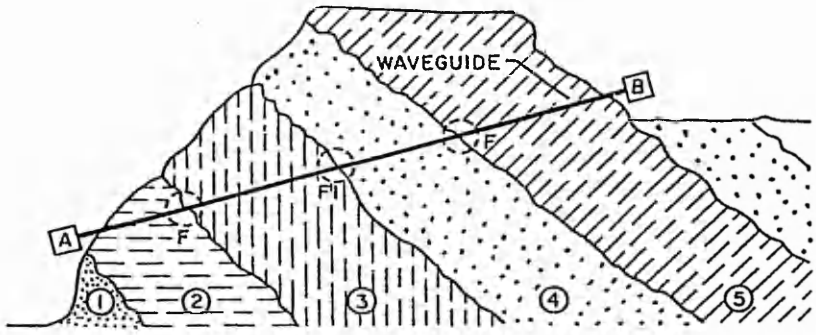


Figure 2.16 Dual transducer wave guide configuration applied to rock mass monitoring (A & B denote transducers) after Hardy *et al* (1988)

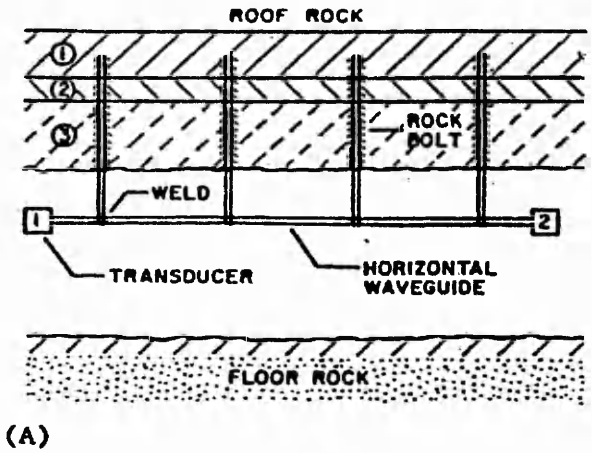


Figure 2.17 Simplified form of roof monitoring system (A), Acoustic characteristics of grouted and mechanical bolts (B) after Hardy *et al.* (1992)

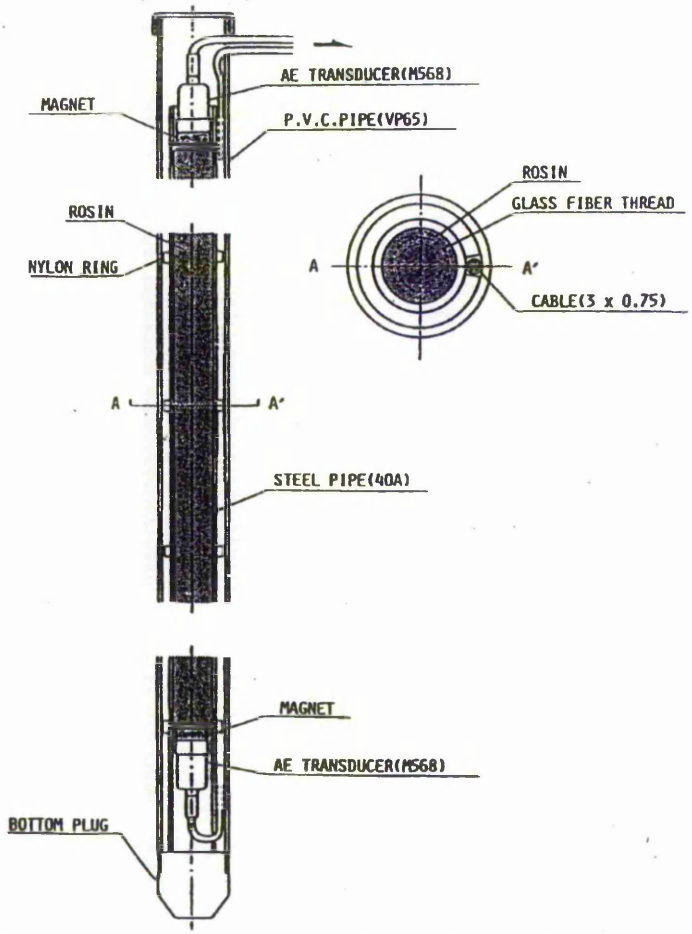


Figure 2.18 Structure of AE monitoring rod Nakajima *et al* (1991)

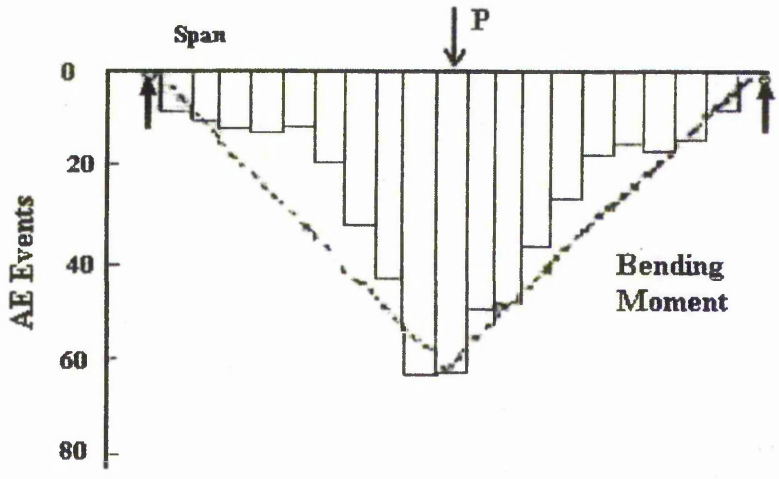


Figure 2.19 Location histogram of AE events on span and diagram of bending moments, after Nakajima (1991)

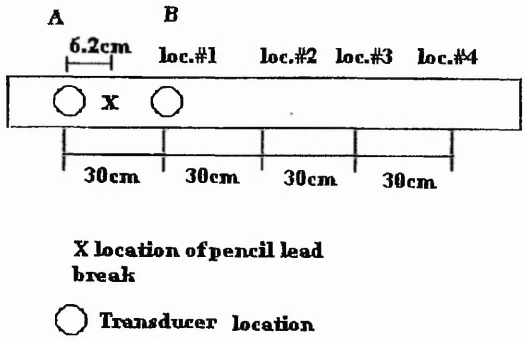


Figure 2.20 Transducer location for source verification after Maji *et al.* (1997).

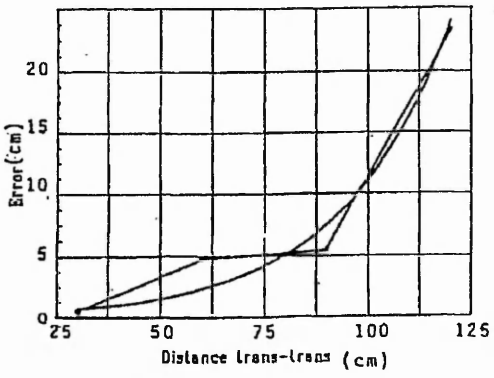


Figure 2.21 Source location error Maji *et al.* (1997).

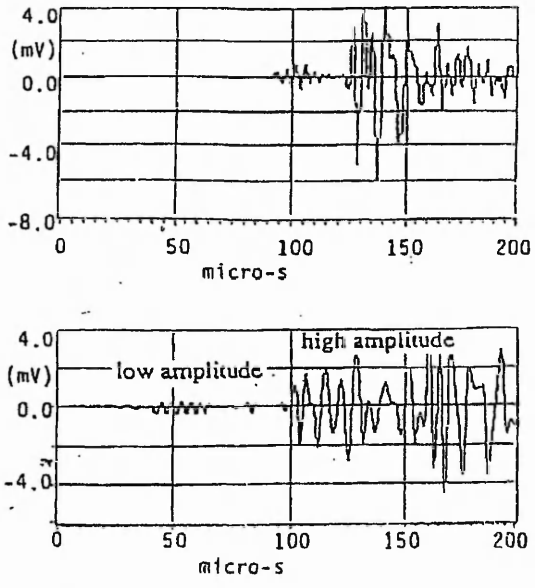


Figure 2.22 Time domain response on 6.3mm plate, Maji *et al* (1997).

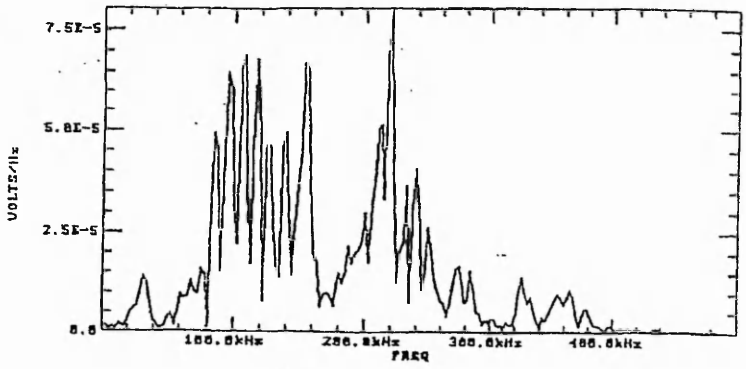


Figure 2.23 Frequency content of AE event, Maji *et al* (1997).

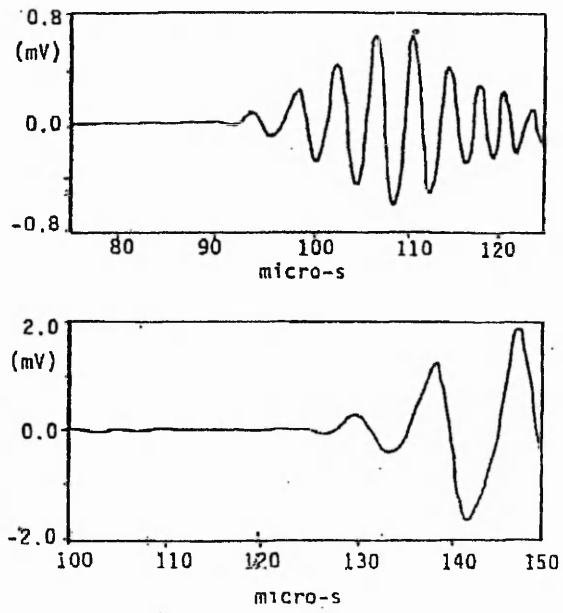


Figure 2.24 Filtered time domain response, top: high-pass filtering and bottom: low-pass filtering Maji *et al* (1997).

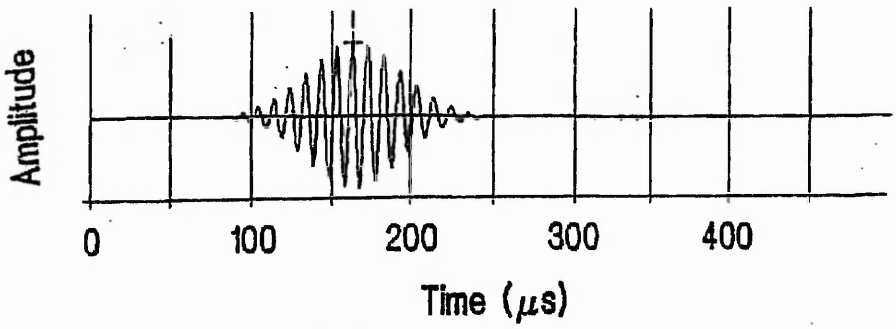


Figure 2.25 Modulate cosine waveform, Ziola *et al* (1991).

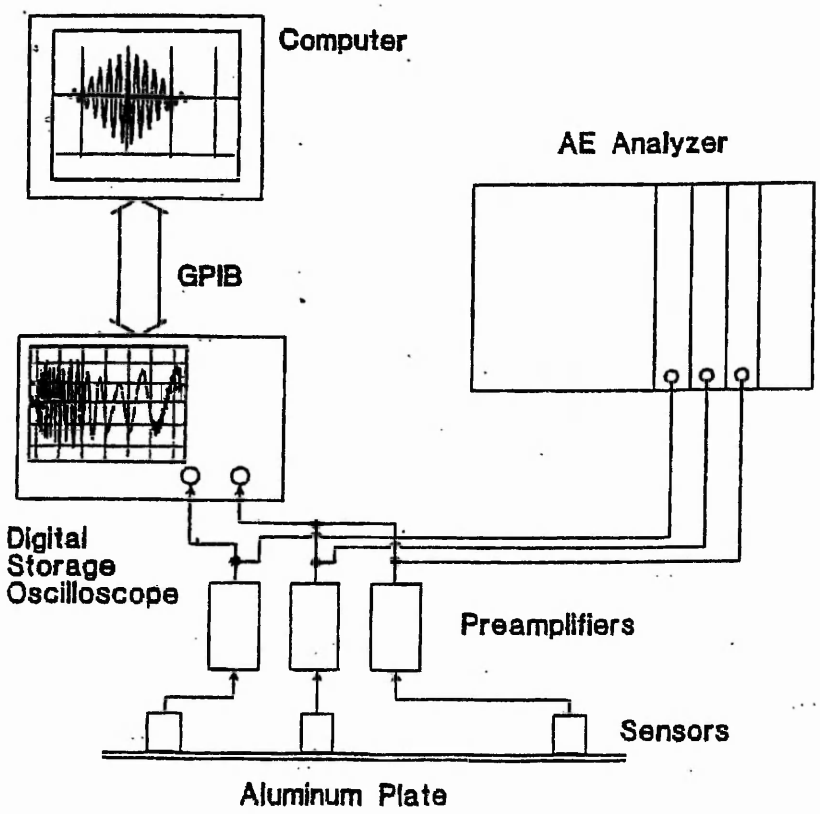


Figure 2.26 Schematic experimental set-up, Ziola *et al* (1991).

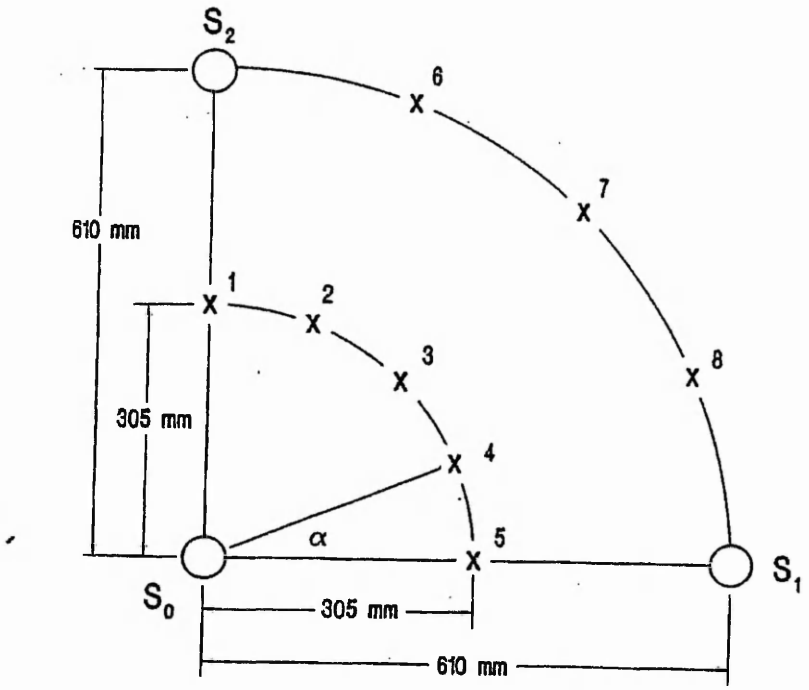


Figure 2.27 Location of lead breaks. For r=305mm, α=90°, 67.5°, 45°, 22.5°, and 0°. For r=610mm α=67.5°, 45° and 22.5°, Ziola *et al* (1991)

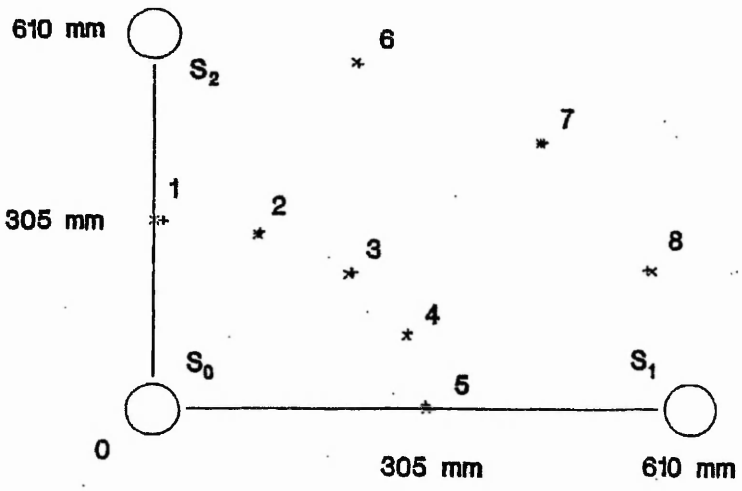


Figure 2.28 Experimental location results for high gain/broad band, conventional AE instrumentation, Ziola *et al* (1991).

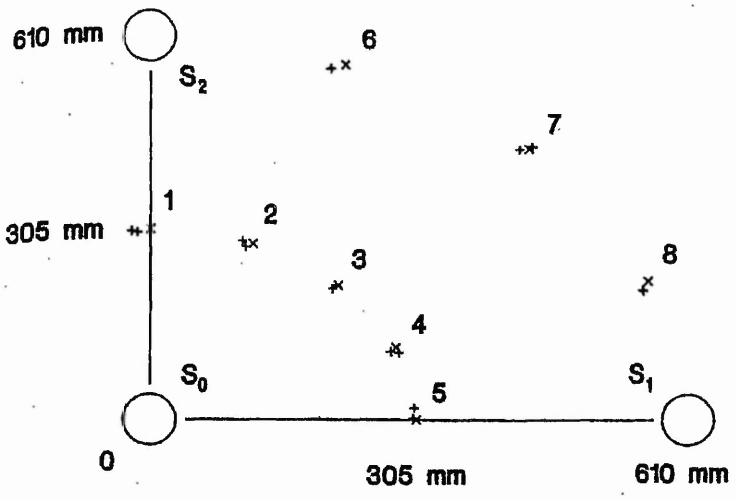


Figure 2.29 Experimental location results for high gain/broad band, conventional AE instrumentation, Ziola *et al* (1991).

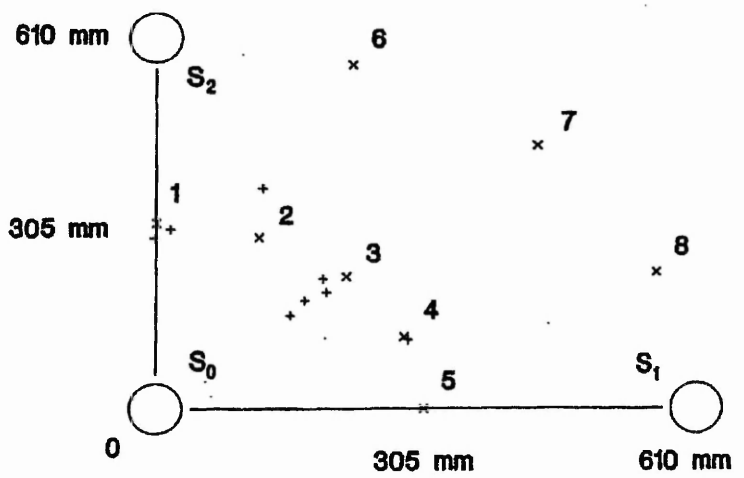


Figure 2.30 Experimental location results for low gain/broad band, conventional AE instrumentation, Ziola *et al* (1991).

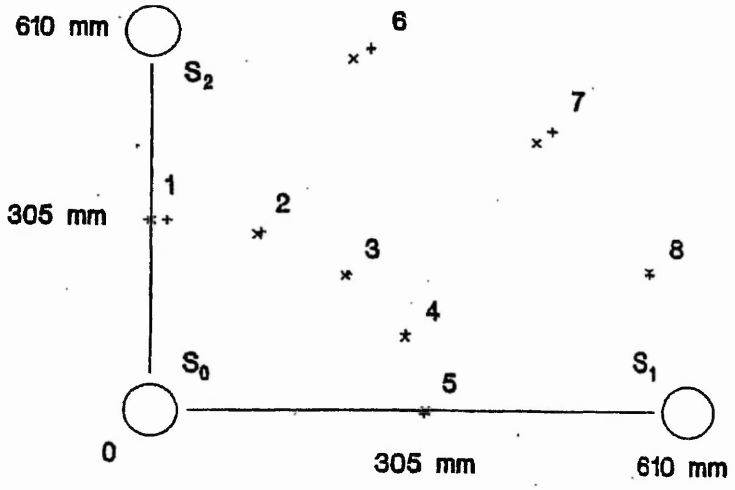


Figure 2.31 Experimental location results for phase point method, Ziola *et al* (1991).

# Chapter 3 - Acoustic Emission Instrumentation and Processing Programs

## 3.1 Introduction

The AE instrumentation components used in the field studies carried out by Kavanagh (1997) are shown in Figure 3.1. Kavanagh's study showed that the AE data obtained using this system were related to the soil displacement rates. Therefore, it was decided to use a similar monitoring system for the present laboratory study. Each element of this system was investigated and modified in order to design an improved monitoring system. This section describes each component of the instrumentation and its function.

## 3.2 Elements of monitoring system

### 3.2.1 Backfill Soil

In Figure 3.1 it can be seen that the borehole accommodates the wave guide tube and the backfill soil. Backfill soil is placed between the wave guide and the soil that is to be monitored. The soil type of the backfill can be sand, gravel or clay. The granular soils (sand and gravel) are used in this study since they produce higher AE levels than clay which is known as a "AE quite soil".

The use of the backfill soil not only improves the contact between the monitored soil and the wave guide, but also plays an important role in reducing the number of factors that influence the AE signal. How the backfill achieves this, is discussed extensively in chapter 5.

### 3.2.2 Wave Guide

Metal wave guides can take the form of steel reinforcing rods, various metal instrumentation pipes, (for example aluminium inclinometer tubes) or construction units

(for example tiebacks, anchors, piles or soil reinforcement units). It is possible for the length of a wave guide to be in excess of 30 m when used in field monitoring.

In the present study the wave guide used was steel tube sections of 1.62 m in length and of 60 mm diameter. The wall thickness of the tube was 6 mm. To construct a longer wave guide the steel tube sections (1.62 m each) were joined together using a 50 mm length steel threaded collar. The ends of the wave guide section were threaded and screwed inside the collar on both sides. The threaded parts of both wave guide and the collar were greased before being screwed together to achieve a robust connection i.e. both wave guide sections had to come in contact with each other about half way inside the collar ring.

The choice of the steel tube AE wave guide has the advantage that it can be easily fabricated to the required cross-section and length, and has a low ultrasonic attenuation coefficient. The "active" wave guide system measures the emission generated by the frictional motion of the soil particles which are in contact with or close to the wave guide once it is installed in a borehole and had an annulus of backfill soil placed around it.

This type of "active" wave guide and connection system was what Kavanagh (1997) used in his field study. The present study investigates the advantage and disadvantage of this system and compares it with other designs of wave guide systems. Wave guides of various diameter and wall thickness or with different type of connection, (i.e. collar or welded connection), and using different type of backfill soil (i.e. sand or gravel) are assessed to suggest the most reliable wave guide design.

### 3.2.3 Sensor

The sensor used for these studies was an AE Technology piezoelectric transducer with a resonant frequency of 30 kHz. This means that the waves arriving to the sensor with/or close to the resonant frequency will clearly appear in the captured signal with higher AE amplitude than the other waves further away from the 30kHz frequency.

The piezoelectric effect is the phenomenon whereby mechanical pressure or tension is applied to the crystal of the transducer and this is converted into an electric charge at the crystal surface. The magnitude of the electric charge produced is directly proportional to the mechanical pressure or tension applied. The sign of the electric charge changes when the mechanical force changes from compression to tension. Therefore, the transducer converts mechanical micro-seismic waves to a variable electrical voltage which can be stored, processed and analysed.

The choice of 30 kHz resonant frequency transducer is due to the need to minimise low frequency background noise and at the same time keep the frequency of the system as low as possible so as to avoid high levels of attenuation (the higher the frequency the higher the attenuation).

### 3.2.4 Preamplifier and Filter

A preamplifier was used to amplify the low level signals from the sensor by 40 dB. From the definition of dB expressed in equation (3.1), the output Voltage was the input Voltage multiplied by 100.

$$dB = 20 \cdot \log\left(\frac{V_{out}}{V_{in}}\right) \qquad (3.1)$$

The signal was filtered by a band pass filter with a bandwidth of 15 - 45 kHz. Hence the output signal consisted of waves with frequencies between 15 kHz and 45 kHz . This ensured that any low frequency background noise was not included in the recorded signal. High frequency waves above 45 kHz were also filtered out. Within this frequency range few wave modes could be captured. This filtering simplifies the gross recorded signal and facilitates the identification of wave modes that do not suffer high attenuation and distortion. Further explanation on the frequency and wave modes is presented in chapter 4.

### 3.2.5 Main Amplifier and an AE processor

The Acoustic Emission Technology (AET) model 204GR is an acoustic emission monitoring system which is designed to measure and process AE data obtained in field applications. It can provide measurements of AE in terms of total ring counts, count rates, total events, event rates and signal strength. These AE measurement criteria are defined in Figure 3.2. It operates within a bandwidth of 30 Hz to 200 kHz and can amplify the signal between 50 and 108dB.

In this study the AET model 204GR was used as a main amplifier only. The AE basic processing facilities were not used since data capture and processing were carried out and saved into files by the DAS50 board and the advance software package called "viewdac". These two are described below.

### 3.2.6 Data Capture

A DAS50 A-to-D board was used to convert the analogue voltage to a digital value. The maximum sampling rate of the board is 1 MHz. By directly writing data to the DAS50 board, via the digital ports, it is possible to set the A to D board default to capture a stream of data including data points before any trigger time or voltage set by the operator. The operator via the digital ports of the board is able to set a threshold level precisely and command when it is to be activated. The triggering could be activated on a rising or descending voltage when the threshold level is crossed.

### 3.2.7 Data Processing

A standard processing software package "Viewdac" was used throughout the study. Viewdac is a high-level programming language developed by Keithley Instruments Ltd. for data acquisition and processing. Viewdac consists of single commands named *tasks* which can control or be controlled by other tasks. Suitable programs, named sequence (sequence presents a collection of tasks and operations that perform some functions) are

formed in Viewdac for each experiment. These, save the AE captured data into binary files which can then be analysed. (Viewdac Users Manual Keithley 1998)

## 3.3 Monitoring and analysis programs developed in Viewdac

Three software programs were created to capture and process the AE data. Two in viewdac language and one in FORTRAN 77. The function of each programs is explained in the following sections.

### 3.3.1 Data Capture Viewdac Sequence

A program sequence responsible for the capture of acoustic emission was developed. The main aims of the sequence are:

1. to prepare the A to D board for fast sensing of acoustic emission events;
2. acquisition and digitising of the oscillating voltage; and
3. efficient storage of AE data.

Fast sensing was achieved by keeping the operations of this sequence to a minimum. This way the board is able to capture and store the events at small time intervals. For example an events consisting of 1000 AE data and the sampling frequency is set to 236842 Hz will result to a capturing time of 0.004 sec (1000 x 1/236842). This is the minimum time that is required to capture the 1000 AE data only. Additional time is required to save these 1000 data into a file. Assuming that this saving procedure takes 2 sec, then the time interval where the board is unable to capture the next triggered event is 2.004 sec. Hence, events are lost within this short time interval.

The sequence layout, including the specific tasks (jobs) performed, are shown in Figure 3.3. The sequence begins with the DAS50 Block. This block of commands sets the analogue to digital board (DAS50) default to capture a stream of data including pre-trigger points. The pre-trigger points are necessary to capture and view the original data of each event which is triggered. The amount of these data are defined by the author and could vary in different cases according to the nature of the experiment and its

requirements. The trigger is set to activate on a rising voltage going through a set threshold value. A 255 unit scale between -10 V and +10 V sets the resolution of the trigger level. For example the threshold voltage value 131 is equivalent to 0.28 volt. The DAS50 is in a state of readiness to begin the acquisition of events while waiting for the trigger to be activated. The majority of the triggered event data could have an amplitude smaller than the threshold level but if only one point of the event data exceeds the threshold level the event will be captured by viewdac. This capture arrangement meant that fewer events, dependent on the pre-set threshold level, were stored compared to ready streaming.

The Filename Block follows in which the operator can type the name of the file in which the acquired data will be stored and saved. Having the A to D board ready and the filename specified a push button is used as a switch to allow the initiation of data capturing.

Loop1 is activated by the push button. The sampling of the selective input event is controlled by an acquisition command, (A to D). This command specifies the number of channel which data is acquired, sets the sampling rate and the number of data points to be captured and stored. It has been suggested that the sampling frequency required to define closely a signal, should be at least three times the frequency of the receiving waveform. In this study, the signal provided includes waveforms of frequencies between 15 kHz and 45 kHz. This is mainly due to the filter which cancels out any other frequency waveforms received from the 30 kHz resonant transducer. Therefore, it was decided to specify a sampling frequency of 150 kHz, which is approximately three times the maximum frequency of the captured signal (150/45=3.3).

After the data are captured in each run loop, storage of the digitised information in permanent memory was achieved. The acoustic emission data were saved to a binary file. Binary files were used in order to occupy less memory space than that of the ASCII file. Each data in a binary file occupies four bytes instead of eight bytes in an ASCII file.

### 3.3.2 Post-filtering AE events Viewdac program

The sequence described above allows any event with an amplitude bigger than or equal to the threshold level to be captured and stored into a file. Unfortunately, not all of these events are of interest. It was common to capture electronic spikes (Figure 3.4) caused from other electrical equipment and these needed to be rejected before processing was carried out. Events with initial points distorted were also captured, and these had to be rejected as well. The DAS50 board dwelling on the negative rail caused recording of events with first points as -10 Volts (see Figure 3.5). The pre-triggered points pay an important role at this stage to indicate if the event has already started inside the digitised window.

Above is described three types of events, electronic noise, original data of -10 Volts amplitude and the absence of low amplitude pre-triggering data. All, are characterised as "bad" events. A sequence called (GDEVENT) was written in Viewdac to filter out these events from the recorded bulk data. A layout of the sequence is shown in Figure 3.6.

In addition to the filtering operation the same sequence proceeds to evaluate the Mean, Standard Deviation and the Root Mean Square of the remaining "good" events.
The arithmetic mean standard deviation and root mean square are defined by the following equations:

For a set of $n$ data points $x_1, x_2, x_3, \ldots\ldots, x_n$

i) The arithmetic Mean is: $$\bar{x} = \frac{1}{n}\sum_{j=1}^{j=n} xj \qquad (3.2)$$

ii) The Standard Deviation (Std.Dev.) $$s = \sqrt{\frac{1}{n-1}\sum_{j=1}^{j=n}(x_j - \bar{x})^2} \qquad (3.3)$$

iii) The Root Mean Square (RMS) $$RMS=\sqrt{\frac{1}{n}\sum_{j=1}^{j=n} x_j{}^2} \quad (3.4)$$

The outcome of this sequence is the creation of two ASCII files. One file with an extension *.ndc includes the good event indices. For example, suppose the original file recorded 10 events and after the filtering the indices file (*.ndc) might include the following numbers: 3,4,6,7,9,10. This means that out of the ten events recorded, four of them are filtered out (first second fifth and eighth) as bad events, with the remaining six listed as good events. Only on these 'good' events is statistical analysis carried out.

The results of the statistical analysis are saved in the second file with the extension *.stc. According to the above example the first row of the *.stc file will include the statistical values of the third event.

### 3.3.3 FORTRAN 77 program

The good event statistical values obtained for a certain laboratory test would not be of any significant if not related to the actual displacement or the real time of the test. In the following chapters 6 and 7 AE generation was obtained by applying measured displacements to the backfill soil. It was useful to relate the AE events generated while a certain displacement interval takes place with the corresponding displacement value. To achieve this relationship between AE and displacement a Fortran 77 (F77) program was constructed. The program was called "grouping" and is included in Appendix 1. It requires three old files to read and produces two new files.

At this stage it has to be noted that while testing the response of the backfill soil an additional file was created carrying the extension *.cm. In this file the cumulative events occurring at equal time intervals were recorded. The operator specifies the time interval, which dependes on the nature of the test. This operation was added to the data capture viewdac sequence described above in section 3.3.1. For example, a test of 15

minutes duration and with a time interval set to 5 min the *cm file could look like the following.

| Time(min) | (filename).cm |
|---|---|
| 0 | 0 |
| 5 | 16 |
| 10 | 23 |
| 15 | 39 |

This means that in the first five minutes 16 events without distinction of good or bad events were generated. In the next 5 minutes an additional 7 events occurred but as the *.cm file reports the cumulative events is shown as 23. The total number of events occurring in this test is reported in the last row of the *.cm file which in this case is 39 events.

The three existing ('old') files the F77 program "Grouping" uses are:

1. (filename)*.stc. This file includes the three AE statistical values of the "good" events (i.e arithmetic mean, root mean square and standard deviation).
2. (filename)*.ndc. Where the true event indices are saved in a single column arrangement and indicate how many good events were captured.
3. (filename)*.cm. Includes the AE cumulative event record as defined above.

Having read the above three files the program processes the statistical data and groups them under the corresponding time interval that they occur. The outcome of this program is two new files:

1. (filename)*.dat where the average of the grouped events is listed and
2. cnt(filename).dat where the amount of only the good events occurring in each time interval is listed.

The final files can be related to the real time monitoring as they have the same amount of rows as the *.cm file. Assuming the above example once more the new files will be as follows:

| Time(min) | (filename).cm | Cnt*.dat | (filename) *.dat |
|---|---|---|---|
| 0 | 0 | 0 | 0 |
| 5 | 16 | 10 | Average statistic value of the 10 events |
| 10 | 23 | 7 | Average statistic value of the 7 events |
| 15 | 39 | 12 | Average statistic value of the 12 events |

These last two files were used extensively in chapter 6 and 7 to create plots and investigate the AE response of the backfill with respect to displacements.

## 3.4 Summary

The instrumentation components described in this chapter allows the capture of high frequency events between 15 to 45 kHz. This range of frequency used in this instrumentation did not allow low frequency background noise to interfere with the signal of interest and at the same time was not too high to suffer from high attenuation. Steel tube wave guides were used to guide the signal from the source to the sensor with little attenuation.

A program was constructed using the viewdac-software to capture the experimental AE emissions. This program did not include data processing operations so as to minimise time delay between capturing the events. Post-processing was carried out on filtered AE events, with bad events removed to obtain statistical values of the events. Finally, statistical values of the good events were related to corresponding real experimental time intervals in which they occurred. Hence they could be related to displacement rates and magnitudes.

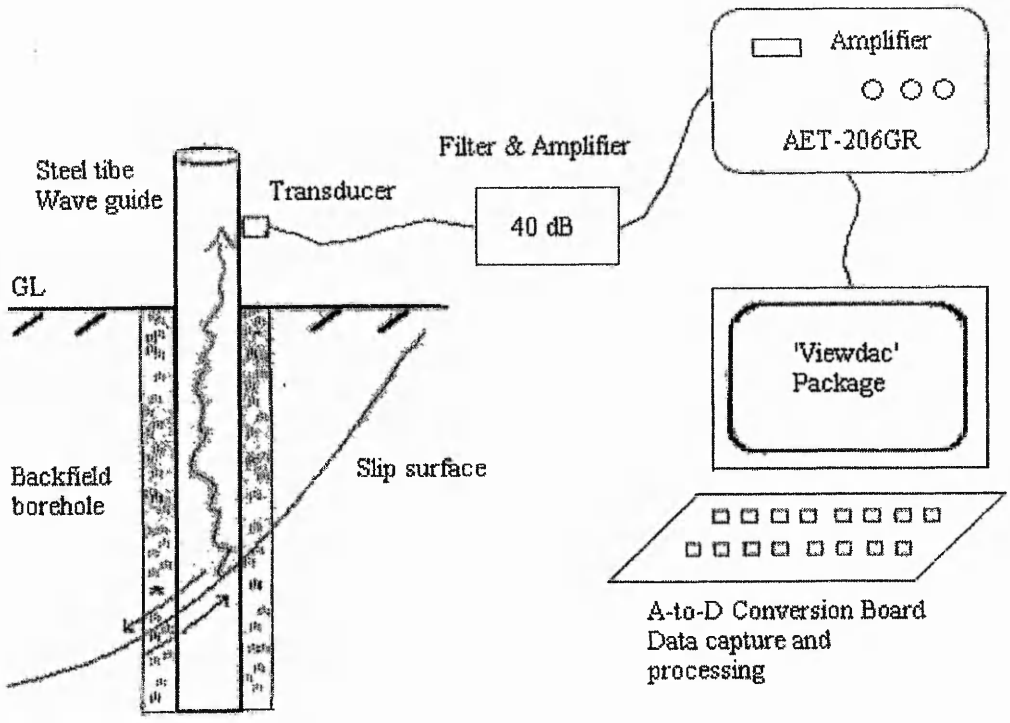


Figure 3.1 AE instrumentation components

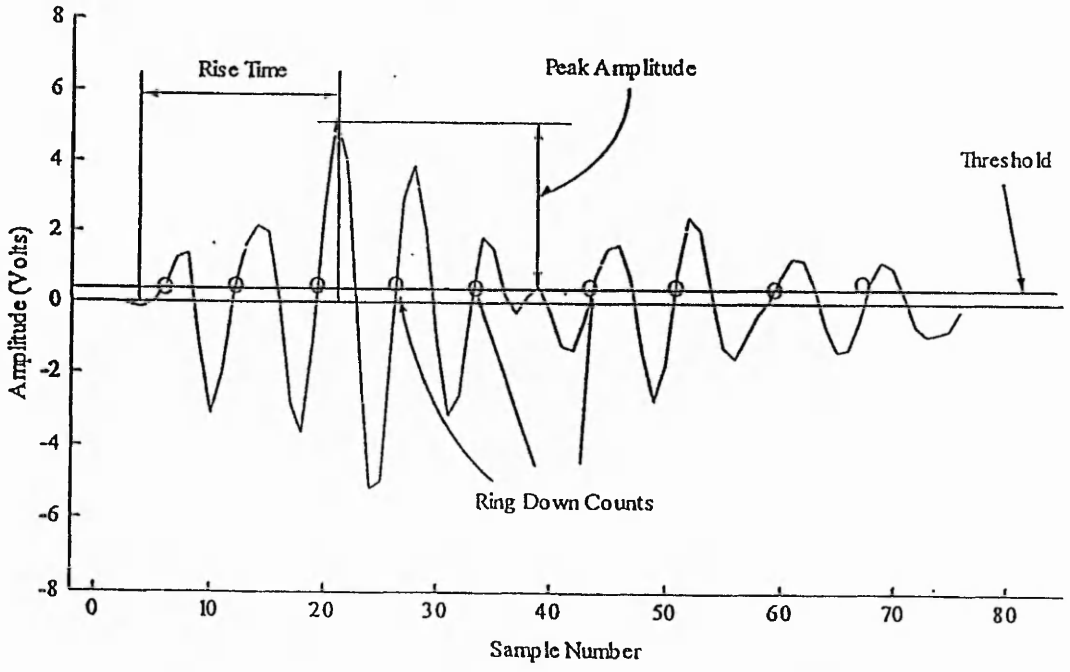


Figure 3.2 AE signal measurement criteria Kavanagh (1997)

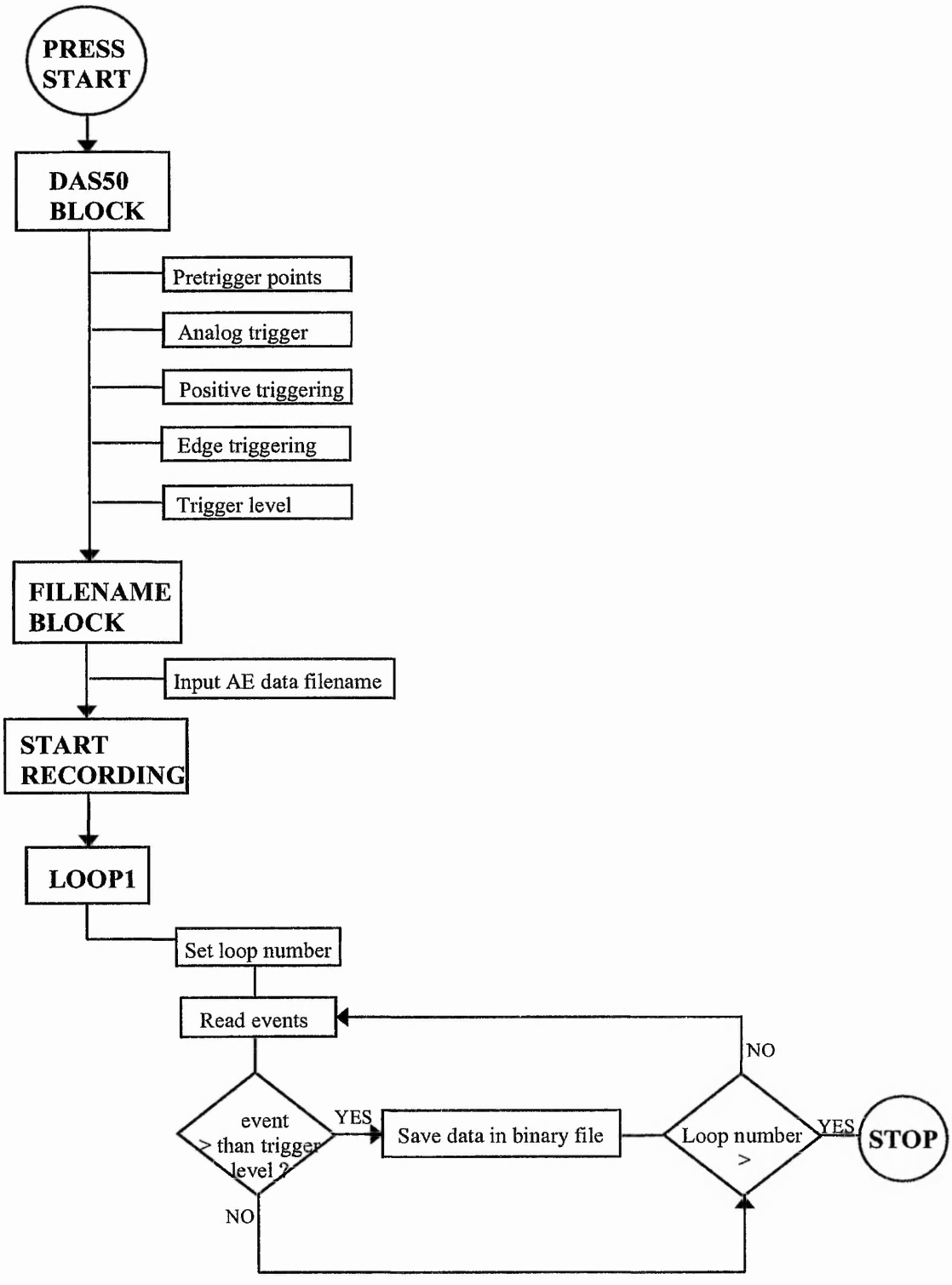


Figure 3.3 Viewdac sequence layout used to capture the test AE data.

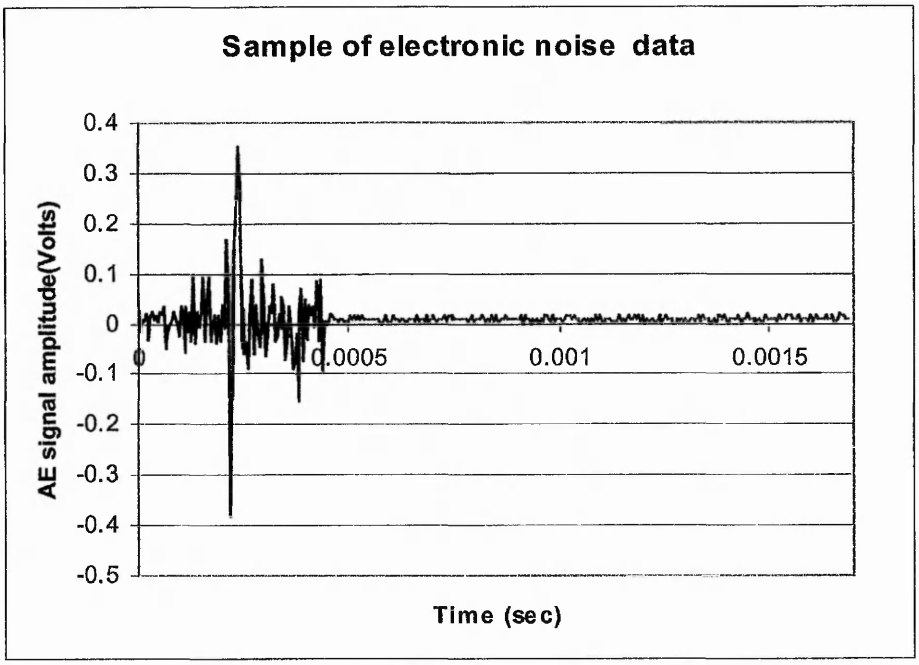


Figure 3.4 Electronic noise event which was filtered out by GEVENT sequence.

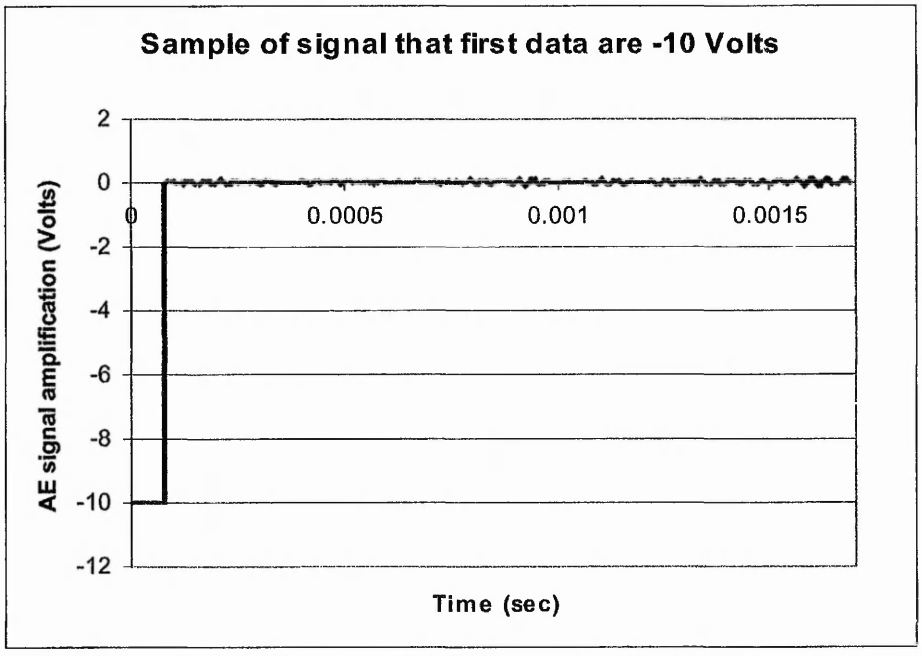


Figure 3.5 DAS50 board dwelling on the negative rail (-10)

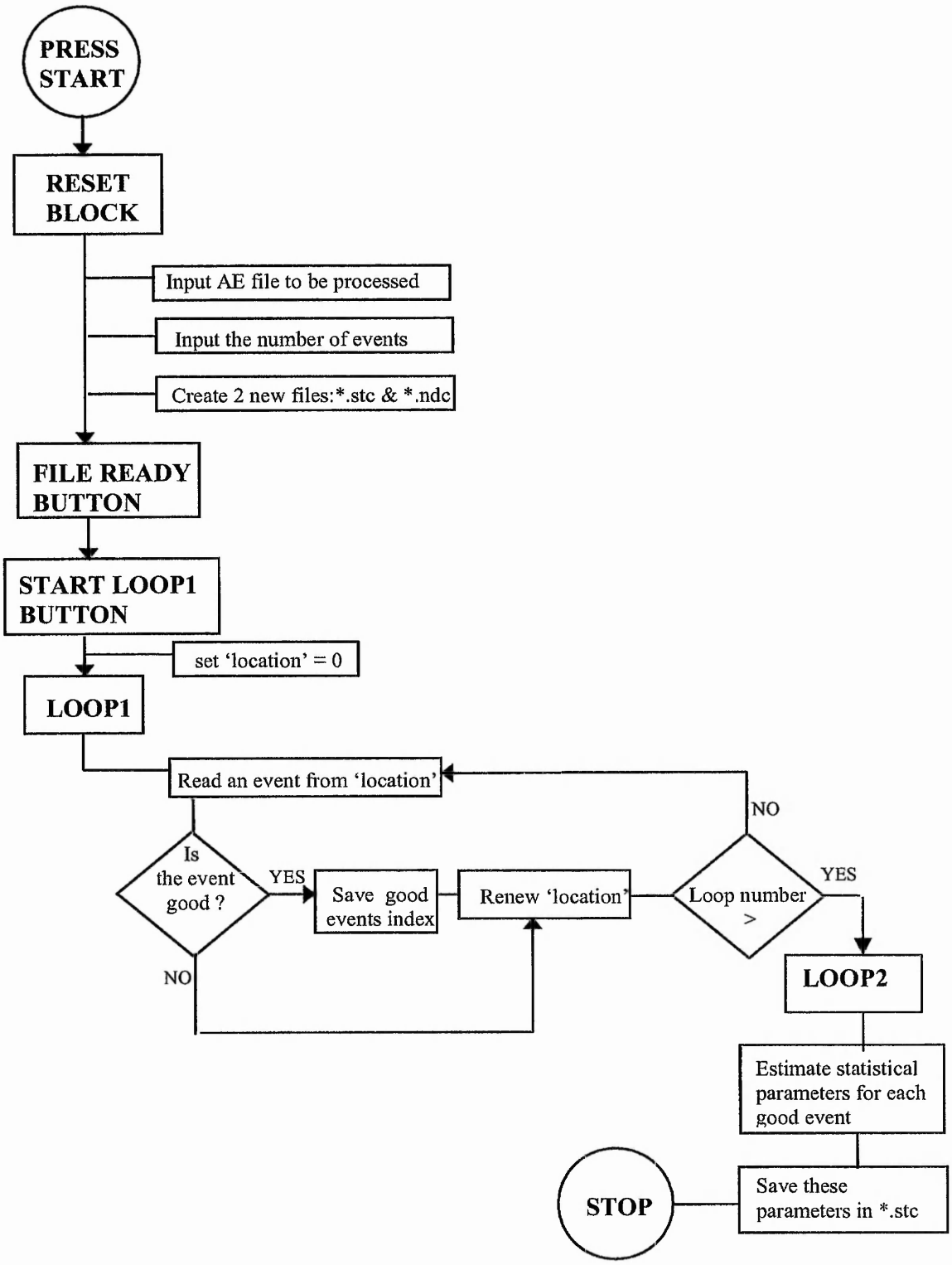


Figure 3.6 Viewdac sequence layout used to filter out bad events

# Chapter 4 –Wave Guides and Lamb Waves

## 4.1 Instrumentation Design Philosophy

In the previous chapter the instrumentation components and their function were described. This section discusses in detail the generation of emissions in the soil and how according to the monitoring system these propagate through the wave guide to the sensor. The expected type of waves (or signals) propagating through the wave guide are outlined. The types of waves the operator is able to capture given the selected instrumentation components are also considered.

## 4.2 Soil and wave guide interaction

The main function of any wave guide system is to guide the signal from the source to the sensor.

In assessment of slope instability it is preferable to install the wave guide at a location and depth where it passes through the slip surface of the slope being monitored. However, this is not always achievable as the location of the slip surface is not known and it is usually necessary to install a number of wave guides to ensure some wave guides intersect with the slip surface (see Figure 4.1). Even if the wave guide is not intersecting with the slip surface is still possible to capture AE emissions due to the internal shearing of slide mass of non-circular slip surface.

There are two models of wave guides that could be used for slope monitoring: the passive and active wave guide. In the passive wave guide model the noise is generated in the soil and propagates through the soil mass before it reaches the wave guide. This signal is known to suffer high attenuation while propagating through the soil. In the active wave guide model the noise is generated as a result of the interaction between the wave guide and the material surrounding the wave guide with the driving force being the slope movement. This model does not suffer as much attenuation as the passive model and this is the main reason that it is preferred. The material surrounding the wave

guide can be sand, gravel, grout or even bentonite clay. In this study sand and gravel were used to surround the wave guide. Both gravel and sand are referred to in this work as backfill material.

## 4.3 AE signals propagating in wave guides

The wave guide, which is used in this study, is a 60 mm diameter steel tube of 6 mm thickness wall. The types of waves that can propagate in this structure are very similar to those that can propagate in a steel plate. The description of these types of waves and their characteristics are presented below.

It is common at normal ultrasonic testing frequencies for elastic vibrations to propagate in thin plates in a manner distinctly different from simple bulk longitudinal or shear waves. In flat plates and in tubes ultrasound propagates in the form of Lamb waves. Lamb waves are surface waves and in most of the literature are described in conjunction with Rayleigh waves which are surface waves in solids. The Rayleigh waves, are effectively limited to a stratum extending approximately to a wavelength below the surface, and on decreasing the thickness of the solid a stage will be reached, on becoming a plate, when the Rayleigh surface waves can no longer exist since their wavelengths will exceed the plate thickness. Various forms of plate waves are possible. One form of waves, are the Lamb waves. These resemble Rayleigh waves.

Lamb waves theoretically can be generated and vibrate a plate in an infinite number of modes. These modes are grouped into two main types according to the direction of particle displacement : symmetrical ($L_{11}$, $L_{12}$) and asymmetrical ($L_{21}$, $L_{22}$). These two types of Lamb waves can be seen in Figure 4.2 after Maji *et al.* (1997). The various modes in each type, travel with a velocity that is dependent upon the thickness of the plate, the frequency of the wave and the material of the propagating path. The frequency and thickness dependence of the different modes is illustrated in Figure 4.3 after Bray *et al.* (1989) which shows the group velocities for the different modes from Lamb's equation in steel. The modes are also generally dispersive, which means that the shape

of a propagating wave changes with distance along the propagation path. It can be seen that at any given frequency there are at least two modes of Lamb waves. Considering wave propagation along pipes, it is found that their behaviour is more complicated than in plates. In pipes three classes of modes are recognised. The modes include a family of axially symmetric and non-axially symmetric motion of the pipe wall, as would be expected from an understanding of Lamb modes if the pipe was considered simply as a curved plate (Lowe *et al.*, 1998). In cylindrical systems, the waves propagate around the circumference, and there may be an integer (n) number of wavelengths around the circumference until they are received by the AE sensor. When n = 0 the system is axially symmetric. The axially symmetric types can be subdivided into Longitudinal modes $L(0,m)$ (m = 1,2,3,...) and torsional modes $T(0,m)$ (m =1,2,3,..). When n > 0 the propagating waves have components in both the circumferential and axial directions where non-axially symmetric flexural modes exist $F(n,m)$ (m = 1,2,3,..). These Lamb wave characteristics and modes of the cylindrical system make the signal interpretation difficult.

However, cylindrical Lamb waves are preferable in AE monitoring due to their ability to propagate over considerably longer distances than bulk waves, and with little attenuation. Bulk waves are three dimensional and will radiate energy three dimensionally which means that when excited from a point source their amplitude decreases inversely as a function of distance squared. In contrast, since cylindrical Lamb waves in pipes are guided along the pipe, no lateral spreading occurs and the propagation is essentially one dimensional. As the wave propagates, the different frequencies disperse and propagate at different velocities. These two characteristics of Lamb waves can be used for this research since a low attenuation wave guide system which can detect a source occurring at a long distance from the sensor is required. Secondly there is the potential for Lamb waves to be used to locate the source within a reasonable error by identifying modes with different velocities, and hence by the difference in their arrival times.

## 4.4 Instrumentation and Lamb wave modes

The instrumentation components used in the present study (i.e. 30 kHz resonant transducer and 6 mm thickness steel tube) provide the possibility of capturing a signal consisting of two Lamb wave modes $a_0$ and $S_0$ (see Figure 4.4) which are within the predominant signal frequency monitored (signal consists of waves within a frequency window 15-45 kHz). At this stage it must be noted that for simplicity reasons the steel tube has been studied considering it as a curved plate. The mode $S_0$ arrives first at the sensor based on a velocity of around 5500 m/sec, and then the $a_0$ mode follows with a velocity of around 3050 m/sec. As it can be seen these two modes have distinctly different velocities which enables the location of the source by considering the difference of their arrival times in the same event. These, can be captured by a single transducer. However, the challenge is to identify each mode. Careful signal analysis is required in order to identify the Lamb modes which are of interest and to isolate them by filtering the original captured signal.

## 4.5 Source Location

Laboratory work has been undertaken in order to investigate the wave guide response, and to estimate the source location from observing the histogram (waveform in time domain) records.

In this study two 1.63 metre sections of 6 mm wall thickness and 60 mm diameter steel tubes were used. The two sections were connected by a steel threaded collar of 50 mm in length. The whole wave guide body (two sections with the collar) was lifted from the ground and supported by three wooden supports (see Figure 4.5). This way a free surface all the way around the wave guide was provided and floor vibrations did not interfere with the AE generated by the pencil lead breaks which ware of interest. The 0.3 mm pencil lead of 3 mm length breaking at a constant angle, was used to generate a consistent reproducible event. The breaking took place at five different locations, of 0.36 m, 0.54 m, 0.72 m, 0.90 m, and 1.08 m distance away from the sensor. At each position ten pencil lead breaks were carried out.

The signals were sensed and processed by the instrumentation described in chapter 3. The main amplifier (AET 204GR) was set up to 50 dB and the total ring down counts of the signal were measured. The total amplification of the signal was 90dB (40dB pre-amplifier plus 50dB main amplifier). The DAS50 board was set to capture a stream of 400 data including 50 pre-trigger points at a frequency of 236842 Hz. The trigger was set to activate on a rising voltage (positive triggering) going through a set threshold value of 0.04 Volt. Samples of recorded signal (400 data, with a duration of 1.69ms) are shown in Figures 4.6, 4.7, 4.8, 4.9 and 4.10. These figures show the first 400 recorded data of the lead breaking signal arriving at the sensor, which was placed at position A (0.20 m away from the nearest wave guide edge Figure 4.5). The signals generated at a distance of 0.36, 0.54, 0.72, 0.90 and 1.08 m from the sensor, are indicated by the numbers 1, 2, 3, 4, 5 respectively.

Analysis was focused only on the first part of each captured event. The reason being to identify the first two fastest modes and not complicate the study with other flexural modes which travel around the circumference $n > 0$ (integer) times. The time between the triggered point and the first peak was plotted on a graph with respect to the distance between source and sensor. The triggered point was usually coincident with the compressive S0 Lamb wave arrival to the sensor, which has low amplitude. The first peak is the peak of the shear Lamb wave that travels with smaller velocity than the compressive wave but has a significantly larger amplitude. At each distance ten values of arrival time were plotted for the first peak from different pencil lead break records. Figure 4.11 shows a linear relationship between propagating distance and arrival times of the first peak. This is an indication of a constant velocity difference between the fastest mode, which triggers the DAS-board, and the flexural mode, which arrives with higher amplitude. In Figure 4.12 the same plot was applied but the transducer was moved further away from the edge of the wave guide to position B. This was to ensure that signal reflections from the wave guide edge would not be included in the waveform. It can be seen that the slope of the line is very similar to that of the slope in Figure 4.11. This certifies that there is no interference of reflections in the first part of the waveform section that is under investigation and that the results are consistent.

A spreadsheet in excel was also prepared to clarify the above results which are based on the appropriate Lamb wave modes to be captured. In this sheet the theoretical arrival times of the shear wave were calculated and compared with the actual histograms obtained from the pencil lead breaks. The shear wave mode travels once around the tube circumference for mode 1 twice for mode 2 and so on. For sixteen loops of this wave the arrival time was calculated and compared with the experimental arrival times of distinguished pulses in the captured events. The propagating distance was calculated by using the following formula:

$$S_n = [(hxN)^2 + a^2]^{0.5} \qquad (4.1)$$

Where n= no of loops

h= tube circumference

a= source-sensor distance

The velocity of the shear wave when propagating through a 6mm steel plate is 3040m/sec. (see Figure 4.4). The compressive wave velocity also is known to be 5500m/sec. Having the propagating length and the velocity of the wave the corresponding arrival times are estimated and presented in Tables 4.1, 4.2 and 4.3 for source-sensor distances 0.36 , 0.54 and 0.72 respectively. In all the three tables it can be seen that not all modes are available in the experimental results column which are assigned by N/A. However, this doesn't mean that these modes do not exist in the captured event. It was not easy to distinguish in the produced histograms the starting point of a mode, which usually was masked under the proceeded modes. It can also been seen that the experimental arrival times are very close to the estimated arrival times.

## 4.6 Summary

The results of the above tests showed that it is possible to locate the AE source by using one transducer only. The recognition of the two fastest Lamb wave modes can be achieved hence the difference in their arrival times and the location of the source could be measured. However, it has to be noted that the above findings are applicable for

propagating distances of 1.6 m long. At full-scale system might require several metres, and in some cases many tens of metres, of wave guide to reach the slip surface. Therefore, further studies are required to investigate if the particular modes used in this study for source location suffer high attenuation and distortion while propagating longer distances and through multiple connections.

| n (loops) | Propagating Distance (m) | Δt (sec) | Theoretical Arrival time | | Experimental Arrival time |
|---|---|---|---|---|---|
| 0 | 3.600E-01 | | (sec) | Viewdac units (sec x frequency) | Viewdac units (sec x frequency) |
| 1 | 4.064E-01 | 1.885E-05 | 1.540E-04 | 3.647E+01 | N/A |
| 2 | 5.213E-01 | 6.558E-05 | 2.007E-04 | 4.753E+01 | 4.423E+01 |
| 3 | 6.704E-01 | 1.262E-04 | 2.613E-04 | 6.189E+01 | 6.154E+01 |
| 4 | 8.355E-01 | 1.934E-04 | 3.285E-04 | 7.780E+01 | N/A |
| 5 | 1.009E+00 | 2.639E-04 | 3.990E-04 | 9.450E+01 | 9.423E+01 |
| 6 | 1.187E+00 | 3.363E-04 | 4.714E-04 | 1.116E+02 | 1.115E+02 |
| 7 | 1.368E+00 | 4.098E-04 | 5.449E-04 | 1.291E+02 | N/A |
| 8 | 1.550E+00 | 4.841E-04 | 6.192E-04 | 1.466E+02 | N/A |
| 9 | 1.734E+00 | 5.589E-04 | 6.940E-04 | 1.644E+02 | N/A |
| 10 | 1.919E+00 | 6.340E-04 | 7.691E-04 | 1.822E+02 | 1.808E+02 |
| 11 | 2.104E+00 | 7.094E-04 | 8.445E-04 | 2.000E+02 | N/A |
| 12 | 2.290E+00 | 7.850E-04 | 9.202E-04 | 2.179E+02 | N/A |
| 13 | 2.477E+00 | 8.608E-04 | 9.959E-04 | 2.359E+02 | N/A |
| 14 | 2.663E+00 | 9.367E-04 | 1.072E-03 | 2.539E+02 | 2.538E+02 |
| 15 | 2.850E+00 | 1.013E-03 | 1.148E-03 | 2.719E+02 | N/A |
| 16 | 3.037E+00 | 1.089E-03 | 1.224E-03 | 2.899E+02 | N/A |

Table 4.1 Comparison of theoretical and experimental arrival times for PLB events for 0.36 m source-sensor distance.

| n (loops) | Propagating Distance (m) | Δt (sec) | Theoretical Arrival time | | Experimental Arrival time |
|---|---|---|---|---|---|
| 0 | 5.400E-01 | | (sec) | Viewdac units (sec x frequency) | Viewdac units (sec x frequency) |
| 1 | 5.720E-01 | 1.299E-05 | 1.481E-04 | 3.508E+01 | N/A |
| 2 | 6.586E-01 | 4.822E-05 | 1.833E-04 | 4.342E+01 | 4.231E+01 |
| 3 | 7.819E-01 | 9.838E-05 | 2.335E-04 | 5.530E+01 | 6.154E+01 |
| 4 | 9.274E-01 | 1.575E-04 | 2.927E-04 | 6.931E+01 | N/A |
| 5 | 1.086E+00 | 2.221E-04 | 3.572E-04 | 8.461E+01 | 8.462E+01 |
| 6 | 1.253E+00 | 2.901E-04 | 4.252E-04 | 1.007E+02 | N/A |
| 7 | 1.426E+00 | 3.602E-04 | 4.953E-04 | 1.173E+02 | N/A |
| 8 | 1.602E+00 | 4.318E-04 | 5.669E-04 | 1.343E+02 | N/A |
| 9 | 1.780E+00 | 5.044E-04 | 6.395E-04 | 1.515E+02 | 1.481E+02 |
| 10 | 1.961E+00 | 5.778E-04 | 7.129E-04 | 1.688E+02 | N/A |
| 11 | 2.143E+00 | 6.517E-04 | 7.868E-04 | 1.864E+02 | N/A |
| 12 | 2.326E+00 | 7.261E-04 | 8.612E-04 | 2.040E+02 | 2.038E+02 |
| 13 | 2.509E+00 | 8.008E-04 | 9.359E-04 | 2.217E+02 | 2.212E+02 |
| 14 | 2.694E+00 | 8.758E-04 | 1.011E-03 | 2.394E+02 | 2.423E+02 |
| 15 | 2.879E+00 | 9.510E-04 | 1.086E-03 | 2.572E+02 | N/A |
| 16 | 3.064E+00 | 1.026E-03 | 1.162E-03 | 2.751E+02 | N/A |

Table 4.2 Comparison of theoretical and experimental arrival times for PLB events for 0.54 m source-sensor distance.

| n (loops) | Propagating Distance (m) | Δt (sec) | Theoretical Arrival time | | Experimental Arrival time |
|---|---|---|---|---|---|
| 0 | 7.200E-01 | | (sec) | Viewdac units (sec x frequency) | Viewdac units (sec x frequency) |
| 1 | 7.443E-01 | 9.868E-06 | 1.492E-04 | 3.534E+01 | N/A |
| 2 | 8.127E-01 | 3.771E-05 | 1.770E-04 | 4.193E+01 | 4.038E+01 |
| 3 | 9.155E-01 | 7.951E-05 | 2.188E-04 | 5.183E+01 | N/A |
| 4 | 1.043E+00 | 1.312E-04 | 2.705E-04 | 6.407E+01 | 6.346E+01 |
| 5 | 1.186E+00 | 1.895E-04 | 3.289E-04 | 7.789E+01 | N/A |
| 6 | 1.341E+00 | 2.524E-04 | 3.918E-04 | 9.278E+01 | N/A |
| 7 | 1.503E+00 | 3.185E-04 | 4.578E-04 | 1.084E+02 | 1.077E+02 |
| 8 | 1.671E+00 | 3.868E-04 | 5.261E-04 | 1.246E+02 | N/A |
| 9 | 1.843E+00 | 4.567E-04 | 5.960E-04 | 1.412E+02 | 1.346E+02 |
| 10 | 2.018E+00 | 5.278E-04 | 6.671E-04 | 1.580E+02 | 1.577E+02 |
| 11 | 2.195E+00 | 5.998E-04 | 7.391E-04 | 1.751E+02 | N/A |
| 12 | 2.374E+00 | 6.725E-04 | 8.119E-04 | 1.923E+02 | 1.904E+02 |
| 13 | 2.554E+00 | 7.458E-04 | 8.852E-04 | 2.096E+02 | 2.077E+02 |
| 14 | 2.735E+00 | 8.196E-04 | 9.589E-04 | 2.271E+02 | N/A |
| 15 | 2.918E+00 | 8.937E-04 | 1.033E-03 | 2.447E+02 | 2.423E+02 |
| 16 | 3.101E+00 | 9.682E-04 | 1.107E-03 | 2.623E+02 | 2.615E+02 |

Table 4.3 Comparison of theoretical and experimental arrival times for PLB events for 0.72 m source-sensor distance.

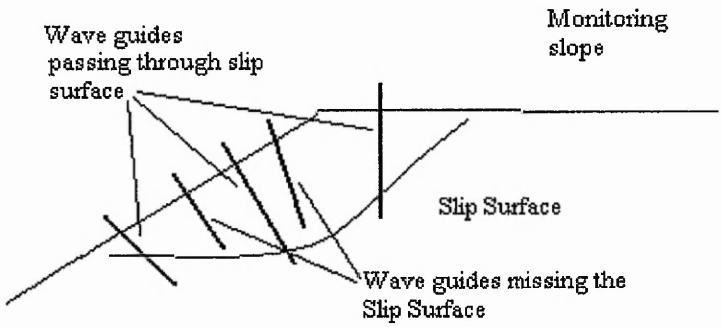


Figure 4.1 Group of wave guides monitoring an active slope.

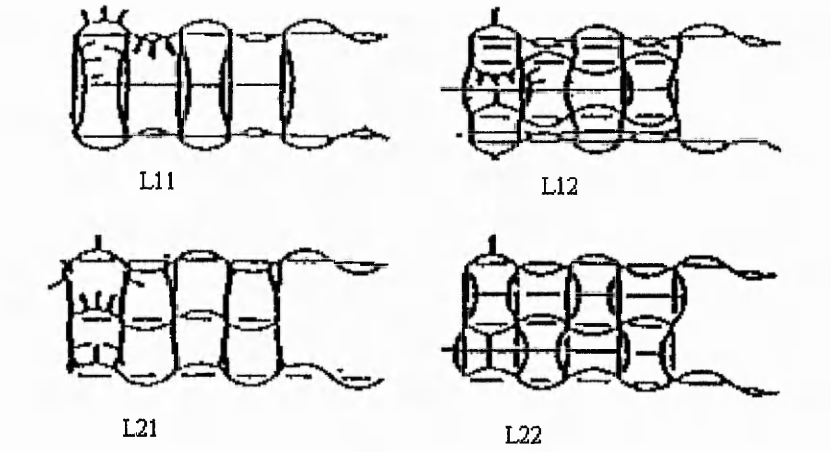


Figure 4.2 Lamb wave mode shapes after Maji *et al.* (1997).

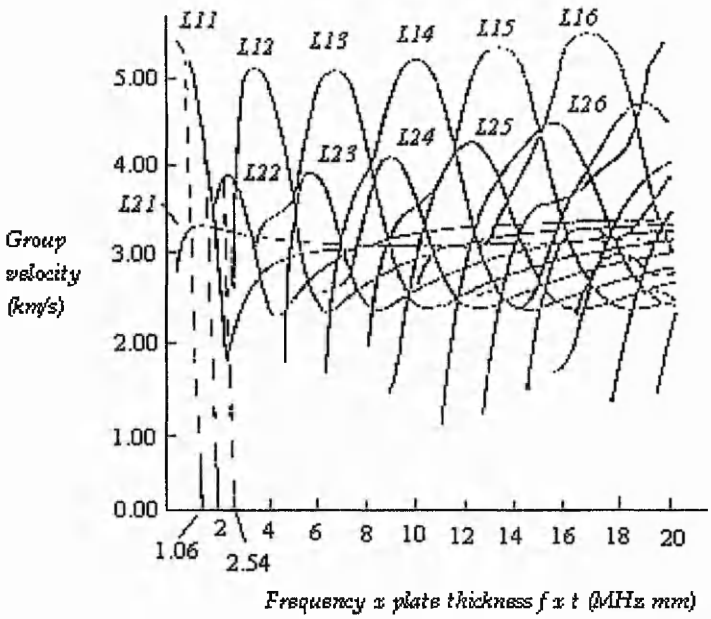


Figure 4.3 Variation of Group velocities and modes after Bray *et al.* (1989)

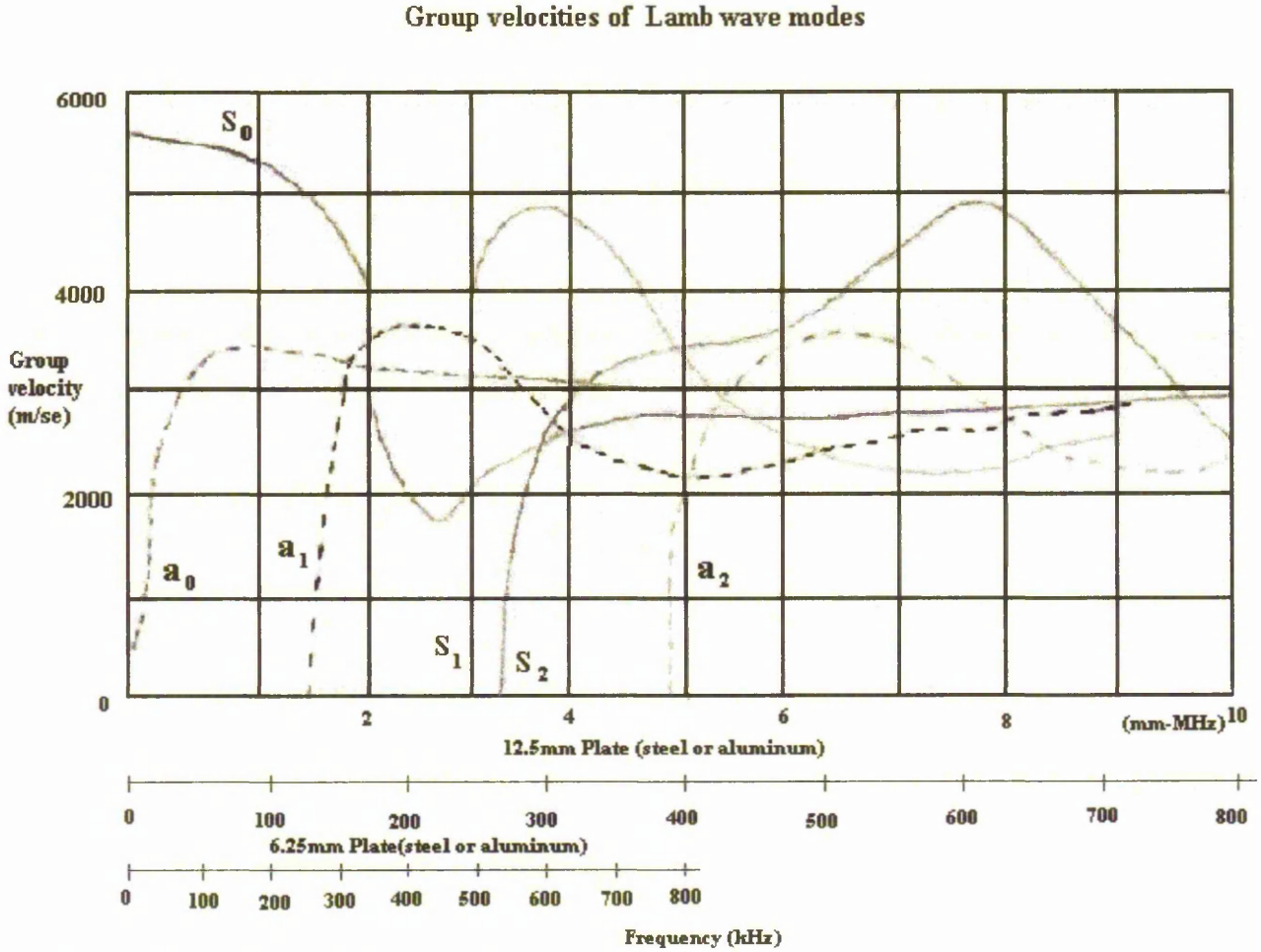


Figure 4.4 Frequency dependence of the different Lamb wave modes after Dunegan Engineering Consultants Inc

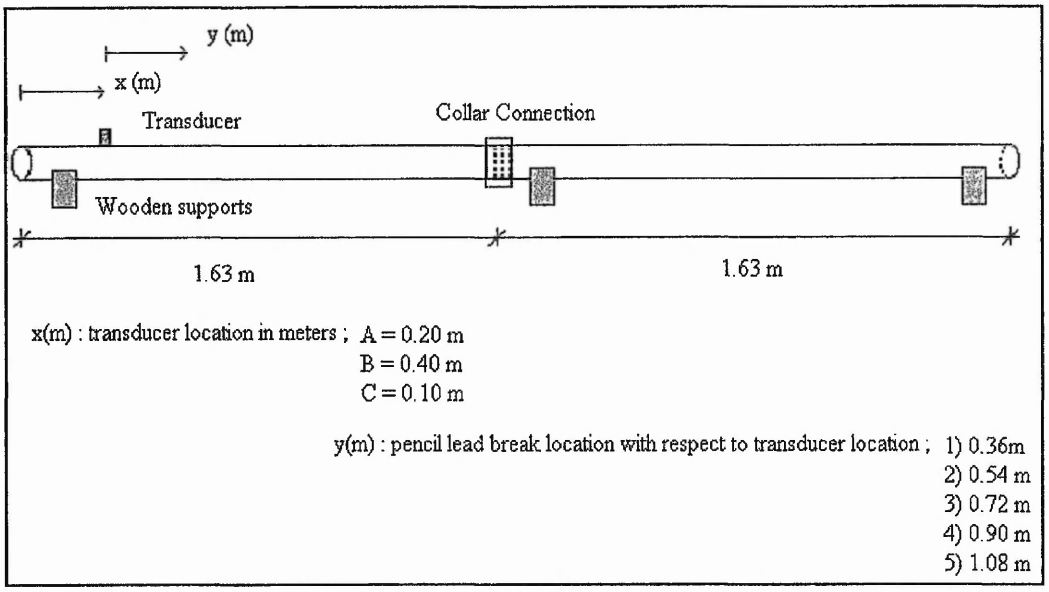


Figure 4.5 Experimental set up for source location investigation

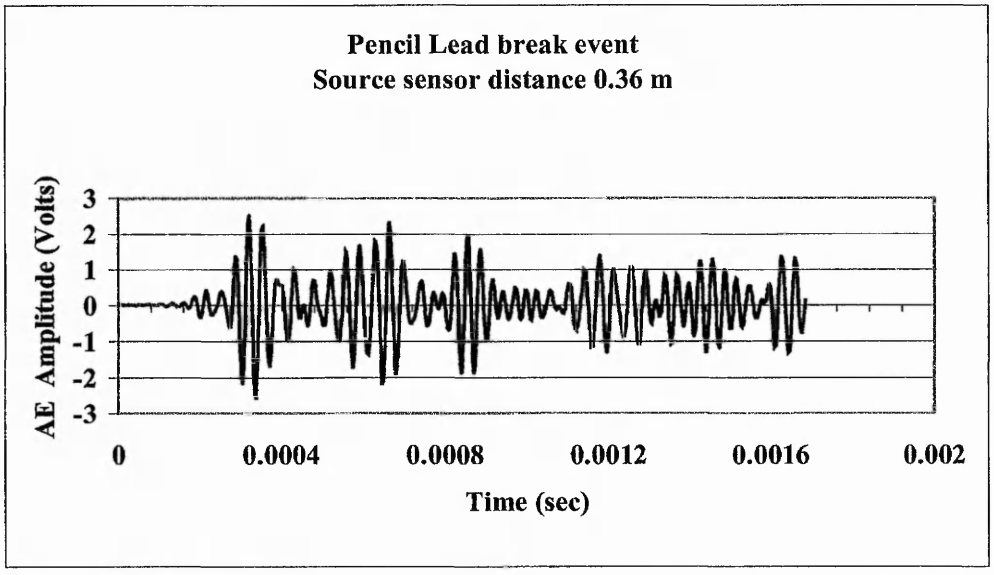


Figure 4.6 Pencil lead break event histogram, source sensor distance 0.36m trasducer position A

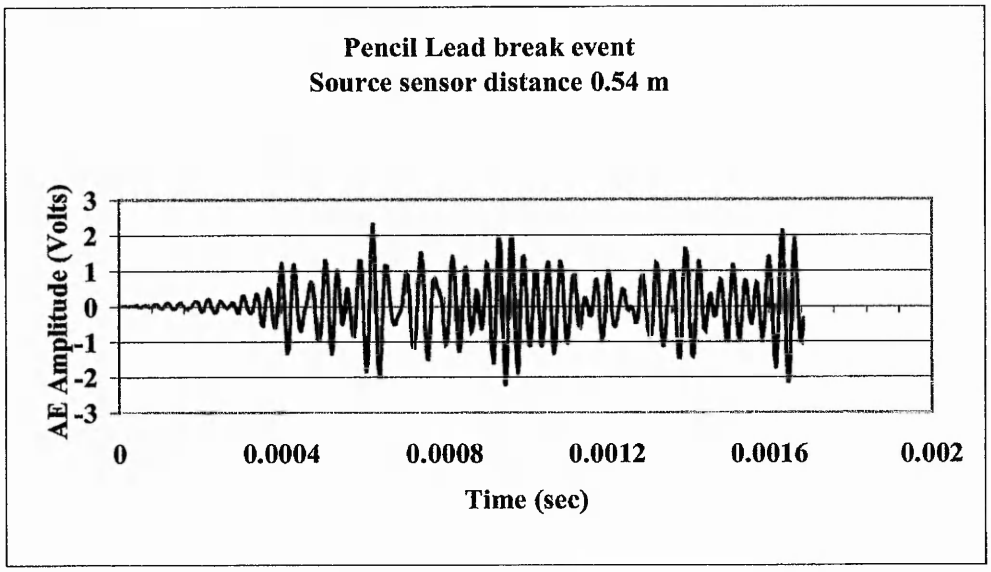


Figure 4.7 Pencil lead break event histogram, source sensor distance 0.54m trasducer position A

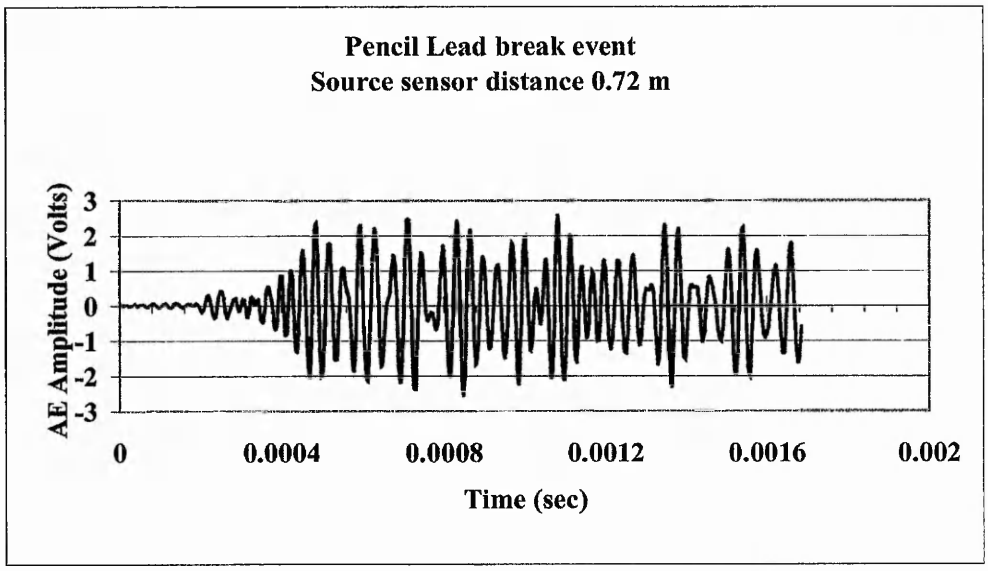


Figure 4.8 Pencil lead break event histogram, source sensor distance 0.72m trasducer position A

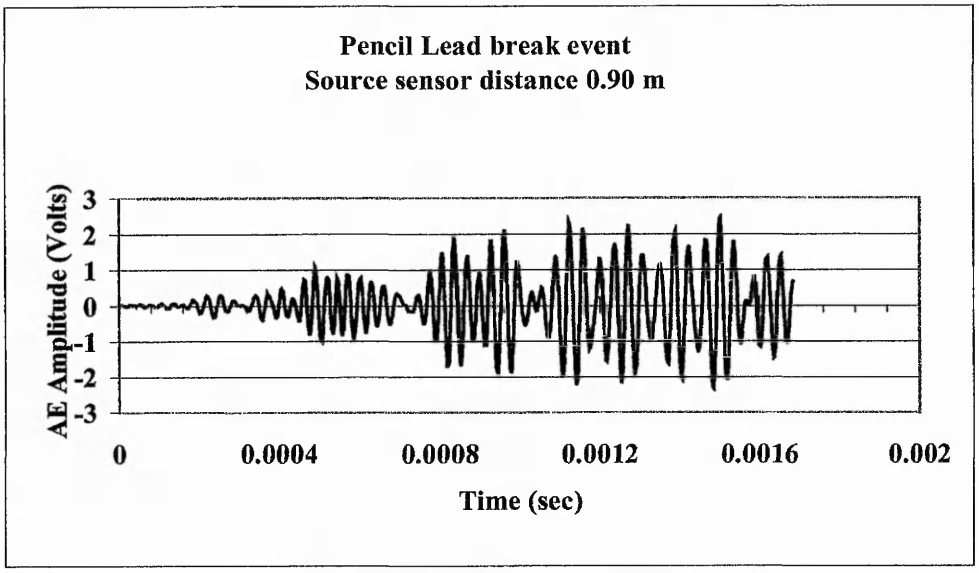


Figure 4.9 Pencil lead break event histogram, source sensor distance 0.90m trasducer position A

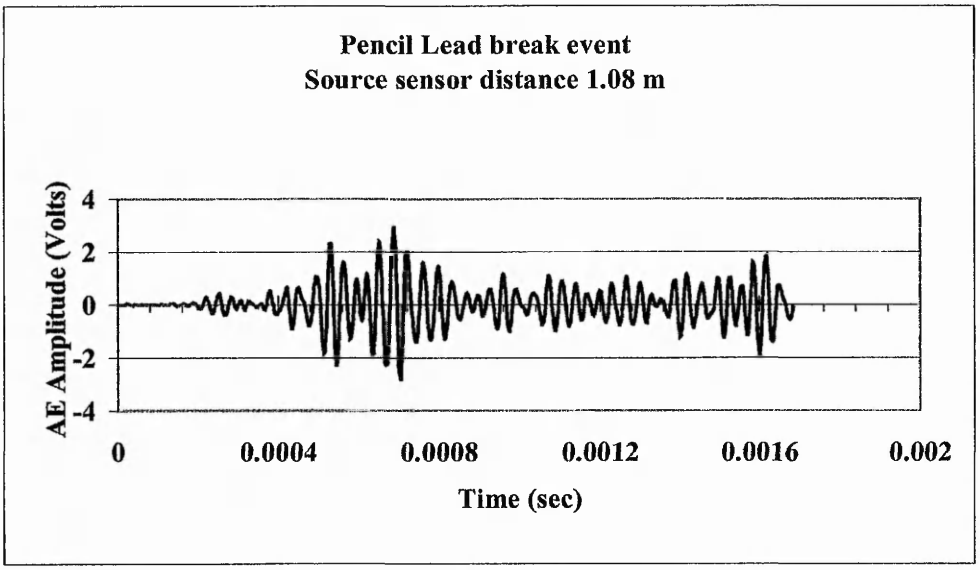


Figure 4.10 Pencil lead break event histogram, source sensor distance 1.08m, trasducer position A

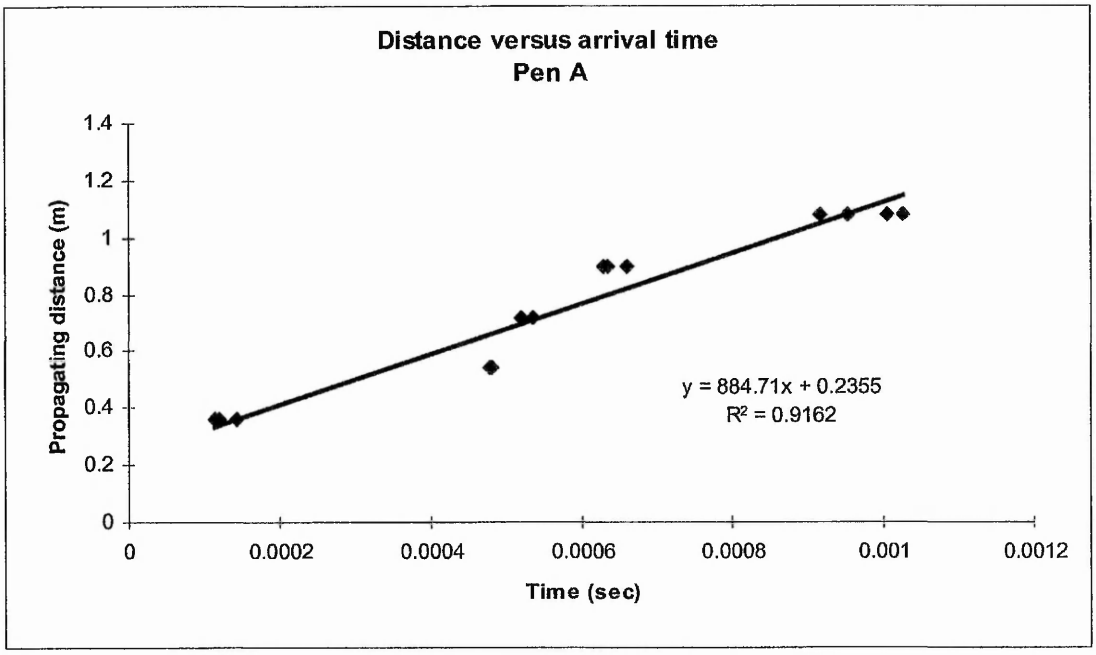


Figure 4.11 Propagating PLB distance with respect to time difference between triggered point and first peak of the shear wave. Transducer loc:A.

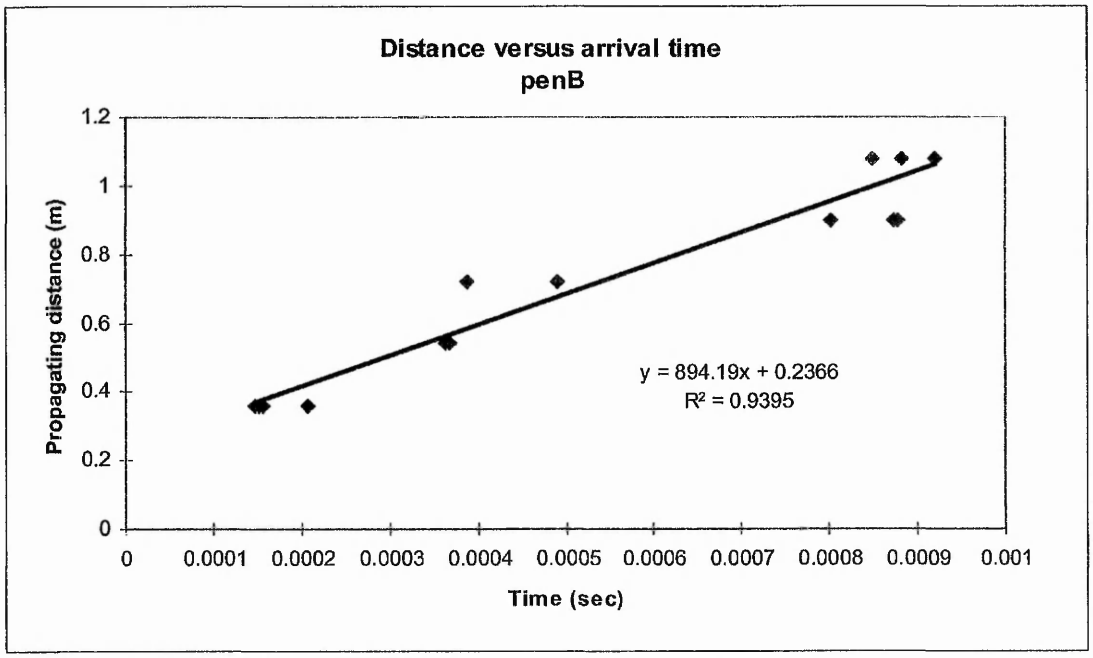


Figure 4.12 Propagating PLB distance with respect to time difference between triggered point and first peak of the shear wave. Transducer loc:B.

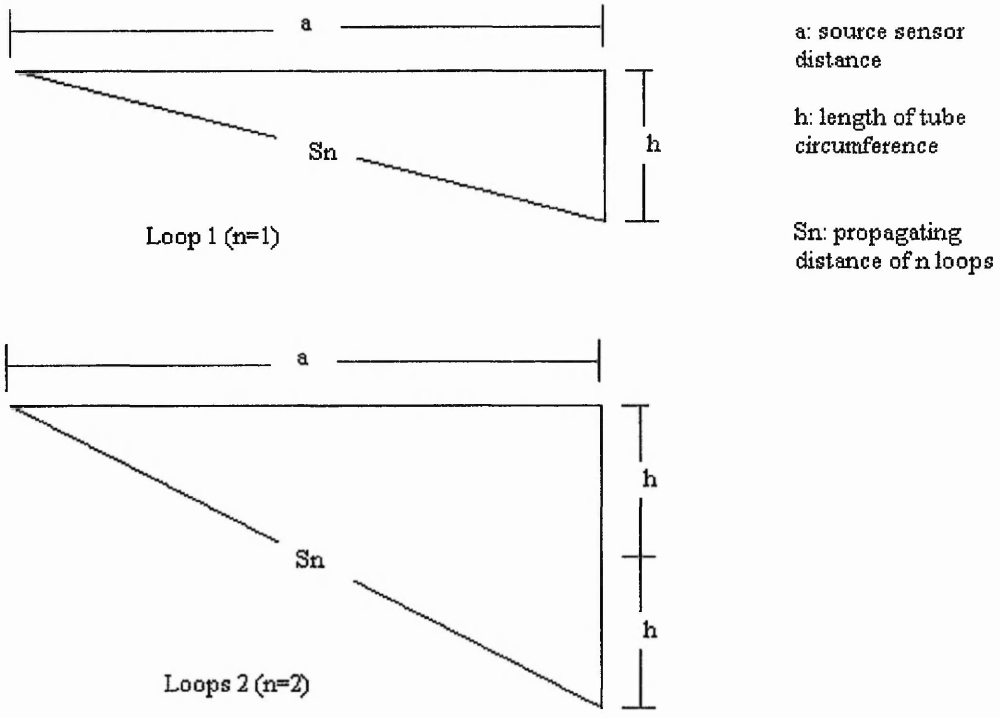


Figure 4.13 Propagating distance graphic presentation of wave travelling around the tube circumference.

# Chapter 5 - Factors Controlling AE Wave Guide Design

## 5.1 Introduction

The Acoustic Emission monitoring technique has the advantage that is sensitive enough to detect the slightest movement of the soil particles surrounding the wave guide and due to this ability provide an early warning system. However, due to the same sensitivity the captured signal depends on the dynamic properties of the monitoring system which can be grouped into two categories:

a) Soil properties of both the soil annulus around the wave guide and the monitoring mass (i.e. moisture content, soil plasticity, grain shape and size, soil density).

b) Material properties and dimensions of the wave guide (i.e. material type, elastic modulus, Poisson ratio, wall thickness, diameter, connections).

Figure 5.1 illustrates these factors graphically. It is well known that every field site is individual. Parameters such as, the type of soil, soil strata, particle grading, moisture content, and water level, differ radically from one site to another. The AE signal is modified by these parameters and the signal response will be different accordingly. In order to quantify the AE monitoring system it is necessary to investigate the effect of each parameter separately. However, while this is scientifically sound, it would be time consuming and not feasible or sensible to do in every case. The high sensitivity of the AE system means that it is not simple to quantify the effect of each parameter on the signal. The high variability of the surrounding in situ soil is of particular concern.

To overcome a lengthy, costly and complex procedure the backfill soil is introduced. The primary purpose of the backfill soil is to introduce a soil with known properties to improve the contact surface between the host soil and the wave guide and to aid interpretation of the results. In an active wave guide systems however, the AE signal is

generated and captured due to the frictional movement between the backfill soil and the steel wave guide tube. Hence, the investigation of each parameter of the host soil one by one is not necessary and instead the investigation can concentrate on to the physical properties of the homogenous annulus of backfill soil. The investigation of the backfill soil properties influencing the AE signal characteristics is discussed extensively in chapter 6 of this thesis.

Background noise is another factor that influences the AE signal. Background noise can be a low frequency noise generated by traffic close to the monitoring area or the noise of an airplane flying over the area. Using high frequency transducers however can eliminate this factor. As it stated in the previous chapters the monitoring system employed in this study uses a 30kHz narrow band transducer. This frequency is high enough so the low frequency background noise is not included in the captured signal.

As the signal propagates through the wave guide, the geometry, dimensions and material type of the wave guide influence the AE signal significantly. This chapter presents laboratory tests and results, which illustrate how each parameter of the wave guide structure in isolation affects the AE signal.

## 5.2 Pencil Lead Breaks generate AE events along the wave guide

The aim of this study was to investigate propagation of AE through a steel tube wave guide. It was not suitable to use soil to generate the AE events, since soil particles generate multiple and non-consistent events depending on many parameters (i.e. soil properties). Hence at this stage it was necessary to generate a signal that is short in duration and "simple". The concept of "simple" signal is that this includes a small number of pulses that can be distinguished easily by the researcher.

Laboratory studies using pencil lead breaks generate a signal in the form of a Transient Step Force Function. The signal generated mainly consisted of one event with short duration and is reproducible and consistent. Therefore, this method was used in the laboratory for the generation of events used, to investigate the wave guide AE response.

### 5.2.1 "Contact shoe" effect

The transducer was attached on the external wall of the wave guide. The contact area between the cylindrical surface of the wave guide and the flat face of the piezoelectric transducer was of concern. Therefore, a small steel "contact shoe" was designed to enlarge the contact area between the wave guide and the sensor. A diagram of the cross section and plan dimensions of the contact shoe is illustrated in Figure 5.2.

Pencil lead breaks were carried out with and without the "contact shoe" at a distance of 0.41 m away from the sensor at location PLB1 shown in Figure 5.3. The recorded AE signals were compared in time and in frequency domain by using (FFT) Fast Fourier Transform equations. It was observed that the "contact shoe" changed the shape of the waveform and decreased the signal amplitude significantly. This can be seen clearly in Figure 5.4 where both signals without and with "contact shoe" are plotted on the same graph. The statistical analysis on the histograms indicated that the statistical mean of the signal amplitude was reduced by 79% when the "contact shoe" was used. The presence of the contact shoe introduced an additional body through which the AE signal had to propagate and an additional boundary at which signal reflections could occur. This resulted in a different shape of the recorded signal and to a different frequency response, as shown in Figure 5.5. It can be seen that both the high peaks appearing at 25 kHz and 35 kHz were significantly reduced when a contact shoe was used. It can be seen also that a third peak exists without the contact shoe which is not present for the contact shoe frequency response.

This study showed that the presence of the contact shoe complicated the recorded signal and did not offer any benefit to the operator of the AE instrumentation. Therefore, in order to avoid producing more complicated signals and suffering from high attenuation, in future studies the transducer was attached firmly and directly on the wave guide steel tube.

### 5.2.2 Collar Connection effect

The connection between the wave guide steel tube sections was achieved in the past (Kavanagh, 1997) by using a steel tube collar. The collar was 0.05 m long steel tube and was internally threaded (the same system was used in the studies described in chapter 4). The two externally threaded ends of the steel wave guide sections were screwed into the collar until the sections come into contact with each other at the centre of the connection as shown in Figure 5.6. This connection arrangement is simple and is easy to use on site. However, it must be ensured, that the two steel tube section ends are in good contact with each other in order the AE signal to propagate with minimal attenuation. The AE performance of the collar connection was investigated as discussed below.

The test set-up was identical to the one described in the previous test used for the contact shoe assessment in section 5.2.1. Once more pencil lead break events were used to generate the AE events. It was expected that there would be some energy loss for the signals propagating along the steel tube connecting collar. Hence, two locations shown in Figure 5.3 as PLB2, PLB3 were used to generate events. PLB2 is 0.80 m away from the sensor and is located just before the collar connection and PLB3 is located after the connection at 0.88 m away from the sensor. Comparison between the recorded AE events generated from the pencil lead breaks at the two locations PLB2 and PLB3 is shown in Figure 5.7 It can be seen that the connection reduced the amplitude of the AE signal by a significant amount (about 73%).

Viewing the frequency domain response it can be seen that the signals propagating through the connecting collar do not consist of high frequency waves between 40 and 45 kHz, or these waves might now have very low amplitude and hence do not appear (Figure 5.8). This high reduction in signal amplitude is a big disadvantage. Especially when carrying out field monitoring studies, where more than one connection will be needed so the wave guide could pass through deeper slip surfaces.

It is possible however, to use other types of connection as those mentioned in table 2.2 of chapter 2 (i.e. welding, brazing, clamping etc.). Hardy *et al.* (1992) indicated that the welded connection performed better with less signal attenuation. Hence, in the 5.2.3 an

investigation of the affect of the welded connection is presented and compared with that of the collar connection.

### 5.2.3 Welded connection affect

Two steel tube sections of the same 60 mm diameter and 6 mm wall thickness were welded together to investigate the AE response of the welded connection. The threaded parts at the end of each section were trimmed off before welding the sections together. Pencil lead breaks were carried out on the surface of the wave guide after the welded connection at 0.88 m distance away from the transducer to generate events. These captured signals were compared with those generated at location PLB3 on the previous tests while investigating the collar connection. The propagating distance in both tests is the same as well as the location of the transducer with respect to the edge of the wave guide.

Figures 5.9, 5.10, 5.11 show three histograms of pencil lead breaks carried out beyond the two types of connection at distance 0.88 m away from the transducer. It is interesting to see that the first part of the wave is similar for both connection types. Providing that there is a good contact interface between the two steel wave guide sections in the collar connection, it is expected that the first part of the signal arrive (i.e. the faster compressive Lamb wave mode) is similar fro the two types of connection. However, the rest of the event seems to be significantly different. For the welded connection the high amplitude shear wave that follows the first pulse seems to be unaffected. However, for the collar type connection it seems that the shear wave mode is not present. This was expected, as the shear wave could not propagate directly from one section to another whereas the compressive wave is able to do. The shear wave has to travel through the collar and back to the second section, which results in the high attenuation.

The welded connection improves the contact between two wave guide sections since the welded metal between the sections forms a solid continuous path between them and both compressive and shear wave modes propagate through the connection almost unaffected.

### 5.2.4 Attenuation coefficient along wave guide

In chapter 4 the source location study was presented by applying pencil lead breaks at five different locations along the wave guide. It was mentioned that the arrival time of the shear wave first peak was used to estimate location of the source. In this section the amplitude of this peak is assessed with regard to what degree this AE amplitude is attenuated with increasing propagating distance.

Figure 5.12 and Figure 5.13 show how the amplitude reduces with distance. It can be seen that the attenuation coefficient for when the transducer was placed at location A, which is 20cm away from one end of the tube, is 2.73 dB/m. However Figure 5.13 shows a higher attenuation coefficient of 5.15 dB/m when the transducer is place 40 cm away from the end of the wave guide to avoid end reflections. The reason for this difference in the attenuation coefficients is not obvious. It should be noted that the linear equation (trendline) plotted in both Figures is not accurate as the squared error tolerance is far form unity ($R_A$=0.32 and $R_B$=0.21). The PLB method provides a consistent event and was used successfully in previous studies. However, the degree of amplitude variation in the generated events is too large for use in an attenuation study. Further investigations need to be carried out using another method for generating an event with constant amplitude in order to estimate the attenuation coefficient of the wave guide accurately.

## 5.3 Wave guide AE response under deflection

The aim of this experiment was to investigate if there was any significant emission generated while the wave guide itself was deformed in bending.

In this study a section of 1.6 m long and 60 mm diameter (i.e. same as used in previous studies) steel tube was used. The tube was simply supported by two wooden blocks and loaded at its longitudinal centre by a point load. The load was applied by a manual hydraulic pump connected to a loading cylinder with a maximum capacity of 20 kN load. Readings of the applied load were obtained and the displacement measurements

were taken by a dial gauge fixed on solid steel plate extending as a cantilever from the loading point. The same AE instrumentation components were used as in the above experiments.

The program sequence responsible for the capture of emitted acoustic emission was called *"beam.seq"*. This program was written in Viewdac language and was set up to capture 1000 data including 100 pre-trigger points when the signal exceeded a threshold of 0.11 Volts. The signal was amplified before reaching the A-to-D board (DAS50) by 110dB (40dB pre-amplifier plus 70dB main amplifier: AET204GR). The captured signals were of insignificant amplitude in comparison with the signal obtained from soil particle movements around a wave guide (Figure 5.14). These results indicate that the wave guide system employed is sensitive to the movement of soil particle in contact with the steel tube but not to the deflection of the tube itself.

## 5.4 Summary

Pencil lead break is a useful tool for assessing AE performance and characteristics of a wave guide. It provides a consistent single event with short duration and is repeatable (although the amplitude of the event can show significant variation). The single reproducible event of the PLB make the assessment of different wave guide designs achievable.

The use of a contact shoe was expected to improve the propagation of the signal from the wave guide to the transducer. However this study showed that it attenuates the signal significantly and also changes its frequency consistence. In future tests the contact shoe will not be used.

Threaded connection does not affect the compressive fast mode of the signal but attenuates significantly the shear wave mode. Whereas welded connections allow both compressive and shear waves to propagate through without significant attenuation.

Wave guide bending deformation emits AE levels of such low magnitude that they are not of any concern. Soil particle movement generates distinctively higher AE levels.

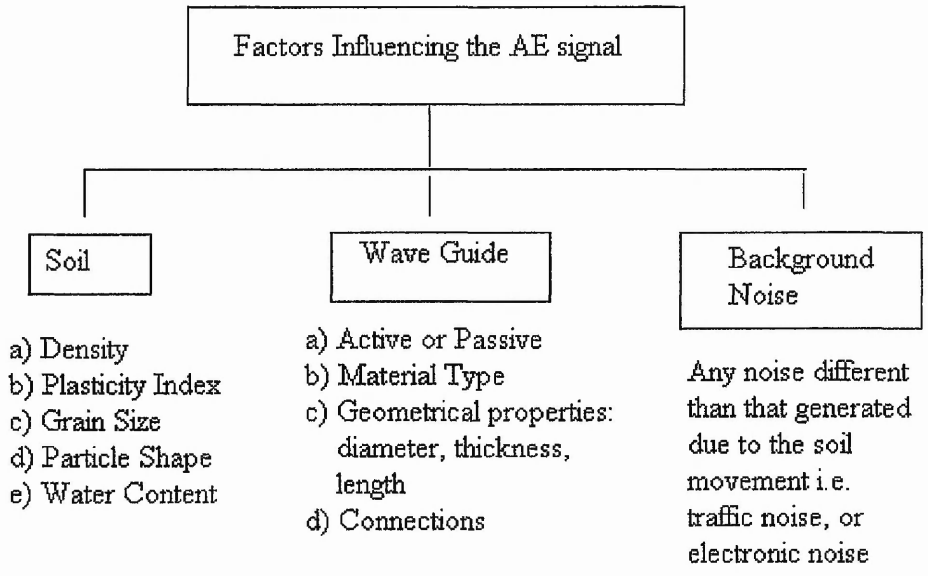


Figure 5.1 Factors Influencing the AE signal

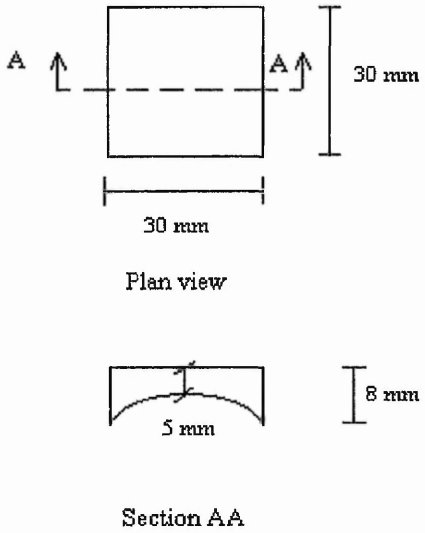


Figure 5.2 Contact shoe plan and section.

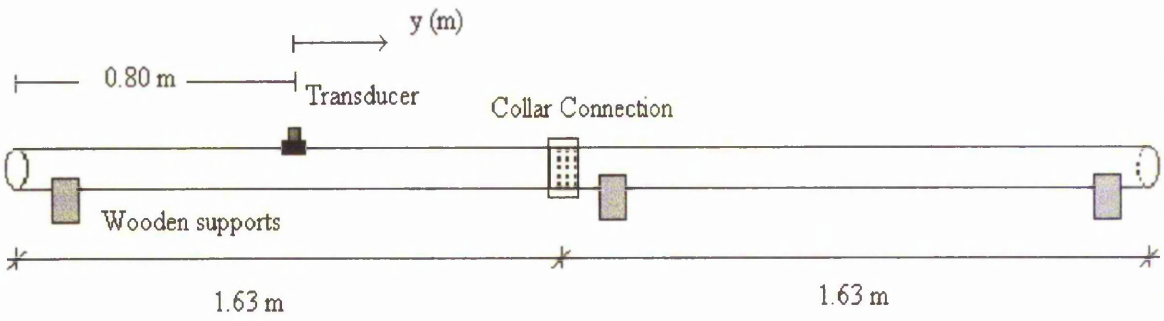


y(m) : pencil lead break location with respect to transducer location ; PLB1 = 0.41 m
PLB2 = 0.80 m
PLB3 = 0.88 m

Figure 5.3 Experimental set-up investigating contact shoe signal effect generated by pencil lead breaks.

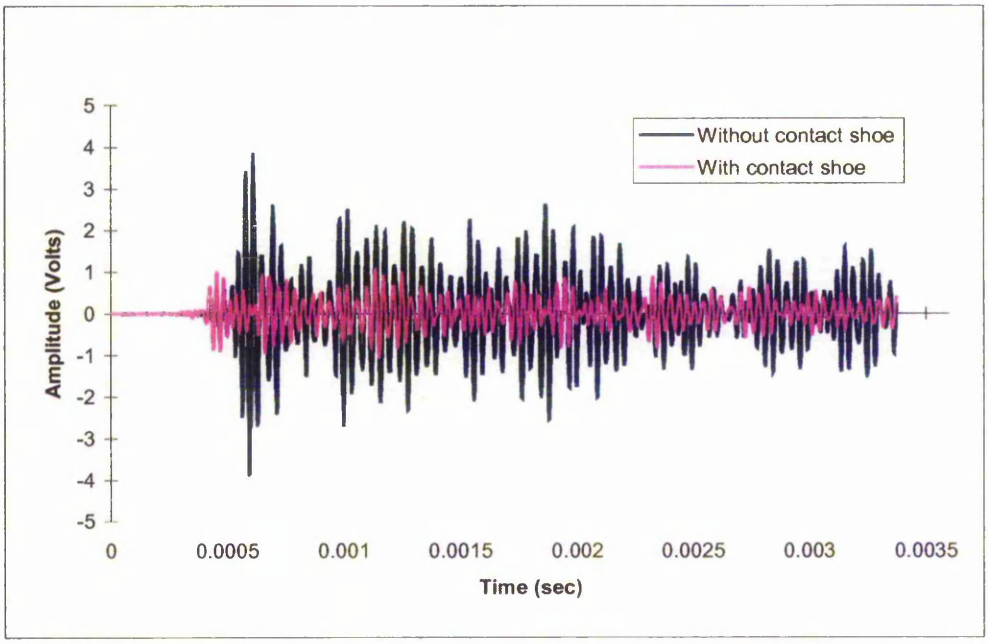


Figure 5.4 AE amplitude effect with and without contact shoe

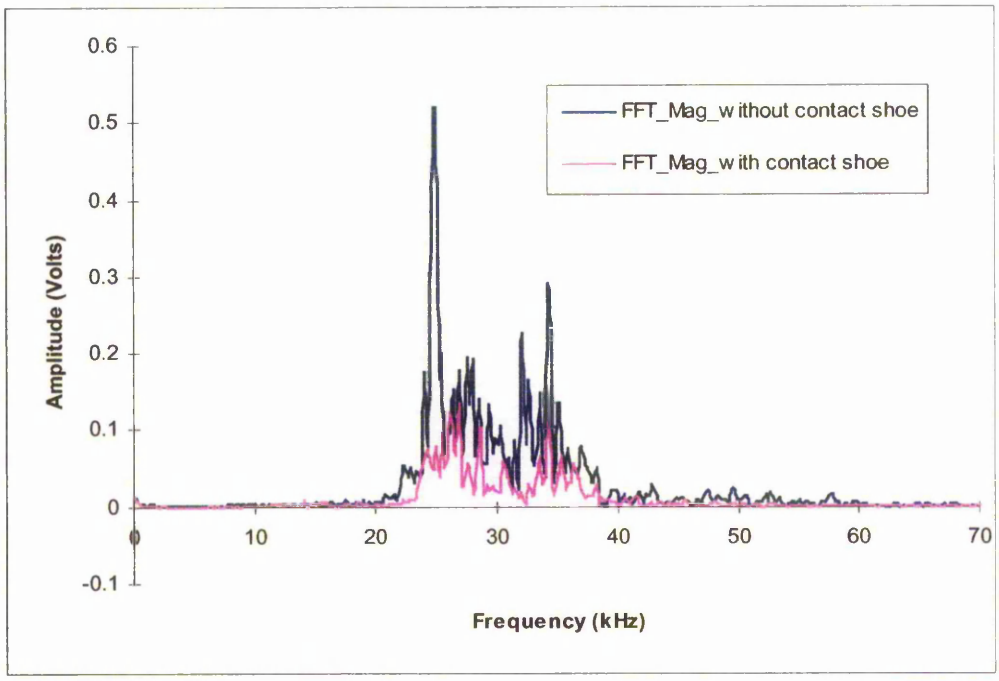


Figure 5.5 AE frequency effect with and without contact shoe

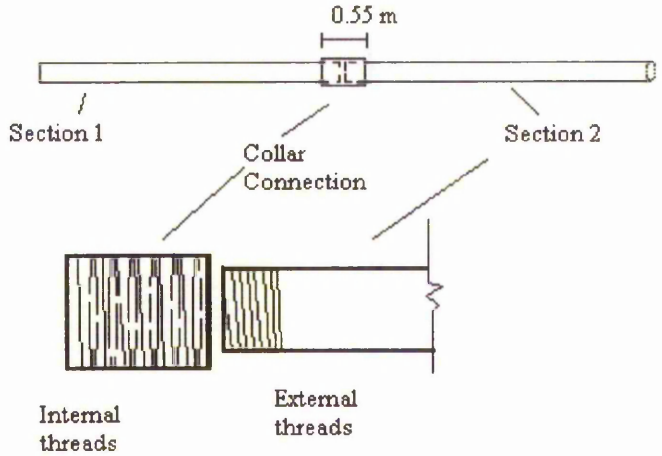


Figure 5.6 Collar connection arrangement

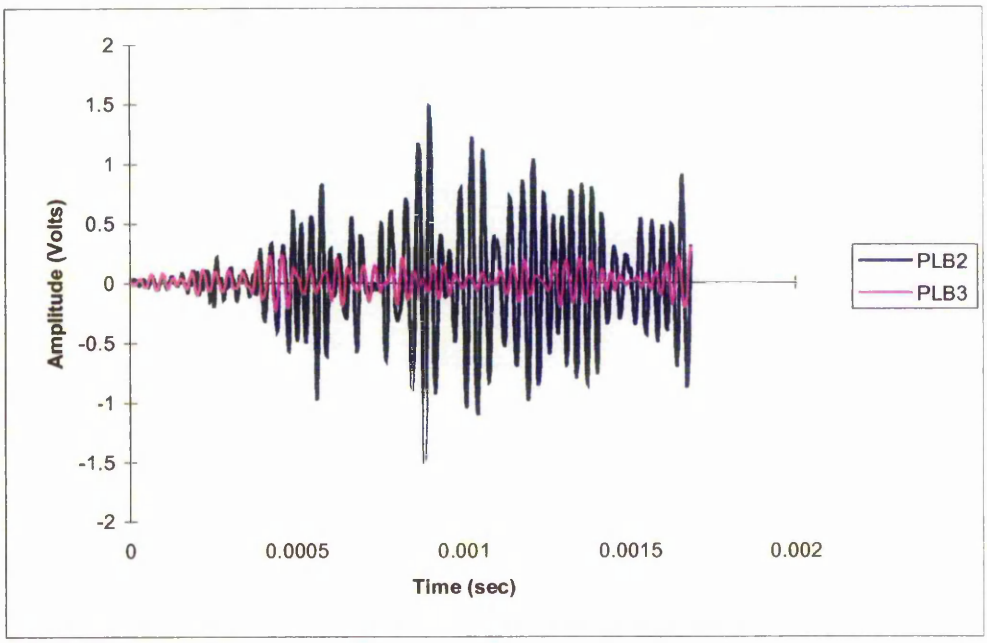


Figure 5.7 AE signal histograms just before (PLB2) and after (PLB3)the collar connection

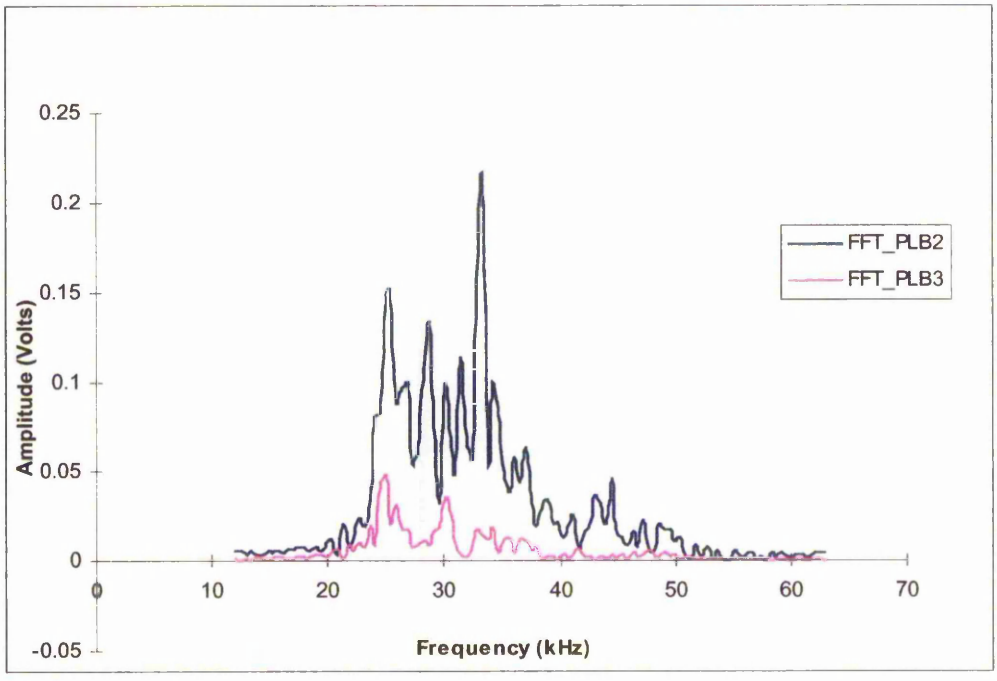


Figure 5.8 AE signal frequency response just before (PLB2) and after (PLB3) the collar connection

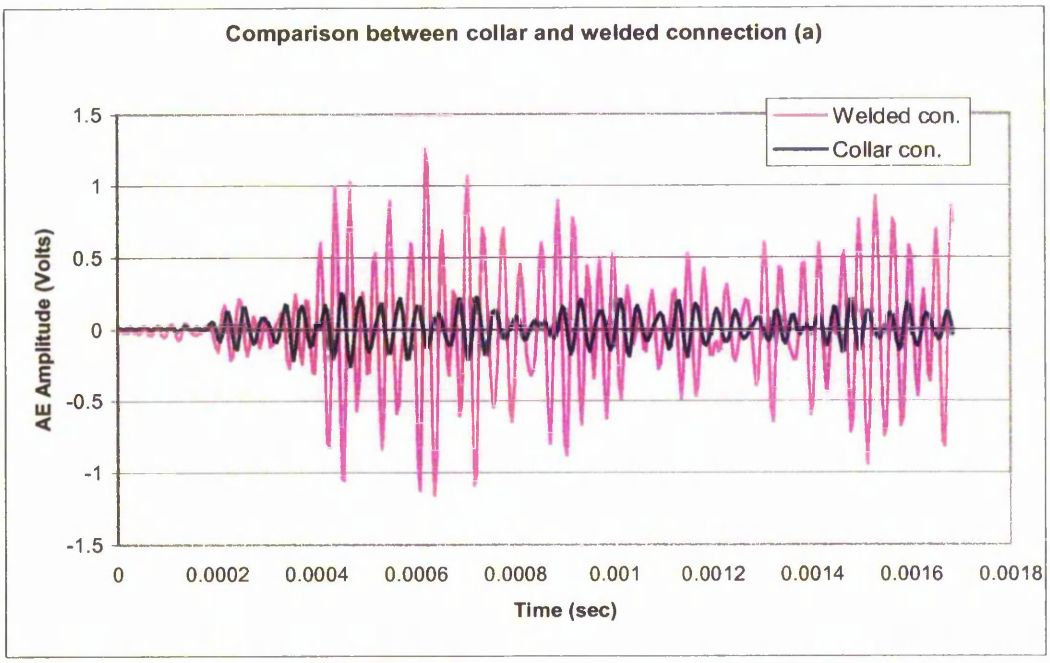


Figure 5.9 Comparison on PLB histograms between welded and collar connection (a)

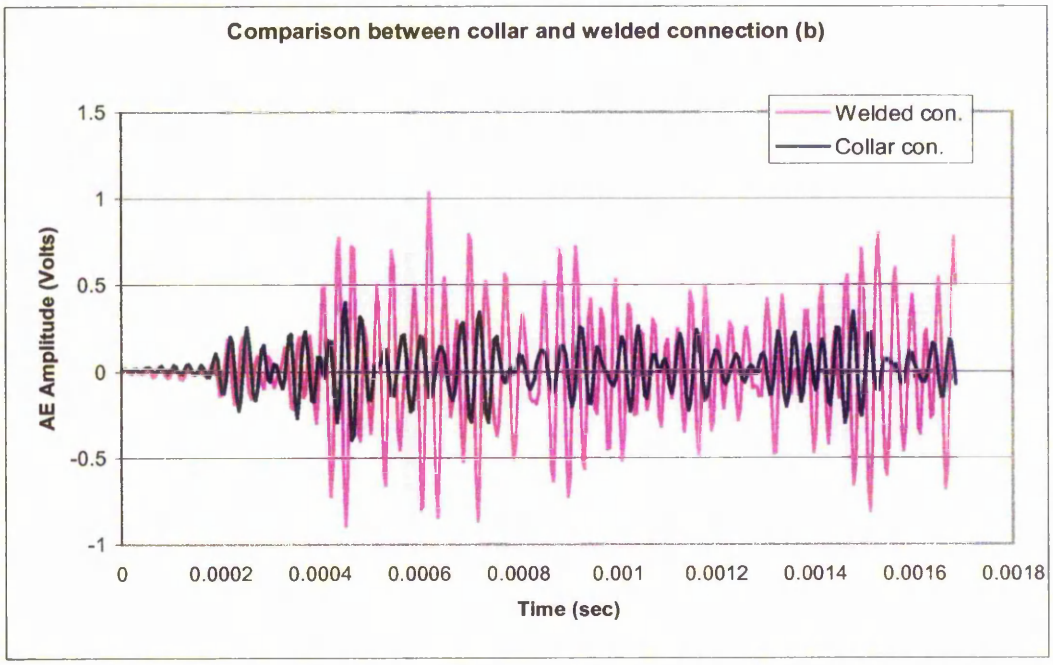


Figure 5.10 Comparison on PLB histograms between welded and collar connection (b)

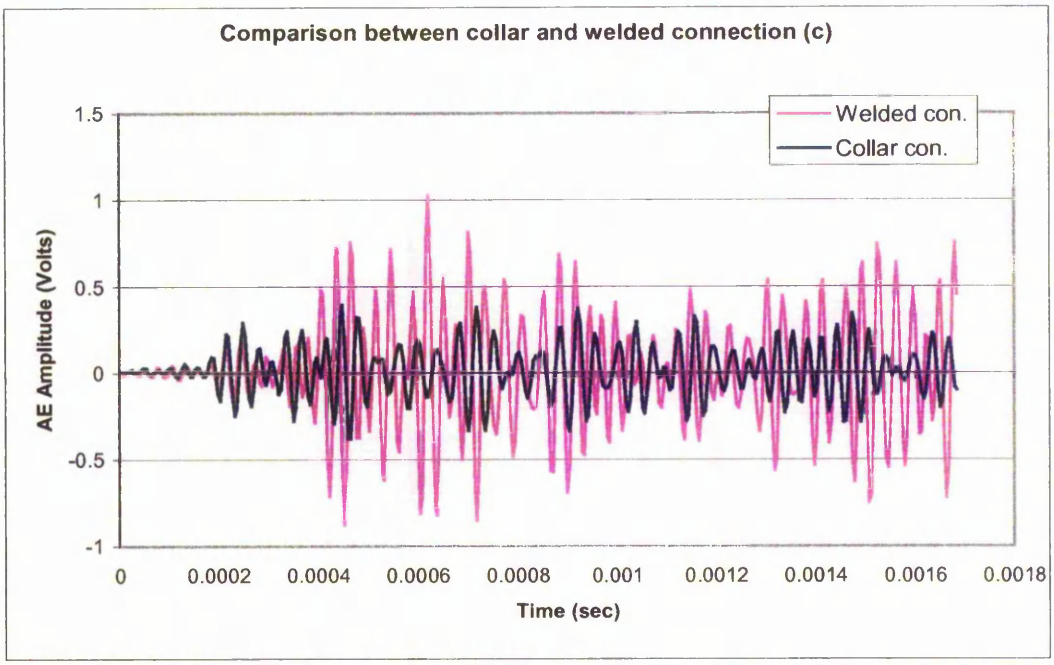


Figure 5.11 Comparison on PLB histograms between welded and collar connection (c)

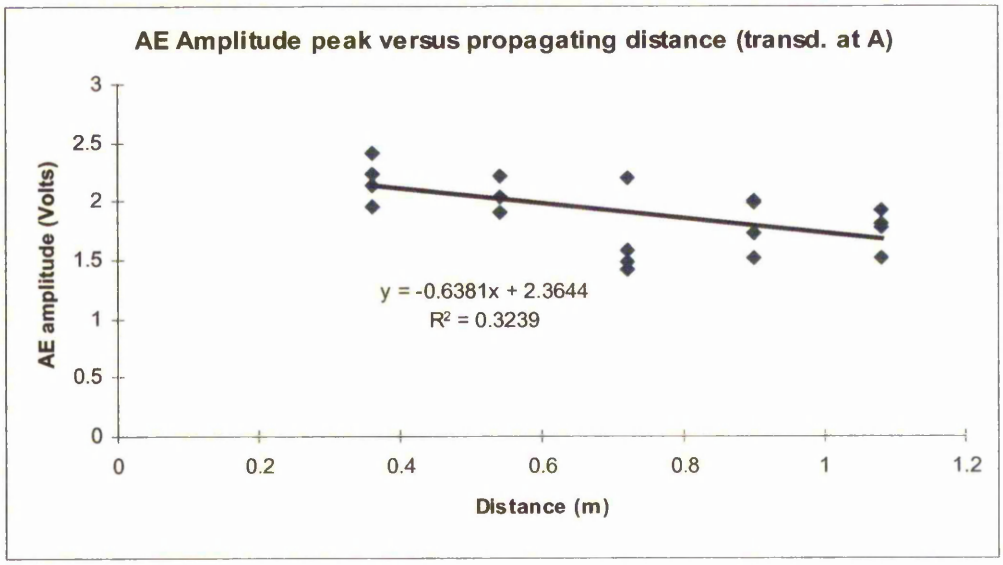


Figure 5.12 First peak AE amplitude with respect to propagating distance, transducer location A.

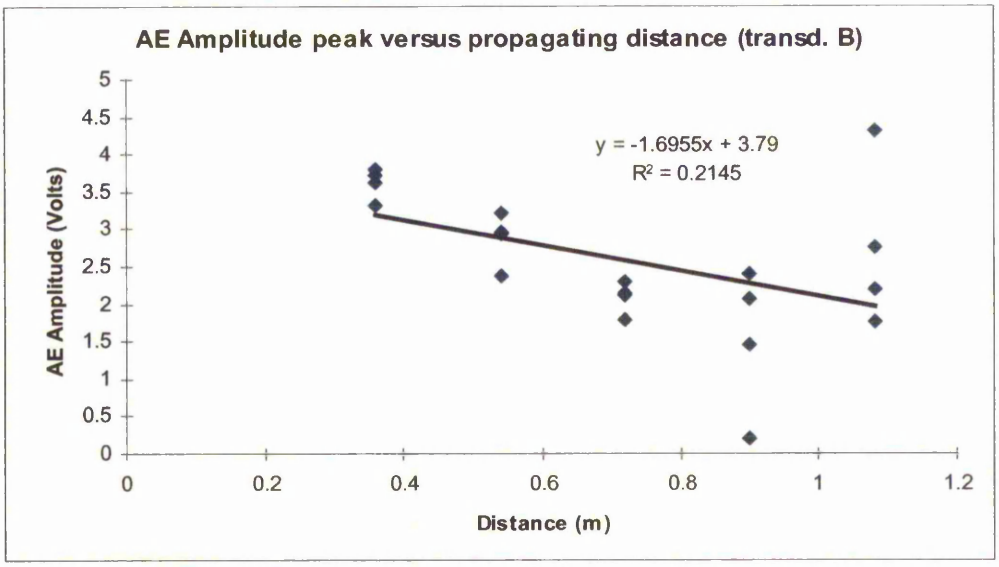


Figure 5.13 First peak AE amplitude with respect to propagating distance, transducer location B.

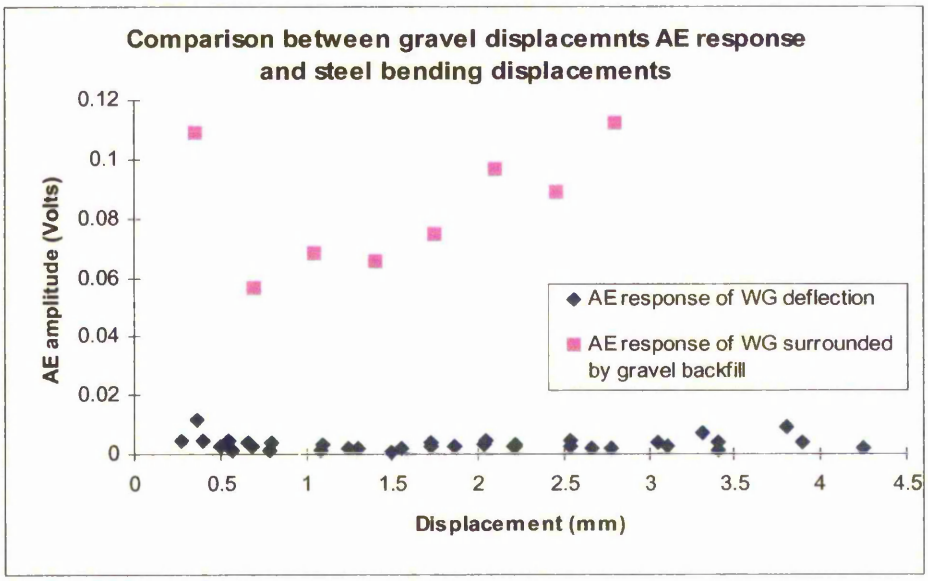


Figure 5.14 AE response of the steel tube under bending deformations in comparison with emissions generated from gravel particle movement around the same wave guide

# Chapter 6 - Active Wave Guide System Investigation Method and Results

## 6.1 Introduction

The work outlined in the Chapter five was limited on investigating the wave guide AE response while generating a signal directly on the tube surface or deforming it.

The response of the soil was not included in the above investigations. In this chapter the AE response of two types of backfill granular soils is presented. The system of backfill soil and wave guide was represented here in two different test set ups. In the first test set up an investigation of the relationship between soil displacement and AE event has been carried out. Whereas, in the second test set up the relationship between displacements as well as displacements rates and AE event, were investigated.

In both tests the behaviour of two types of backfill soil were assessed. A well graded sand and medium size gravel. The grading distribution of the sand is shown in Figure 6.9. The gravel type used for the G-clamp test was a rounded medium size particle gravel. For the controlled displacement rate test angular shaped particles, with medium sized grains up to D=20mm was used. All three backfill soils are granular materials as these emit higher AE levels than cohesive soils.

## 6.2 Backfill displacement and AE response

The study presented in this section relates the AE response of the two backfill soil types with displacement.

A thick polythene tube of 195mm in diameter and 1650mm long was used to contain the backfill material. The soil column was supported vertically by a steel frame. At the centre of the polythene tube one section of 1.65 m long (steel tube) wave guide was inserted before filling the sack with the backfill soil. (see Figure 6.1). The backfill soil

was poured between the wave guide and sack in stages. Approximately 5 kilograms of soil was poured in each stage and was compacted by a rod to distribute the soil evenly and achieve uniform density. At the top a section of the wave guide was left exposed in order to attach the AE transducer. Two elastic bands were used to hold the transducer in place and acoustic gel was applied on the contact surfaces. The AE instrumentation components were the same as the previous experiments described in chapter 5. The event capturing procedure was set up with the following parameters;

- Sampling frequency: 150 kHz
- Event data points (including pre-triggering point) : 1000
- Pre-triggering points captured: 100
- Threshold of level : 0.11 Volts
- Main amplifier was set to: 60dB

A G-clamp was placed around the polythene column and was used to compress the containing soil. The backfill soil was compacted locally with the aid of the G-clamp which forced the soil particles to move around the wave guide thus generating AE events. This compression of the backfill soil was applied at two points along the backfill/wave guide system. The two locations where the AE events were generated were at a distance of 565 mm and 1170 mm away from the sensor.

The clamp progressively reduced locally the soil column diameter by equal displacement intervals of 0.16 mm (or 0.35 mm in some occasions when no AE emission was generated under smaller deformation intervals). Each time the soil diameter was reduced the triggered AE events were captured and saved by the instrumentation as well as the amount of AE events occurring. Then, the soil was left for about 5 minutes to "settle" (being quiet, and no more AE events generating) till the next compression was applied by the clamp. The recorded AE events were analysed by carrying out a statistical analysis. The signal produced in an event consisted of both positive and negative values. To obtain meaningful statistical values in the analysis the signal data had to be converted all to positive values. Otherwise the statistical values will appear all close to zero even if the event is much bigger in amplitude than the other

events. So the statistical analysis was applied on the absolute values of the recorded AE events.

Figures 6.2 (a), (b) and Figures 6.3 (a) and (b) shows plots of the AE events occurring in each displacement interval for gravel and sand backfill at propagating distances of 0.565 m and 1.17 m respectively. In all four plots it can be seen that the event number is smaller at the beginning of the test as the soil is less compacted and then increases as the soil becomes denser. In Figure 6.2 (a) the event occurrence for the gravel backfill seem to fluctuate between values of 5 and 14. Fluctuation also appears to a smaller degree in Figure 6.2 (b). However, for sand backfill the event occurrence seems to increase more evenly with the displacement. This is due to the two different mechanism of grain movement around the wave guide. Sand particles as being much smaller than the gravel can move easier and be re-arranged in a more dense structure which will require higher force to be unlocked and cause movement again. For gravel the unlocking and particle re-arrangement mechanism is more sudden and severe, as it requires only a small displacement to change the position of a big grain which will disturb the balance within the soil. Due to the shape of the gravel particles the interlocking condition is better than those of the sand hence higher loads are required for the next slippage to occur.

At each displacement interval the resulting mean and standard deviation of the AE voltage response of the events were obtained and plotted against the cumulative displacement. This is shown in Figures 6.4(a), (b) and 6.5(a), (b) for gravel and sand backfill respectively. The gravel backfill was displaced only up to approximately 2 mm where sand was displaced further up to 8 mm. It is obvious that the deformation of the gravel emits higher AE levels than the sand. The gravel backfill shows pulses of high and low amplitudes of events without however showing a clear indication that the cumulative displacement is increasing. Sand backfill behaviour in Figure 6.5(a) even if it consists of sporadic releases of energy which results in the AE level dropping temporarily there is a general trend of increase in the AE mean amplitude with displacement. This phenomenon seems to be the "Kaiser effect" (Dunning *et al.*, 1985) in which AE levels are low until the material is stressed beyond that which it has

experienced in the past. Kavanagh (1997) demonstrated this effect on Leighton Buzzard sand subjected to consolidation tests.

The above G-clamp tests were repeated twice more for both backfill soils. The results obtained from these additional tests on the AE response were unfortunately not consistent. This could be due to the fact that as the compression action was applied with the aid of the G-clamp manually the rate of the displacement wasn't constant, which affected the AE signal response. In the light of these a revised laboratory test procedure was developed using a controlled rate of backfill displacement rate.

## 6.3 Controlled strain rate test set-up

A large diameter of 154 mm (inner diameter) steel tube and 1.53 m in length was used to represent the borehole of the AE active wave guide system. The length was small to represent the field set up but the diameter was the same size as a typical borehole drilled on site (Kavanagh 1997). This tube accommodated both the wave guide and the backfill soil. Along the tube length three circular openings were created where three plastic plungers of 40 mm diameter were placed. The three plastic plungers were used to push the backfill soil against the wave guide which was placed at the centre of the 154 mm tube. The wave guide dimensions were 60 mm in diameter and 6mm in wall thickness. The two steel tubes originally were supported vertically so the gap between them could be filled up with the backfill material. Figure 6.6 shows the two-tube system standing vertically and the locations of the plungers. On both ends of the external tube wooden lids were used to keep the soil in place. Both lids had opening of 60 mm at their centre to allow the wave guide length extend through. Once more granular soils were used for the backfill material that were sand and gravel. Filling the tube was carried out in stages so the soil can be compacted and distributed evenly as possible. When the tube was filled up the top wooden lid was placed and the whole system was laid horizontally. Three wooden supports were used to hold in place the filled tube through a compression test machine.

The compression test machine which was used shown in Figures 6.7 and 6.8b. Controlled deformations were applied to the backfill by the compression test machine,

which is capable of applying displacement rates between minimum 0.0001 mm per minute and maximum 9.999 mm per minute. The dial pressure ring gauge

shown in Figure 6.7 was placed directly in line with the plunger that was to be pushed into the backfill soil so the tube could be held in place (not to be lifted upwards) and at the same time obtain readings of the reaction forces. Additionally a recording was kept on the uplifting displacement of the whole tube. This usually occurred when the plunger was pushed a significant distance into the backfill around the wave guide and the locally compacted soil was too dense to allow any further displacements to take place. The result was, lifting of the whole body of the tube.

The sand backfill soil that was used in this test was concrete sand and its particle size distribution is shown in Figure 6.9. The backfill tested was a medium size angular shaped gravel.

For the first time, the transducer in these tests was held by a magnetic clamp on the top of the wave guide steel surface (see Figure 6.8b). This way the contact pressure between the transducer and the wave guide remains the same for all the tests and will not effect the event amplitude.

The AE monitoring was carried out by the same instrumentation mentioned in the previous studies. The signal capturing procedure was carried out using the following parameters set up:

- Sampling frequency: 150 kHz
- Event data points (including pre-triggering point) : 500
- Pre-triggering points captured: 200
- Threshold of level : 0.27 Volts
- Main amplifier was set to: 60dB

Tables 6.1 and 6.2 list the total number of tests carried out for sand and gravel respectively including the test details.

The major tests carried out for the sand backfill are under displacement rates between 0.5 to 2 mm/min. Whereas, for the gravel backfill, tests were carried out with much smaller displacement rates and many more files were created for a given test. This was due to the bad quality of the AE response captured when either sand was tested under small displacement rates and when gravel was tested under larger displacement rates. The different nature of the slip stick mechanism for gravel and sand soil played an important role to the choice of the applied displacement rate and the quality of the AE captured data. The grain size and the grain shape difference between the two granular soils alter the interlocking and released nature of the particles. The sand smaller and rounded shape particles are allowed to be compacted and move by the sides of the plunger before any grain movement occurs at the surface of the wave guide. On the other hand gravel may require higher energy to cause unlocking of its angular shaped particles but the significantylarger grain size will create enough disruption that frictional movement between soil and steel wave guides surface will be present.

However, for comparison purposes Tests 17 and 18 in table 6.1 were carried out to illustrate the AE response of the sand backfill and compared to the gravel backfill soil.

### 6.3.1 Sand Backfill

Sand was the first backfill tested using the controlled displacement rate test set up. It was decided that an upper limit of 2 mm per minute soil displacement rate was to be applied for the sand backfill. Figure 1.1 which defines a slope movement according to its velocity shows, that the displacement rate of 2 mm per minute falls within the velocity range of a rapid slope movement. This justifies the choice of 2 mm per minute as an upper bound. Reduced displacement rates of 1 and 0.5 mm per minute were applied to the sand and their AE response was assessed in this section. Some of the tests were repeated as shown in table 6.1 with slightly different soil density. These were carried out to check if the emitting AE levels are consisted under the same displacement rate by using this test set-up.

As soon as the compressive test started pushing the plunger into the backfill, the 'viewdac' sequence was set ready to capture the events that exceeded the threshold level of 0.28 Volts. Note that the threshold level is higher than the previous test, which was set to 0.11 Volts. The reason for this change was that the motor of the compressive machine generated low amplitude events that were captured under lower threshold level. Tests were carried out without moving the soil but letting the machine operate and the minimum threshold value that could be used without capturing background noise was that of 0.28 Volts. The AE events were recorded and saved into binary files. Filenames are listed in Table 6.1. The same sequence created an ASCII file with an the extension *.cm where an array was created of the cumulative AE events occurring in every 30 sec time interval. The cumulative event time interval was adjusted according to the rate of the AE generated events, which was observed on the computer screen while testing. In fast rates usually the cumulative event time interval recording was set to be 30 sec or 1 min. The choice of 30 sec was decided to be the minimum time interval. This was a sensible time interval to reduce the number of missed triggered events. For example if the interval was set to 10 sec the viewdac sequence used for capturing AE events had to stop every 10 sec to save the amount of events recorded into the ASCII file. This procedure will hold the board busy and cannot record the AE events which could occur during at the same time. For testing on small displacement rates the events are not occurring often and the recording event time interval could be set to 5 min or even to 10 minutes.

In most occasions the 'viewdac' sequence was set to continue recording events even after the compressive machine was switched off (i.e. the plunger was not pushed in). This was done to observe if there was any indication in the AE response or the cumulative event indicates that the soil stopped moving.

The recorded AE data were processed in two stages.

a) Post-filtering the AE data and obtaining the statistical values of the good events .

b) Estimate the average of the statistical values of the good events captured within the time interval specified by the cumulative event recording procedure. (stages a and b were described in detail in chapter 3).

The second stage of processing allows the researcher to plot in a graph the averaged statistical values with respect to actual testing time or displacement, since the displacement rate is constant.

These type of plots are presented in Figures 6.10 to 6.13. Figure 6.10(a) shows the AE response with respect to time when the sand backfill is compressed locally by plunger 1 and with a constant displacement rate of 2 mm per minute (wg12a). It is observed that the AE voltage levels are rising with time till 10 minutes at which time the compressive action was stopped. As the sand backfill remained undisturbed for 6 further minutes the AE levels started reducing gradually to reach the value of 0.1 volts. This means that soil particle movement is still present after the 6 minutes, and probably requires longer time to obtain completely "quiet" response (i.e. no AE events). Figure 6.10(b) shows the AE response plotted against displacement for the same test.

Figure 6.11 shows the results of test 3 which is a repeated test of plunger 1 moving the backfill with the same displacement rate of 2mm/min. The AE amplitude levels are lower than those shown in Figure 6.10. The reason for this difference is not obvious as the density of the soil between the two tests differs only by 1% . However, local density variation is possible, which could be the reason for the difference in the amplitude.

A different feature of high amplitude spikes appears in this figure in the settling phase of the backfill. It seems that these spikes are due to the electronic noise occurring when the compressive machine is switched off and is interfering with the signal. Although it should have been filtered out by the "good event" sequence in Viewdac, is still present because it is not always distinctive and is masked by events generated by the soil particles while settling. These types of spikes were often observed during testing not only at the end of the test, where the compressive machine was switched off, but also at the beginning of the recording. Therefore, the operator had to allow enough time after

switching on the electronic devices so their electronic noise would not interfere with the AE noise emitting from the soil, which is of interest.

Figures 6.12 and 6.13 illustrate the results of plunger 1 compressing the backfill soil with displacement rates of 1mm/min and 0.5 mm/min respectively. The AE amplitude levels seem to be increasing slightly from 0.05 to 0.1 Volts in Figure 6.12 till 15 minutes of testing at which time the movement was stopped. Immediately after the test stopped the AE emissions dropped below 0.05. However, this reduction does not remain below 0.05 volts to give a clear indication that the movement has stopped. Similar behaviour is shown in Figure 6.13 after 40 minutes. It was noted that despite the displacement rate being halved from 1mm/min to 0.5mm/min the AE signal amplitude did not vary. This is more obvious in Figure 6.14 were the three displacement rates responses are compared. Both displacement rates 0.5 mm/min and 1mm/min show a band of average mean values around 0.1 Volts where for the faster rate of 2mm/min the response is significantly higher than the other two.

The cumulative events of the three different displacement rates are plotted together in Figure 6.15 (a) with respect to time. The slopes of these three curves differ with time and are getting steeper as the soil velocity increases. Provided that the slope of the cumulative event for each displacement rate of movement varies within a range of angles it is possible to estimate on site what is the slope movement once a significant volume of data have been obtained. The cumulative plots also give a clear indication at which point the soil deformation is stopped. The same data are plotted in Figure 6.15 (b) with respect to displacement. This figure shows that for the same total displacement larger number of events are captured when the soil is displaced slower. This phenomenon could be due to the readiness of the board to trigger on time under slow rates of movement without missing as many events as when faster rates are applied to the soil. For high rates of deformation it was obvious that more events were occurring than during testing at slower rates. However, since the event flow occurs within a small time interval, the board doesn't have the chance to capture all of them.

### 6.3.2 Gravel backfill

Gravel backfill AE response was investigated under six different displacement rates. In table 6.2 the displacements rates that were applied to the soil are listed under the 'comments' column. It can be seen that they range between the minimum of 0.0001 mm per minute, up to a maximum of 0.25 mm per minute. The maximum rate is only half of the smallest rate that was applied to the sand backfill above.

Figure 6.16(a) and Figure 6.16(b) show the average statistical values plotted with respect to time and displacement respectively when the gravel was displaced 10 mm under a displacement rate of 0.25 mm/ min. During the first 12 minutes, when the soil was at its loosest state it can be seen that the average AE mean reaches a value above 0.3 volts and then drops to 0.1 volts. After 10 minutes the amplitude of the signal picks up again and stays almost constant around 0.15 volts throughout the period time of the test. The higher events that appear in the first 2.5 mm are due to the ability of the less compacted gravel grains to move between the plunger and the wave guide. As the local spacing decreases the particles interlock and move less around the wave guide till the interlocking arrangement breaks and higher amplitude events occur as shown in Figure 6.16 (a) at 48 min. It should be noted that deformation of the plunger was stopped after 40 minutes. However, the plunger remained under compression and can still be stresses the soil.

Further information on the plunger/soil system behaviour is provided by the readings of the resisting force and the tube uplifting displacement that were measured at the top of the outer tube. Table 6.3 shows these readings. In the second column of the table it can be seen that the tube uplift displacements are increasing, which means that, the whole system is moving slightly upwards as the plunger is pushed into the soil. The resisting force also increases with time until plunger penetration was stopped after 40 minutes. The last set of data clearly indicates that the plunger was pushed further after the penetration by the motor was stopped as a result of the residual compressive force in the plunger. After a period of time the compressive force reduced in magnitude. This additional plunger displacement 0.06 mm into the soil produced the high amplitude events appearing at the tail of the AE response plot. Figure 6.17 shows that the

cumulative events also continue to occur in large numbers after 40 minutes and reach a plateau at 47 minutes.

The phenomenon of high amplitude events appearing after the motor was switched off was present again in test gv1Dc4 for which results are shown in Figure 6.18. In this test the soil was not as loose a state as it was in gv1D test. The soil has already been compressed by 1.06 mm. As the initial conditions are not the same as the previous test gv1D the initial AE response is different. (i.e. there are no significantly higher AE levels at the start of the test). However, as soon as the monitor was stopped and the tube was left resting under its own weight and the compressive force that was built up in the dial ring, the high amplitude AE events begin to generate. Once more the readings of resisting force showed that the whole tube was settling as the plunger pushed further into the soil (see table 6.4). These tests showed that by applying a displacement rate of 0.25mm/min to the gravel backfill in this particular experiment set up does not produce reasonable results.

It seems that the soil required more time to respond to the high stresses applied under this rate of movement. The high boundary stiffness of the outer steel tube does not allow much room for the gravel grains to move around the wave guide in such a short time period.

The next step was to reduce the rate of displacement significantly so that this phenomenon of tube uplifting and delayed AE response of the gravel backfill does not occur. Figure 6.19 shows the AE response of gravel displaced by 2.1 mm under both displacement rates of 0.02 (Gv1Z) and 0.01mm/min (Gv1F). It can be seen that a general trend in the average AE mean amplitude appears around 0.15 Volts for both rates. Under the rate of 0.01 mm/min the response is slightly higher than that of 0.02mm/min. Table 6.2 shows that the densities are significant different between these two tests Gv1F and Gv1Z. Test GV1F has 13% higher density than that of Gv1Z. This can explain the higher AE response even when the rate of displacement is smaller (half the magnitude of Gv1Z).

Figures 6.20, 6.21 and 6.22 show plots of the AE response of the gravel backfill with respect to time under the 0.0042 mm/min rate of movement. These plots correspond

to data captured under test 12 (in file Gv1B) and test 14 (in two binary files GvBc1 and GvBc2). In Figure 6.20 it can be seen that at 500 min when the soil was displaced by 2.1mm (0.0042mm/min x 500min), and at which time the compressive motor was switched off, a clear reduction in the average statistical values occur. Similar reductions appear in Figure 6.22 after 225min. For the file Gv1Bc1 a reduction is not present as the event capturing did not continue beyond the time at which the plunger stopped being pushed into the soil. It was expected that the AE level would rise as the soil gets denser between the plunger and the wave guide.

In order to see if there is any AE amplitude increase due to density variation Figure 6.23 presents the results of the three files integrated in one plot. In this figure the average AE mean response of the gravel is plotted against displacement. It can be seen that the AE amplitude levels are almost consistent fluctuating around 0.15 Volts. A significantly higher peak appears just before the end of the test. This could be a point where the grain interlocking is released.

As the displacement rate was reduced, it required a longer time of testing and monitoring to cover the same amount of displacement that previous tests with faster rates had covered. Therefore, for the next displacement rate of E=0.001 mm/min three blocks of displacement intervals were chosen and not a continuous displacement interval as seen in the previous rate tests. Table 6.5 shows that, files (GV1E*) in test 13 cover the soil displacement interval between 0mm and 1.06mm. During test 15 the next displacement interval was between 2.1mm and 3.67mm, with a displacement gap of 1.04 mm and finally, in test 14 the third displacement interval between 3.69 and 4.6 mm was monitored.

Figures 6.24 ,6.25 and 6.26 shows the AE response of gravel with respect to displacement for the three different displacements blocks mentioned above. It can be seen in Figure 6.24 the AE results are plotted beyond 0.182 mm. This is due to the fact

that no "good events" where captured and written to file Gv1E. The total number of events triggered and captured in Gv1E was only six. AE activity occurs between 0.22mm and 0.27mm with significant amplitude and then the soil is quiet until 0.58mm displacement is reached.

In Figures 6.25 and 6.26 the AE activity becomes more consistent without quiet gaps as in the smaller displacements shown previously. There are still some intervals that show zero AE emissions. However, most of them are when the soil was left overnight resting overnight(i.e. no plunger displacement) and the next day the test was continued. These starting points are assigned by the filename id on the plots.

Table 6.5 shows that the combined four displacements rates that they described above (D, B, F and Z) covered the initial 2.1 of mm of displacement. Figure 6.27 compares the four different displacement rates with the same initial conditions covering 2.1mm displacement. Once more it can be seen that the AE amplitude level does not depend upon the speed the soil is deformed.

For the slowest displacement rate of 0.0001mm/min it should be noted that this was applied in to the gravel backfill once the plunger had already been displaced beyond 4.6 mm. The main purpose of the last displacement rate was to test the sensitivity of the AE instrumentation for slope movements as slow as creeping movement.

Figure 6.28 shows that although a lot of quite periods exists (i.e. AE amplitude is zero) there are still significant high AE events occurring that indicates a soil movement.

## 6.4 Summary

The experiments carried out on the two backfill soils using the polythene bag and the G-clamp showed that the deformation of gravel emits higher AE levels than sand. However, this test set-up arrangement did not produce consistent AE responses when the tests were repeated. This inconsistency of AE response was due to the random displacement rates applied to the soil by the G-clamp.

In strain rate controlled tests the sand backfill demonstrated that under fast rates of movement (i.e. in the order of 2mm/min the AE response increases with the cumulative displacements and when plunger displacement stops the AE emissions gradually reduce.

The gravel backfill under the fast rates of movement responded with higher levels of AE after the compressive motor was stopped. This delayed response did not allow the researcher to quantify the signal and was a function of the test set up (i.e. rigid confining tube surrounding the backfill). However the gravel responded well under the slower rates (i.e. below 0.0042 mm/min).

The rate of cumulative events on both backfill soils, gravel and sand, showed an increase with displacement but also with displacement rates. The AE amplitude levels however did not change between the different displacement rates.

| Test No | Soil mass | Soil Density | Filename of AE data (Binary files) | | | Displ. Rate | Comments |
|---|---|---|---|---|---|---|---|
| | kg | kg/m$^3$ | Plunger No | | | mm/min | |
| | | | 1 | 2 | 3 | | |
| 3 | 40.309 | 1711.37 | Wg12b | N/A | Wg32b | 2 | |
| 4 | 40.1 | 1694.5 | Wg12c | N/A | Wg13c | 2 | |
| 5 | 39.85 | 1685.07 | Wg12d | N/A | N/A | 2 | One of the wooden support was broken during testing |
| 6 | 40.26 | 1704.7 | Wg12e | Wg22e | Wg32e | 2 | |
| 7 | 39.87 | 1685.92 | Wg11a | Wg21a | Wg31a | 1 | |
| 8 | 40.26 | 1701.26 | Wg11b | Wg21b | Wg31b | 1 | |
| 9 | 40.11 | 1696.06 | Wg11c | Wg21c | Wg31c | 1 | |
| 10 | 40.05 | 1694.66 | Wg15a | Wg25a | Wg35a | 0.5 | |
| **17** | **40.27** | **1703.97** | SnD1 | N/A | N/A | 0.25 | These tests were carried out for comparison with the gravel backfill tests |
| | | | SnB1c1a | | | 0.0042 | |
| | | | SnB1c2 | | | 0.0042 | |
| | | | SnE1c3 | | | 0.001 | |
| | | | SnE1c4 | | | 0.001 | |
| | | | SnE1c5 | | | 0.001 | |
| | | | SnE1c6 | | | 0.001 | |
| | | | SnE1c7 | | | 0.001 | |
| **18** | **39.98** | **1689.01** | SnB1 | N/A | N/A | 0.0042 | Used for comparison with the gravel backfill tests. |
| | | | SnB1c1b | | | 0.0042 | |
| | | | SnE1b | | | 0.001 | |
| | | | SnE1bc1 | | | 0.001 | |
| | | | SnF1 | | | 0.01 | |
| | | | SnC1 | | | 0.0001 | |
| | | | SnC1c1 | | | 0.0001 | |
| | | | SnC1c2 | | | 0.0001 | |

Table 6.1 List of the sand backfill created files under the controlled strain test.

| Test No | Soil mass (kg) | Soil Density ($kg/m^3$) | Filename of AE data (Binary files) Plunger No | | | Comments |
|---|---|---|---|---|---|---|
| | | | 1 | 2 | 3 | The displacement rates are assigned by the capital letters as follows |
| 11 | 35.85 | 1518.99 | Gv1D | N/A | N/A | |
| 12 | 40.1 | 1694.50 | Gv1B | Gv2B | Gv3B | B= 0.0042 mm/min |
| | | | Gv1Dc1 | Gv2Bc1 | Gv3Bc1 | C=0.0001 mm/min |
| | | | Gv1Cc2 | Gv2Dc2 | Gv3Cc2 | D=0.25 mm/min |
| | | | | Gv2Cc3 | Gv3Cc3 | E=0.001 mm/min |
| 13 | 39.8 | 1682.95 | Gv1E | Gv2D | Gv3F | F=0.01 mm/min |
| | | | Gv1Ec1 | Gv2Ec1 | Gv3Ec1 | Z=0.02 mm/min |
| | | | Gv1Ec2 | Gv2Ec2 | Gv3Ec2 | |
| | | | Gv1Ec3 | Gv2Ec3 | Gv3Ec3 | |
| | | | Gv1Dc4 | Gv2Bc4 | Gv3Ec4 | |
| 14 | 40.26 | 1704.69 | Gv1F | Gv2F | | |
| | | | Gv1Bc1 | Gv2Ec1b | | |
| | | | Gv1Bc2 | Gv2Ec2b | | |
| | | | Gv1Ec3b | Gv2Ec3b | | |
| | | | Gv1Ec4b | | N/A | |
| | | | Gv1Ec5b | | | |
| | | | Gv1Cc6 | Gv2Bc4b | | |
| | | | Gv1Cc7 | | | |
| | | | Gv1Cc8 | | | |
| 15 | 35.46 | 1503.47 | Gv1Z | Gv2Fb | Gv3Z | |
| | | | Gv1Ec1c | Gv2Fbc2 | | |
| | | | Gv1Ec2c | Gv2Dc3b | | |
| | | | Gv1Ec3c | Gv2Z | | |
| | | | Gv1Ec4c | | | |
| 16 | 35.43 | 1502.20 | Gv1Ed | | | |
| | | | Gv1Edc2 | N/A | N/A | |
| | | | Gv1Edc3 | | | |

Table 6.2 List of the gravel backfill created files under the controlled strain test.

| Gravel (gv1D) 025mm/min | | | | |
|---|---|---|---|---|
| **Time (min)** | **Uplifting Displ. (mm)** | **Resisting force (N)** | **Plunger Displ. (mm)** | **Energy (Joules)** |
| 0 | 0 | 0 | 0 | 0 |
| 10 | 0.046 | 148.38 | 2.454 | 0.18 |
| 20 | 0.128 | 410.28 | 4.872 | 1.14 |
| 30 | 0.306 | 973.62 | 7.194 | 4.53 |
| **40** | 0.538 | **1712.47** | 9.462 | 10.69 |
| 46 | 0.478 | 1521.39 | 9.522 | 8.87 |

Table 6.3 Resisting force and uplift displacement readings of gv1d test.

| Gravel (gv1Dc4) 025mm/min | | | | |
|---|---|---|---|---|
| **Time (min)** | **Uplifting Displ. (mm)** | **Resisting force (N)** | **Plunger Displ. (mm)** | **Energy (Joules)** |
| 0 | 0 | 0 | 0 | 0 |
| **10** | 1.3 | **135.4839** | 1.2 | 0.08129 |
| 12 | 1.3 | 64.51613 | 1.2 | 0.08129 |
| 13 | 1.3 | 58.06452 | 1.2 | 0.08129 |
| 15 | 1.29 | 54.83871 | 1.21 | 0.081855 |
| 17 | 1.29 | 51.6129 | 1.21 | 0.081855 |
| 19 | 1.29 | 45.16129 | 1.21 | 0.081855 |
| 22 | 1.29 | 45.16129 | 1.21 | 0.081855 |
| 23 | 1.29 | 45.16129 | 1.21 | 0.081855 |
| 26 | 1.29 | 41.93548 | 1.21 | 0.081855 |
| 36 | 1.27 | 38.70968 | 1.23 | 0.082661 |
| 39 | 1.27 | 38.70968 | 1.23 | 0.082661 |

Table 6.4 Resisting force and uplift displacement readings of gv1Dc4test

| Filename | Displ. Rate (mm/min) | Original displ. (mm) | Final displ. (mm) | Duration (min) |
|---|---|---|---|---|
| **Test 11** | | | | |
| Gv1D | 0.25 | 0 | 10 | 40 |
| **Test 12** | | | | |
| Gv1B | 0.0042 | 0 | 2.1042 | 501 |
| Gv1Dc1 | 0.25 | 2.1042 | 4.6042 | 10 |
| Gv1Cc2 | 0.0001 | 4.6042 | 4.6402 | 360 |
| **Test 13** | | | | |
| Gv1E | 0.001 | 0 | 0.182 | 182 |
| Gv1Ec1 | 0.001 | 0.182 | 0.49 | 308 |
| Gv1Ec2 | 0.001 | 0.49 | 0.74 | 250 |
| Gv1Ec3 | 0.001 | 0.74 | 1.065 | 325 |
| Gv1Dc4 | 0.25 | 1.065 | 3.565 | 10 |
| **Test 14** | | | | |
| Gv1F | 0.01 | 0 | 2.11 | 211 |
| Gv1Bc1 | 0.0042 | 2.11 | 2.761 | 155 |
| Gv1Bc2 | 0.0042 | 2.761 | 3.6892 | 221 |
| Gv1Ec3b | 0.001 | 3.6892 | 3.8782 | 189 |
| Gv1Ec4b | 0.001 | 3.878 | 4.29 | 412 |
| Gv1Ec5b | 0.001 | 4.29 | 4.648 | 358 |
| Gv1Cc6 | 0.0001 | 4.648 | 4.7002 | 522 |
| Gv1Cc7 | 0.0001 | 4.7002 | 4.7458 | 456 |
| Gv1Cc8 | 0.0001 | 4.7458 | 4.7762 | 304 |
| **Test 15** | | | | |
| Gv1Z | 0.02 | 0 | 2.1 | 105 |
| Gv1Ec1c | 0.001 | 2.1 | 2.625 | 525 |
| Gv1Ec2c | 0.001 | 2.625 | 2.987 | 362 |
| Gv1Ec3c | 0.001 | 2.987 | 3.194 | 207 |
| Gv1Ec4c | 0.001 | 3.194 | 3.671 | 477 |
| **Test16** | | | | |
| Gv1Ed | 0.001 | 0 | 0.473 | 473 |
| Gv1Edc2 | 0.001 | 0.473 | 1.114 | 641 |
| Gv1Edc3 | 0.001 | 1.114 | 1.62 | 506 |

Table 6.5 Gravel tests details original and final displacement of the plunger

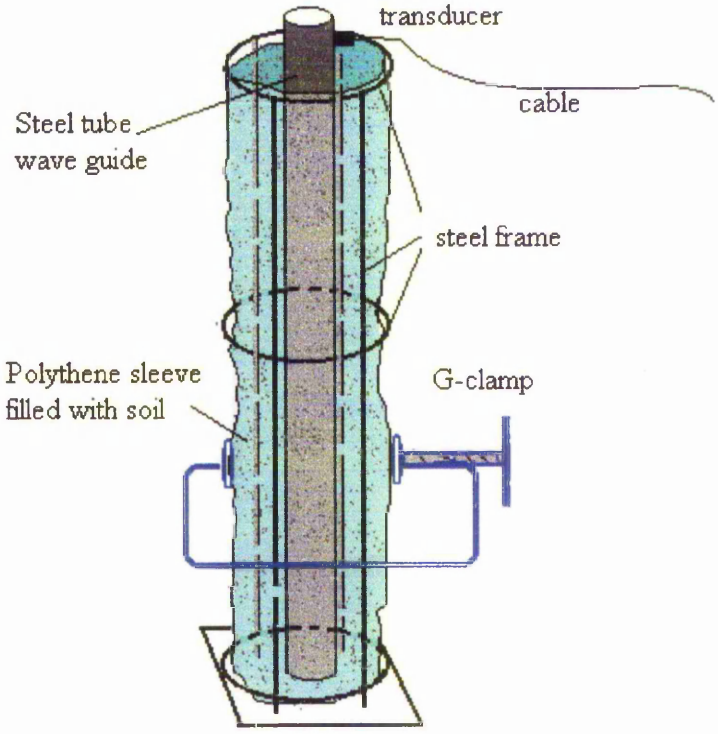


Figure 6.1 Active wave guide system test set-up using a G-clamp to generate AE events

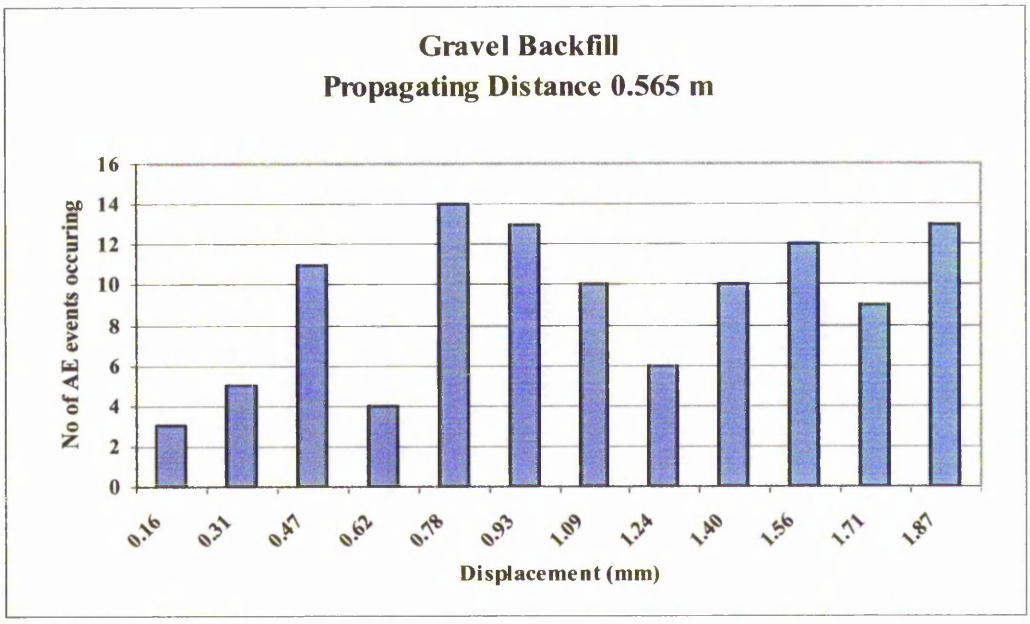


Figure 6.2 (a) AE event No with respect to displacement for gravel and propagating distance 0.565 m.

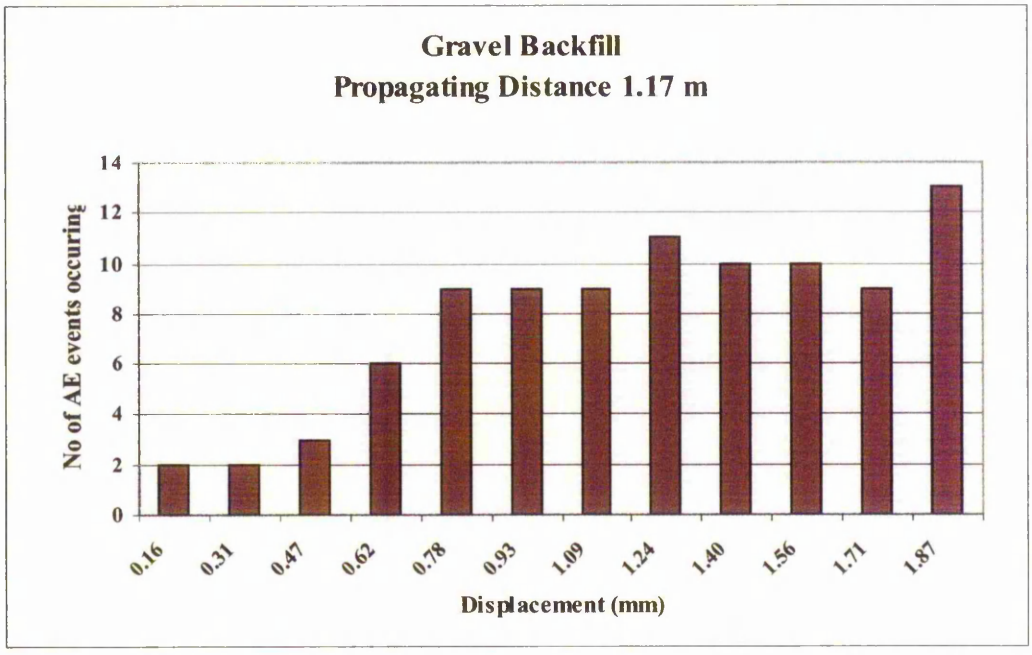


Figure 6.2 (b) AE event No with respect to displacement for gravel and propagating distance 1.17 m.

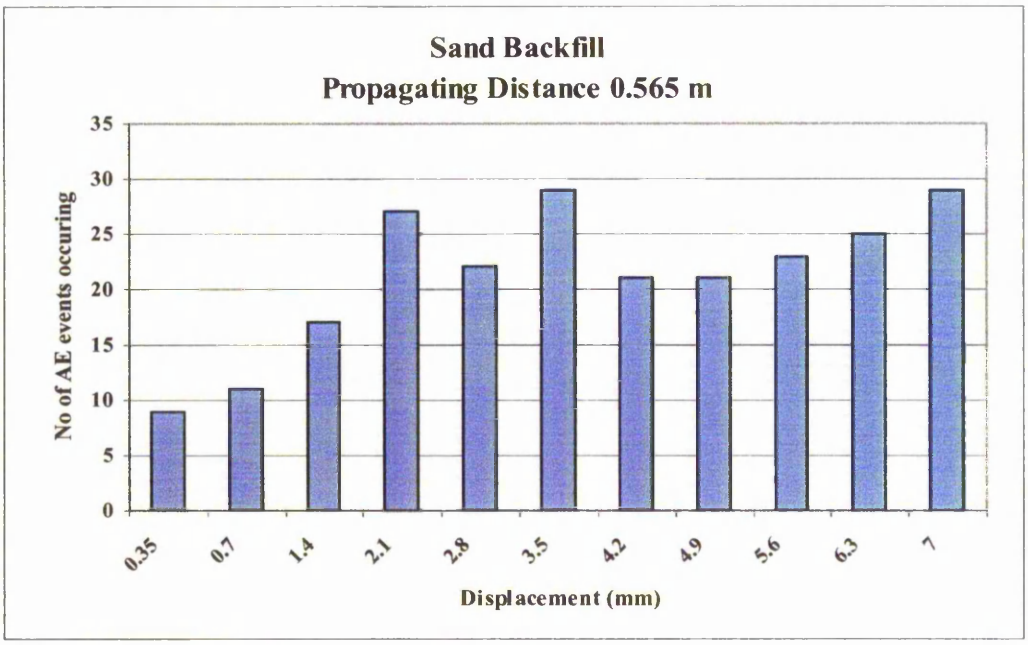


Figure 6.3 (a) AE event No with respect to displacement for sand and propagating distance 0.565 m.

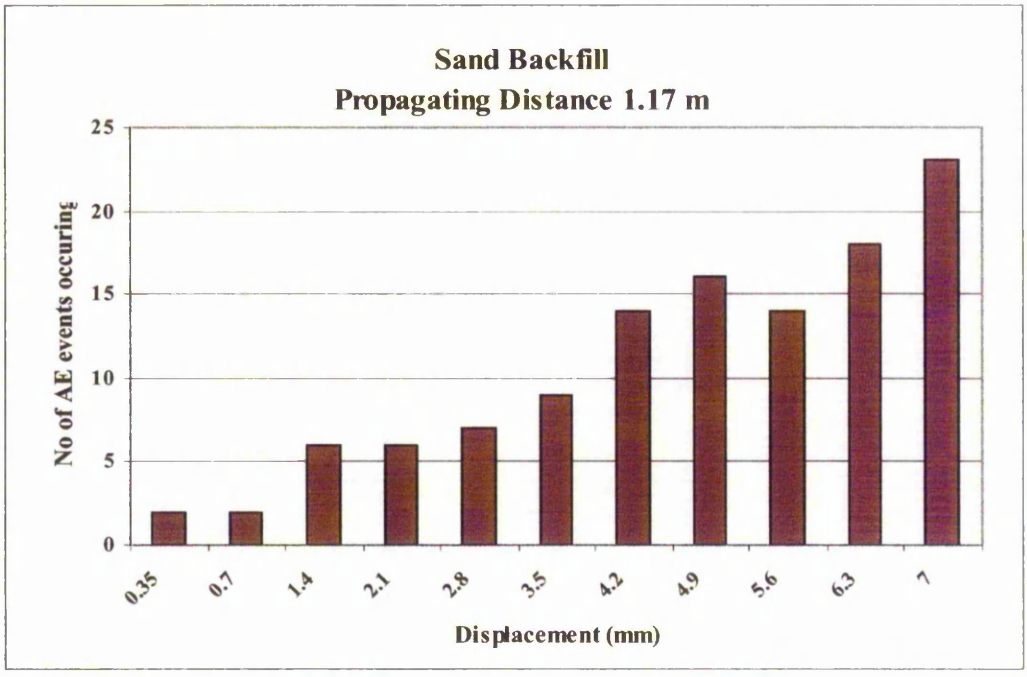


Figure 6.3 (b) AE event No with respect to displacement for sand and propagating distance 1.17 m.

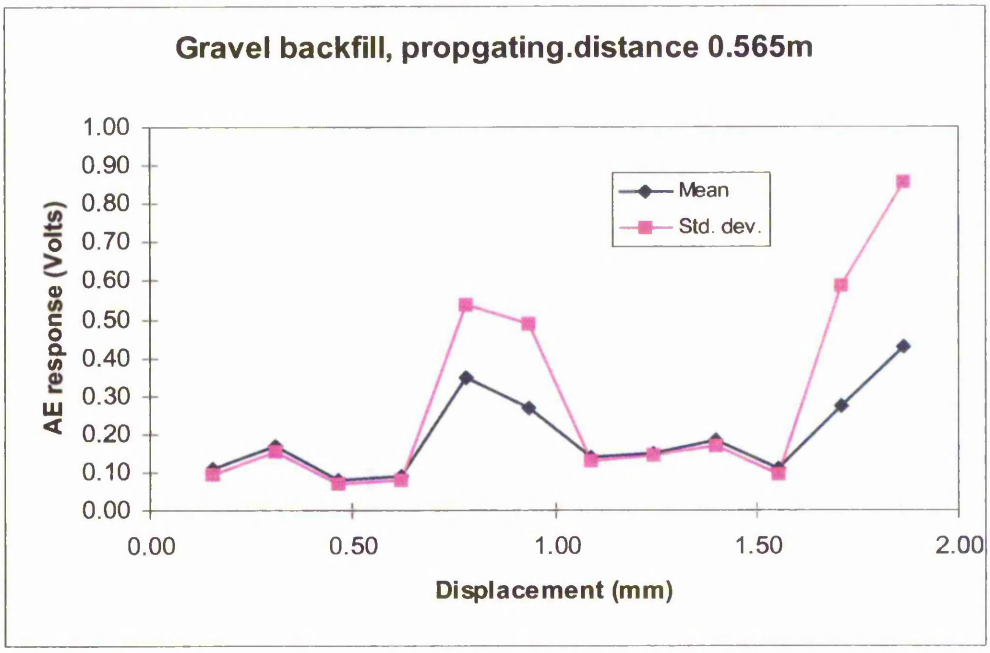


Figure 6.4 (a) AE response of gravel with respect to displacement (0.565 m)

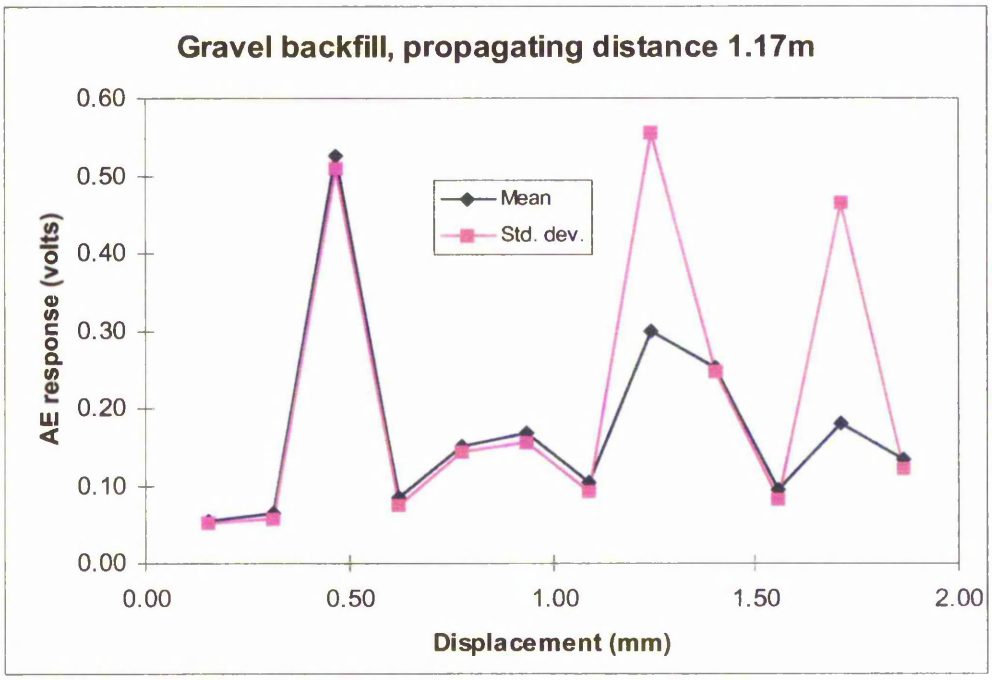


Figure 6.4 (b) AE response of gravel with respect to displacement (1.17 m)

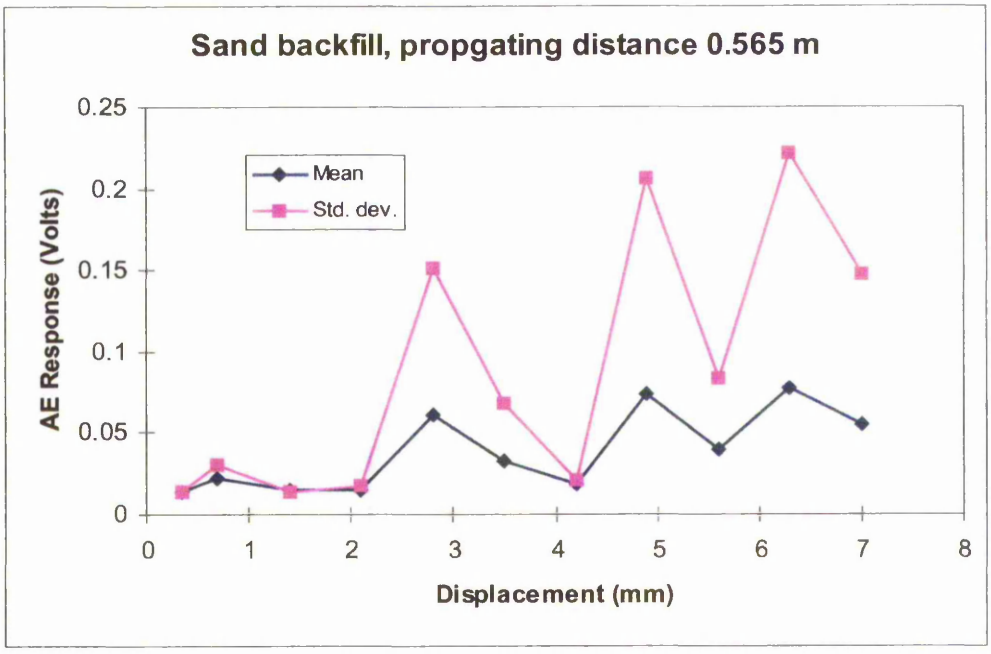


Figure 6.5 (a) AE response of sand with respect to displacement (0.565 m)

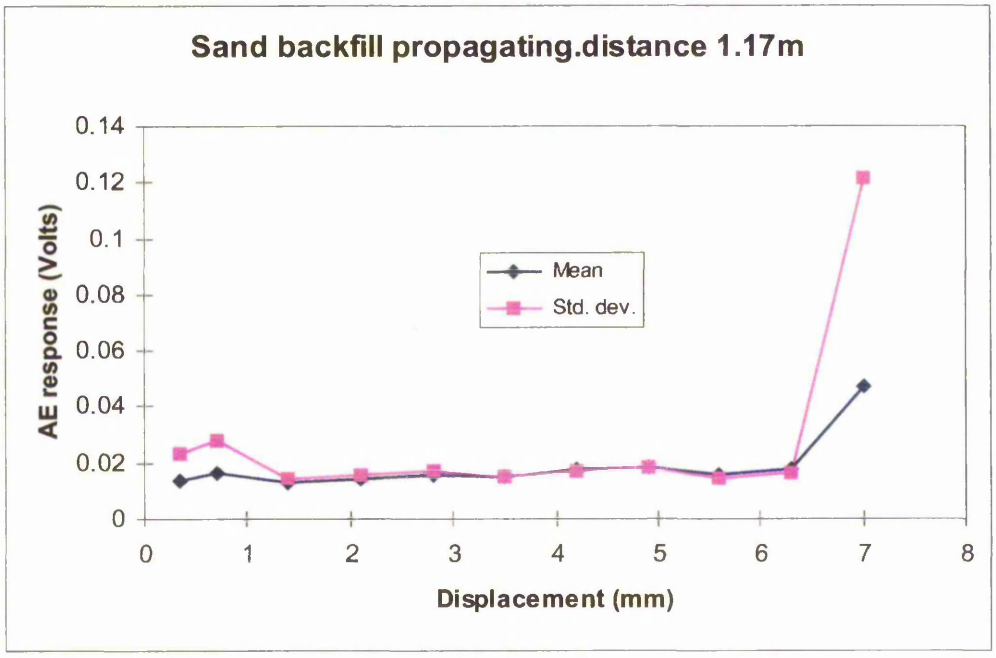


Figure 6.5 (b) AE response of sand with respect to displacement (1.17 m)

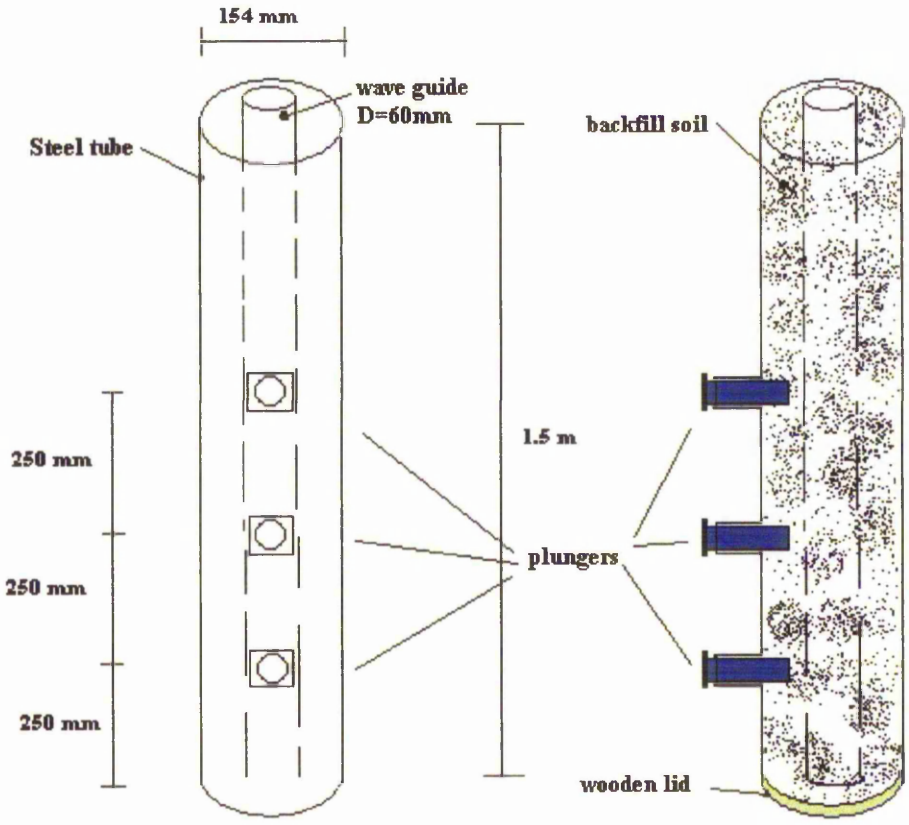


Figure 6.6 Outer steel tube dimensions and plunger locations

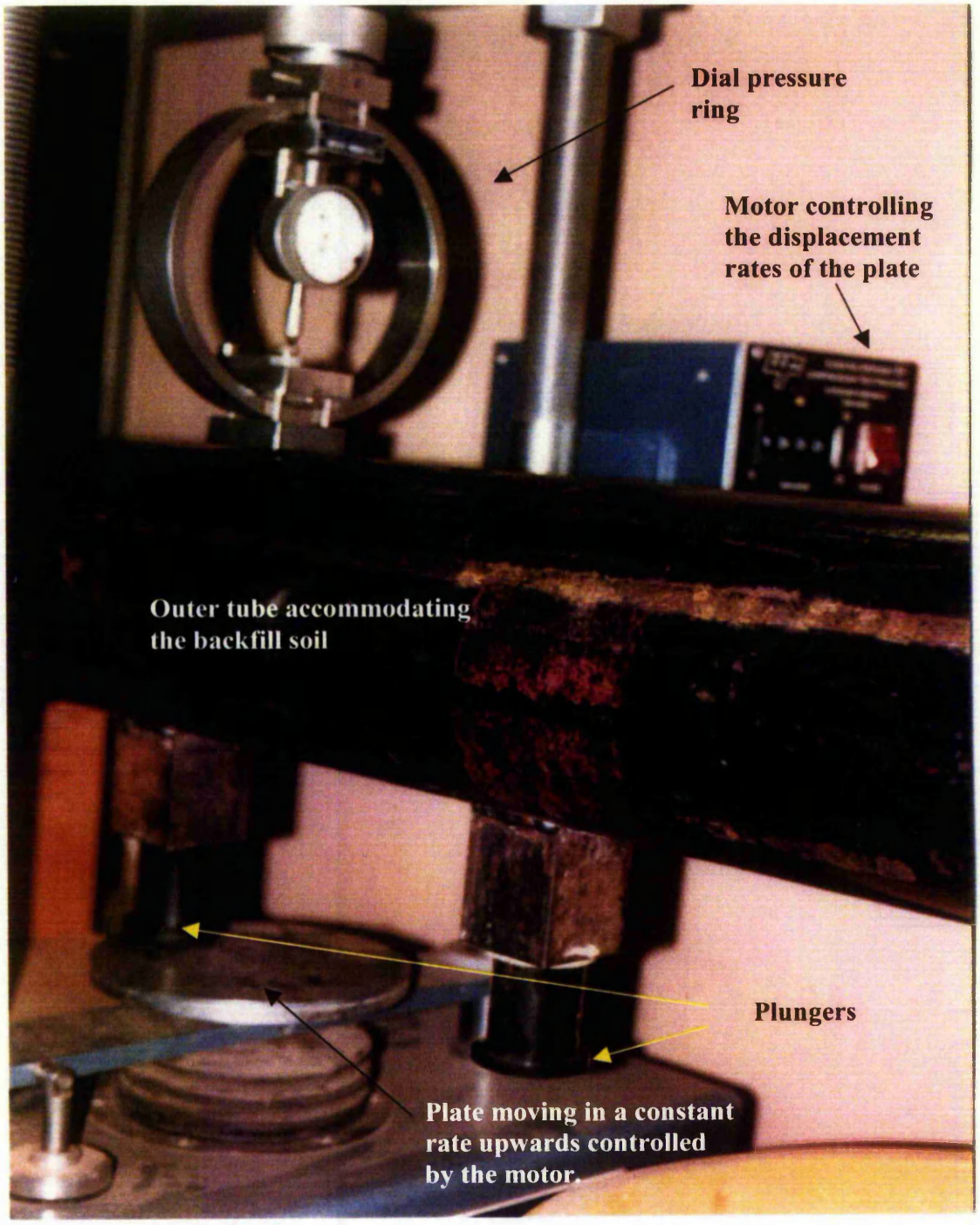


Figure 6.7 Laboratory test set-up for investigating AE response while localised constant rate backfill movement is applied against the wave guide.

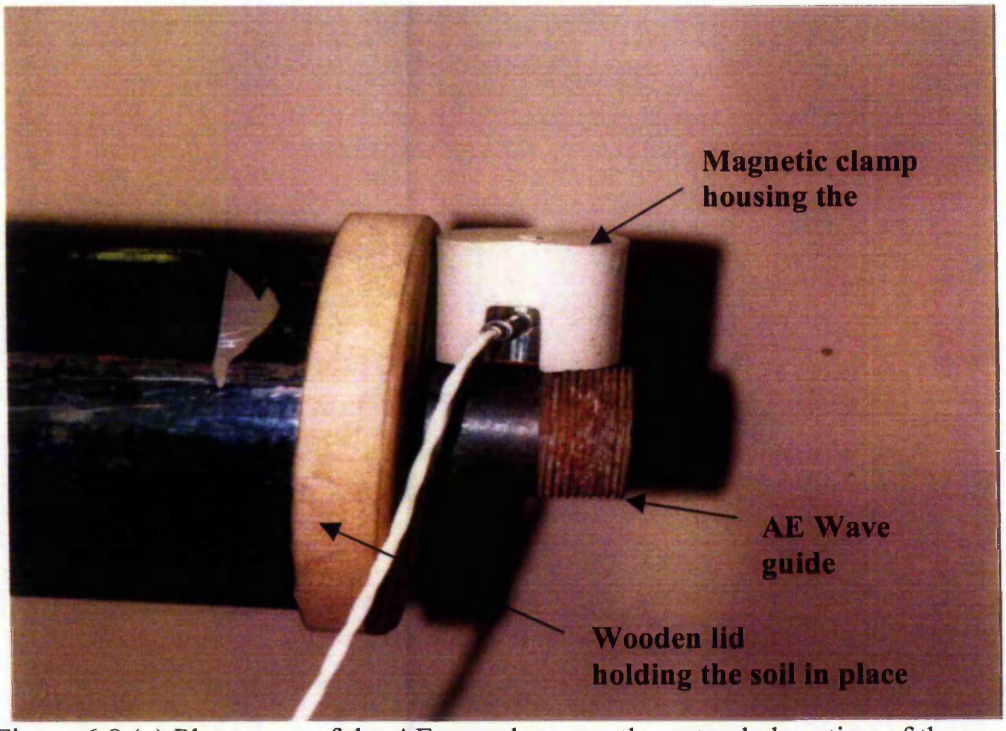


Figure 6.8 (a) Placement of the AE transducer on the extended section of the wave guide.

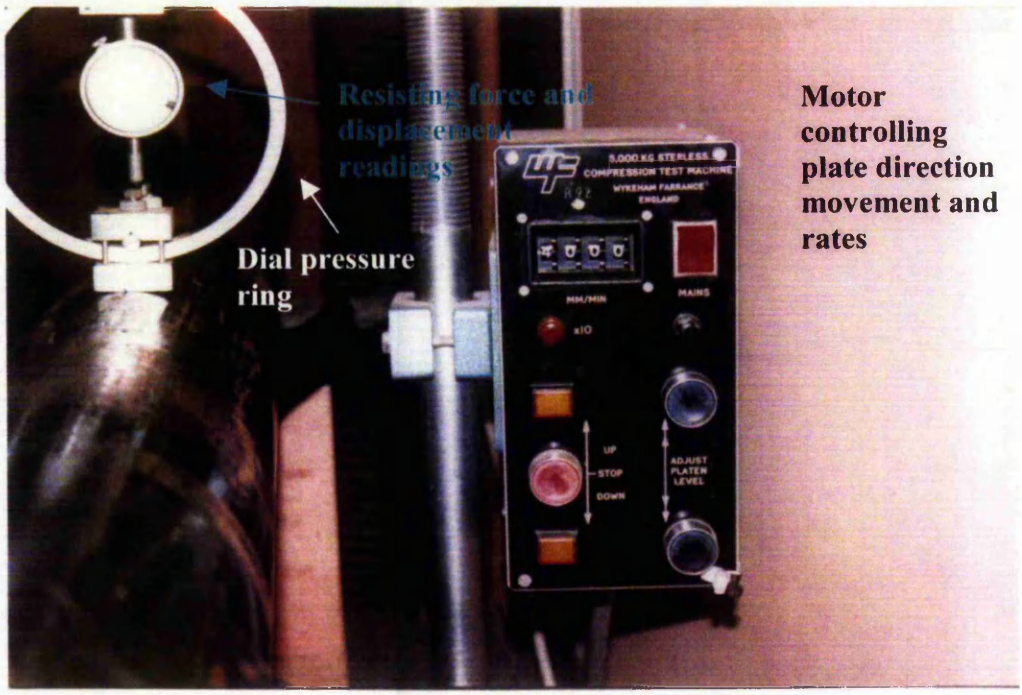


Figure 6.8(b) Active wave guide system placed horizontally through the compression test machine.

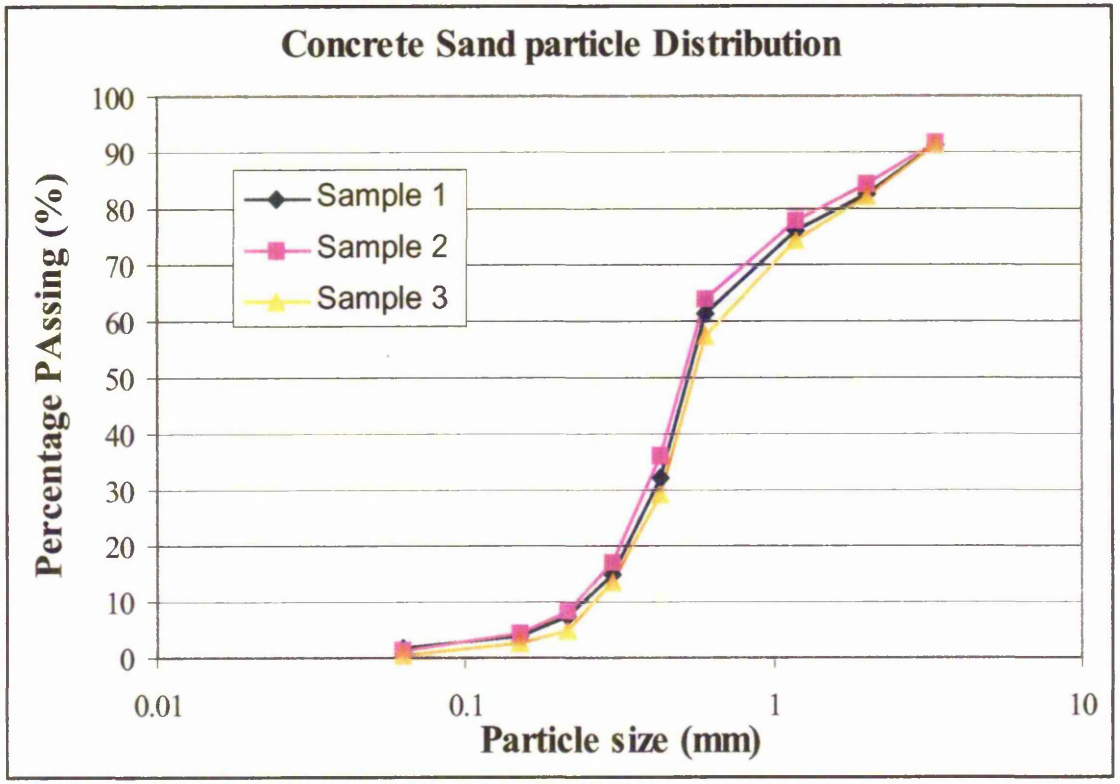


Figure 6.9 Concrete Sand particle distribution on three samples

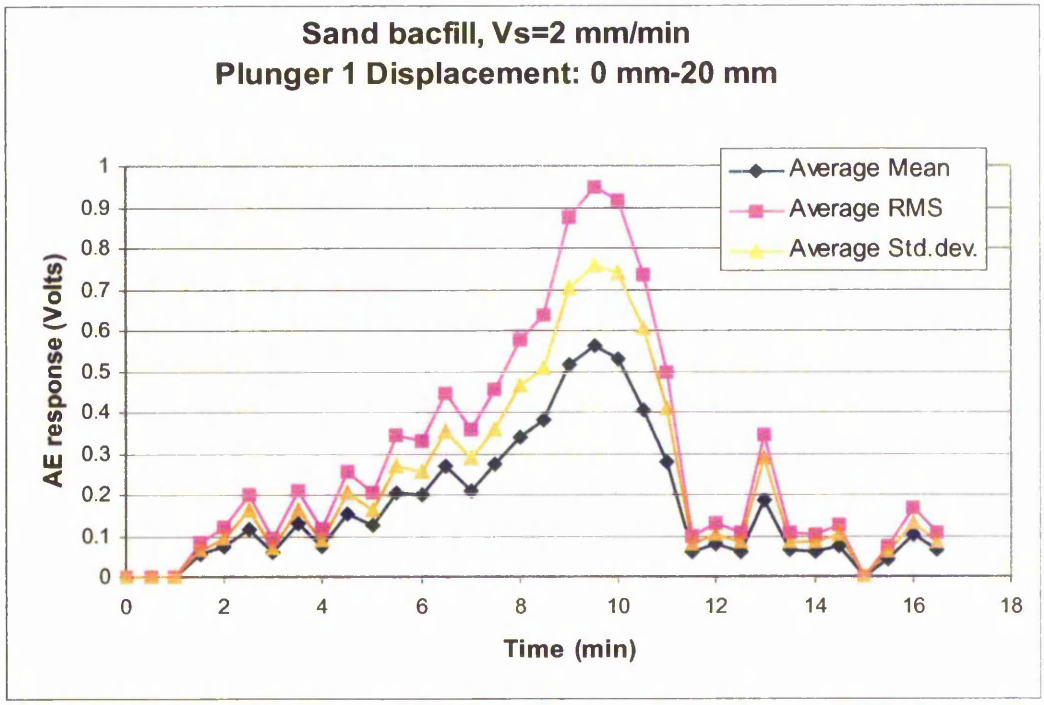


Figure 6.10(a) AE response with respect to time of sand backfill under Vs: 2mm/min (wg21a)

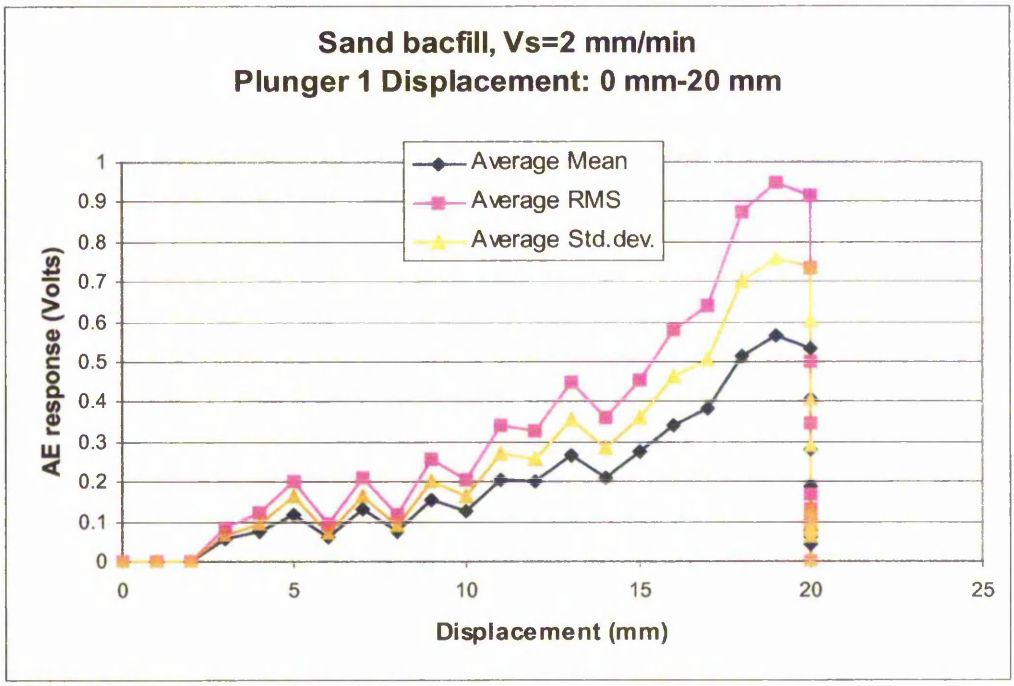


Figure 6.10(b) AE response with respect to displacement of sand backfill under Vs: 2mm/min plunger 1, (wg21a).

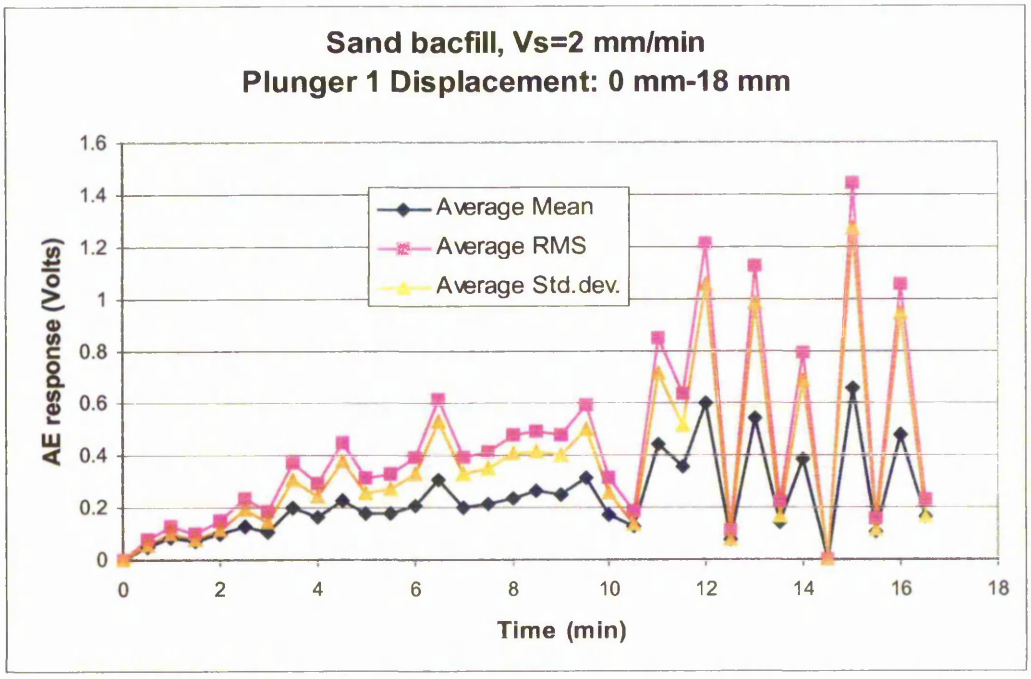


Figure 6.11 AE response with respect to time of sand backfill under Vs: 2mm/min (wg12b)

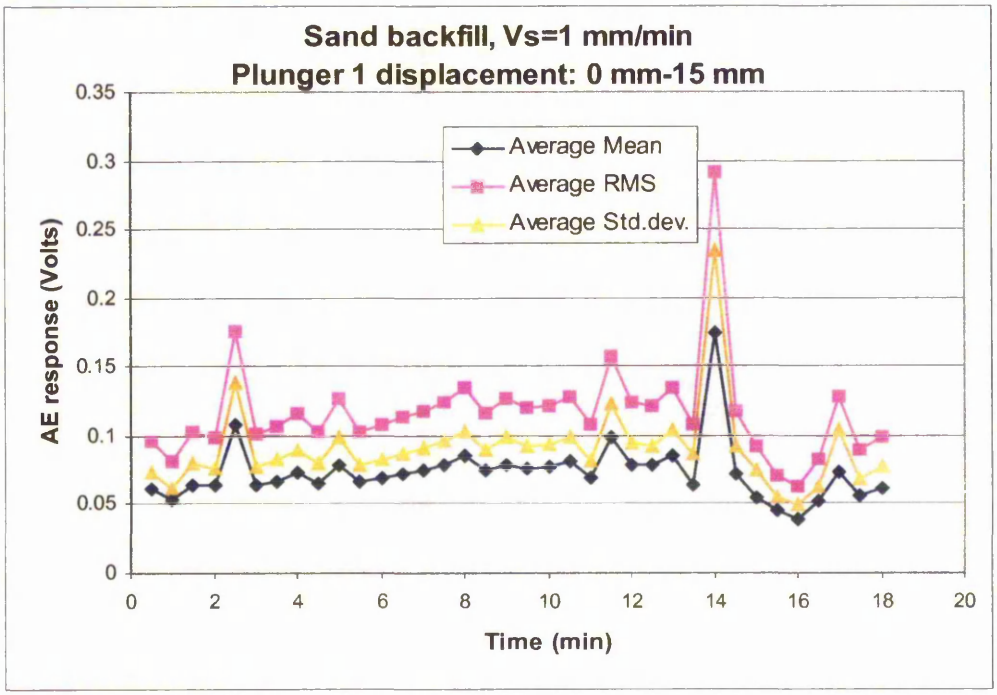


Figure 6.12 AE response with respect to time of sand backfill under Vs: 1mm/min (wg11c)

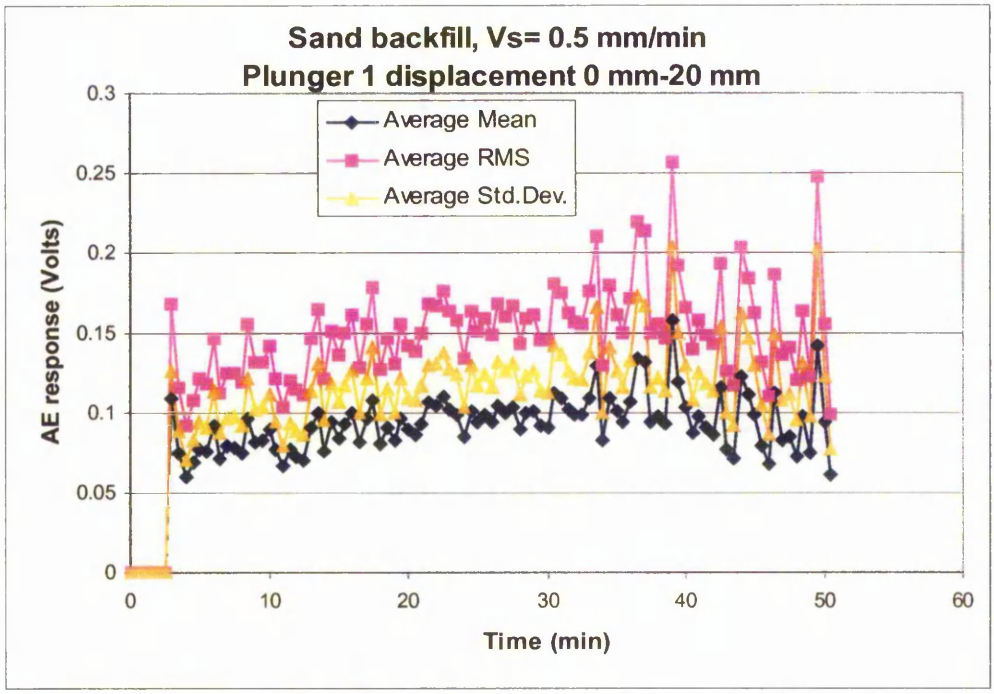


Figure 6.13 AE response with respect to time of sand backfill under Vs: 0.5mm/min (wg15a)

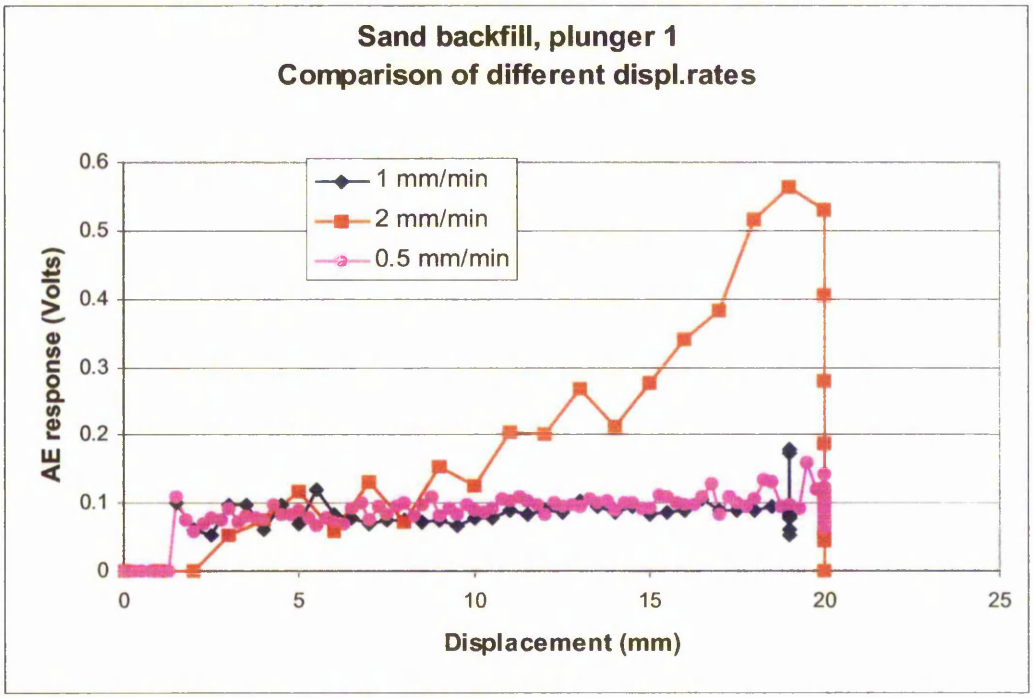


Figure 6.14 Comparison on AE levels of sand backfill under different strain rates.

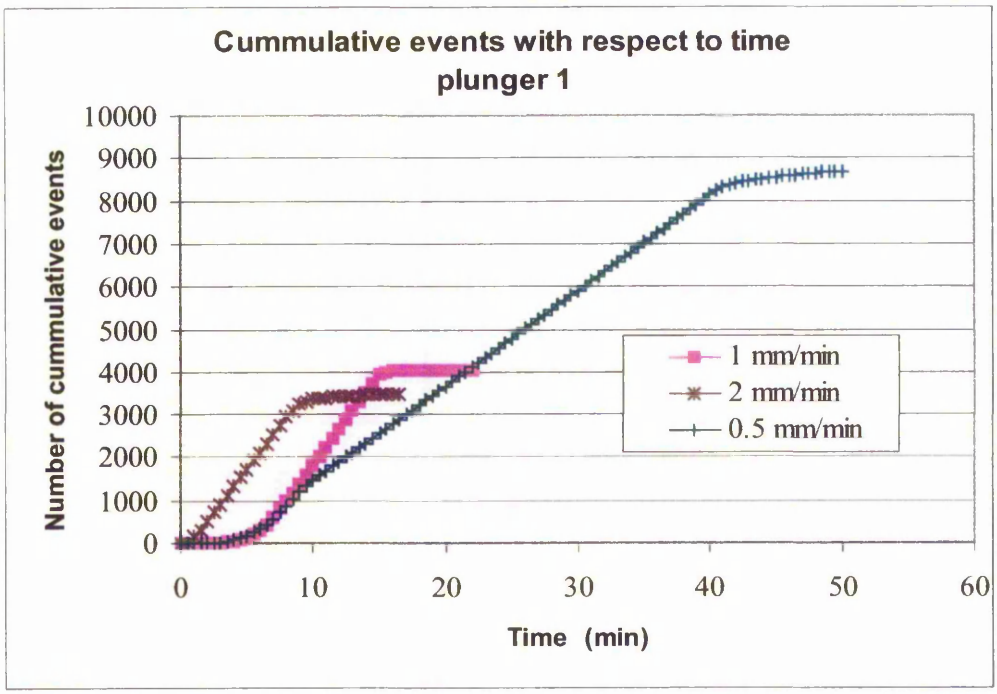


Figure 6.15( a) Comparison on cumulative event occurrence of sand backfill under different strain rates.

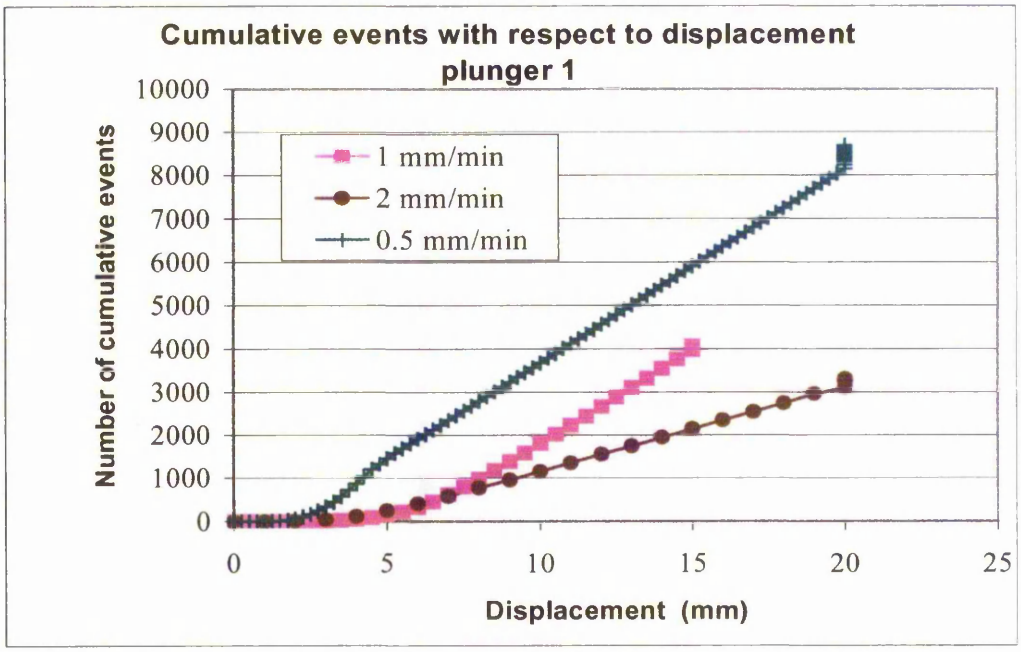


Figure 6.15(b) Comparison on cumulative events occurrence of sand backfill under different strain rates with respect to displacement.

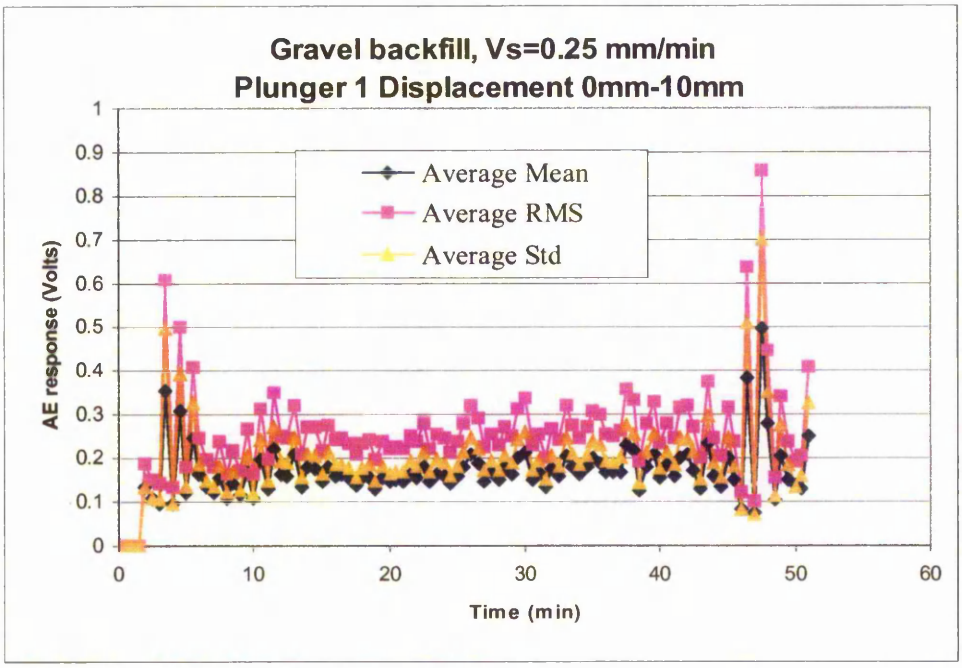


Figure 6.16 (a) AE response with respect to time of gravel backfill under Vs: 0.25mm/min (grv1D)

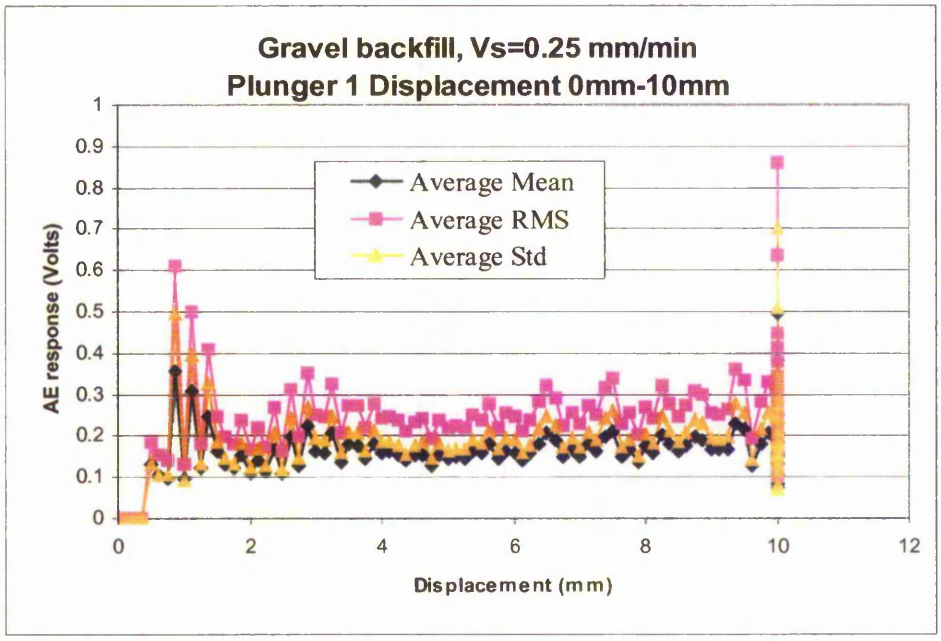


Figure 6.16 (b) AE response with respect to displacement of gravel backfill under Vs: 0.25mm/min (grv1D)

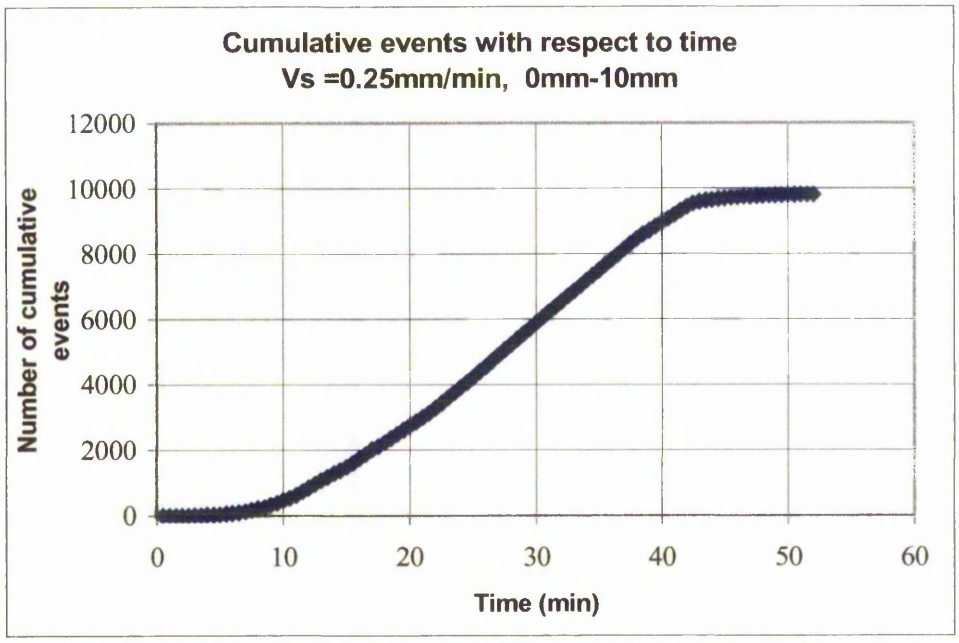


Figure 6.17 Cumulative event occurrence of gravel backfill under 0.25mm/min displacement rate of movement.(gv1D)

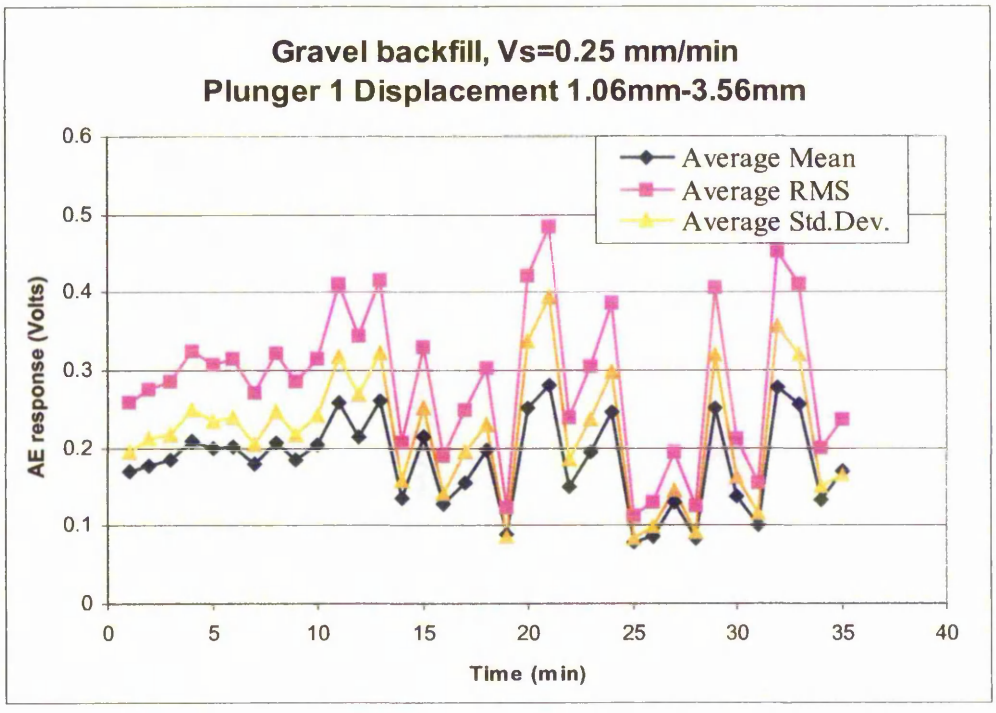


Figure 6.18 AE response with respect to displacement of gravel backfill under Vs: 0.25mm/min (grv1Dc4)

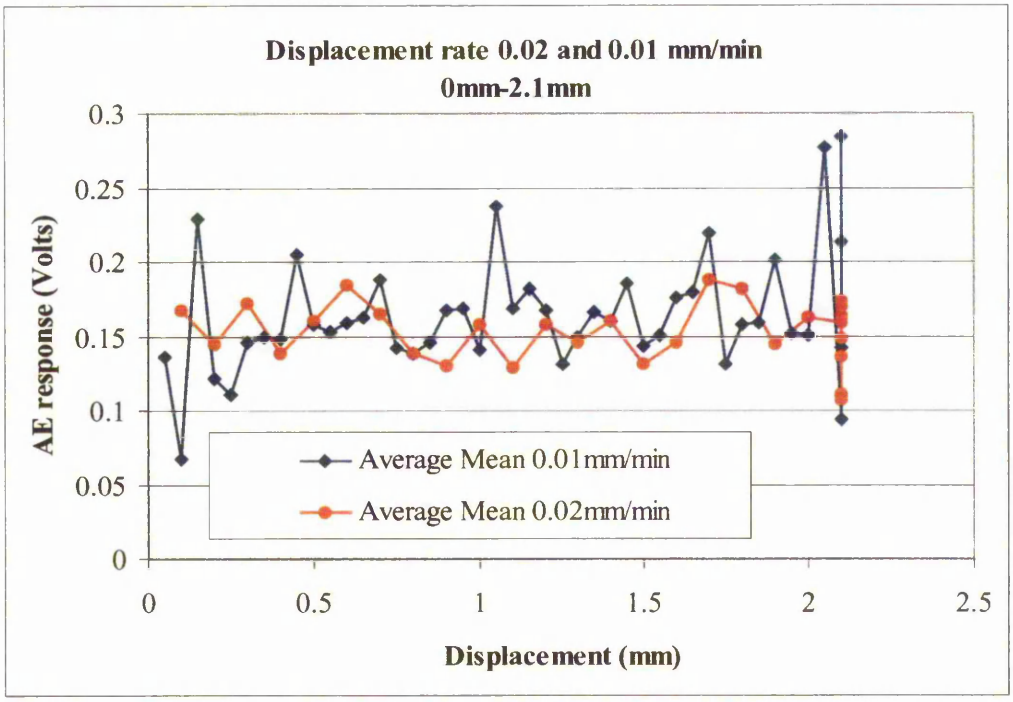


Figure 6.19 AE response with respect to displacement of gravel backfill under Vs: 0.02mm/min (Grv1Z) and 0.01mm/min(Gv1F).

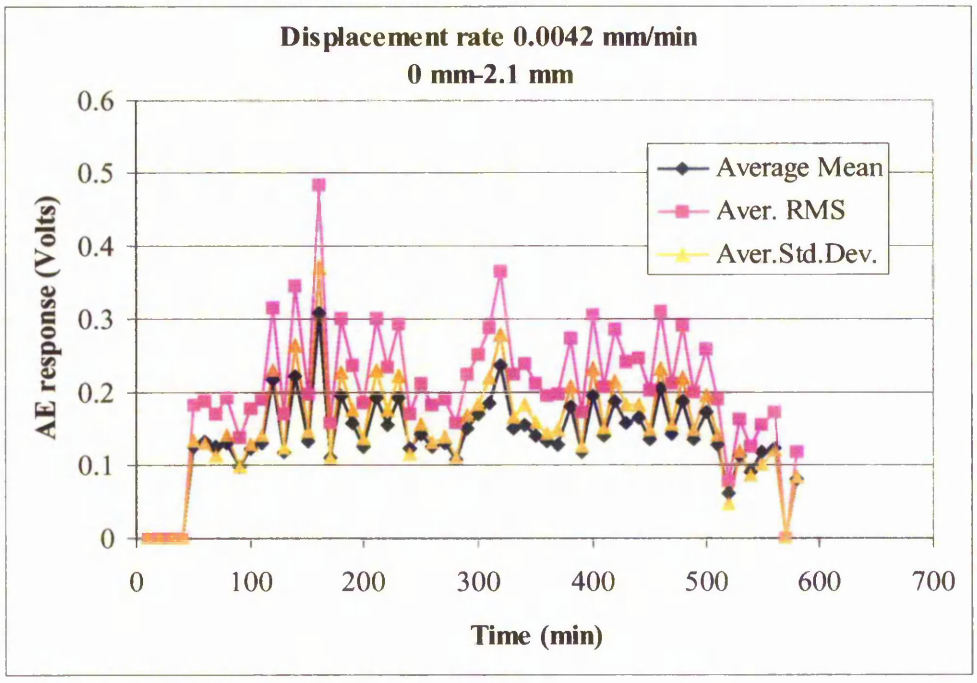


Figure 6.20 AE response with respect to time of gravel backfill under Vs: 0.0042mm/min (Grv1B).

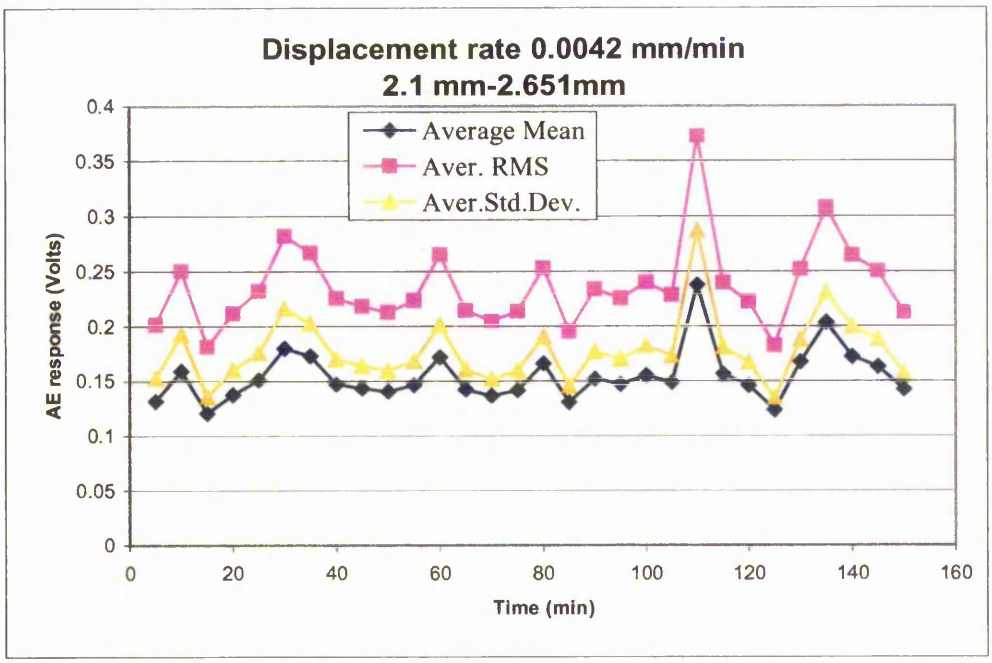


Figure 6.21 AE response with respect to time of gravel backfill under Vs: 0.0042mm/min (Grv1Bc1).

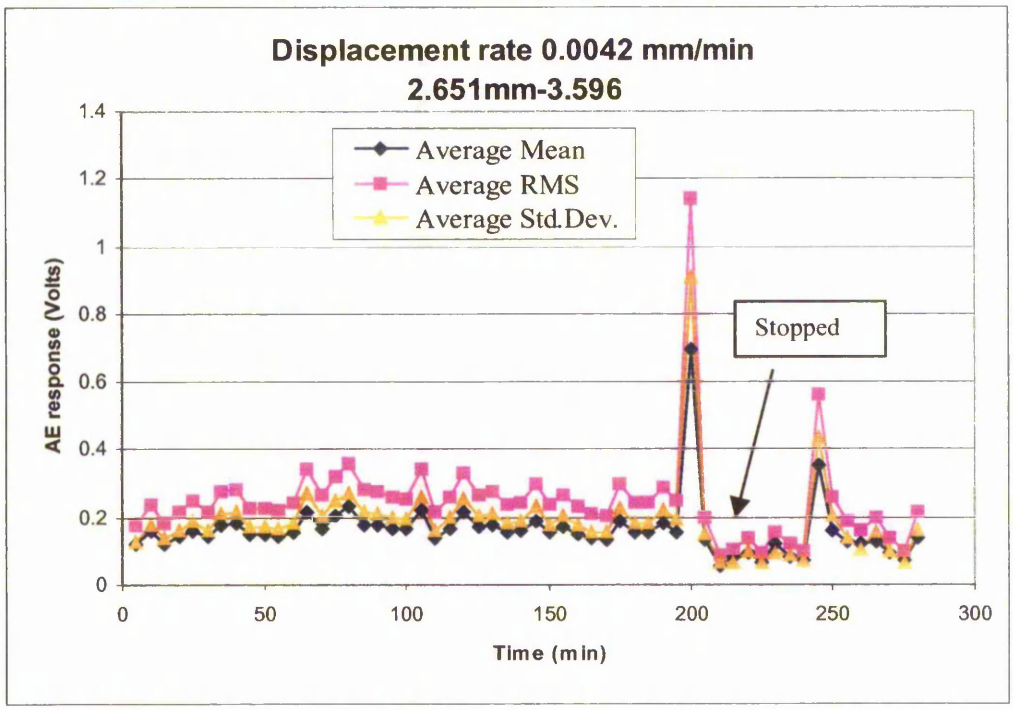


Figure 6.22 AE response with respect to time of gravel backfill under Vs: 0.0042mm/min (Grv1Bc2).

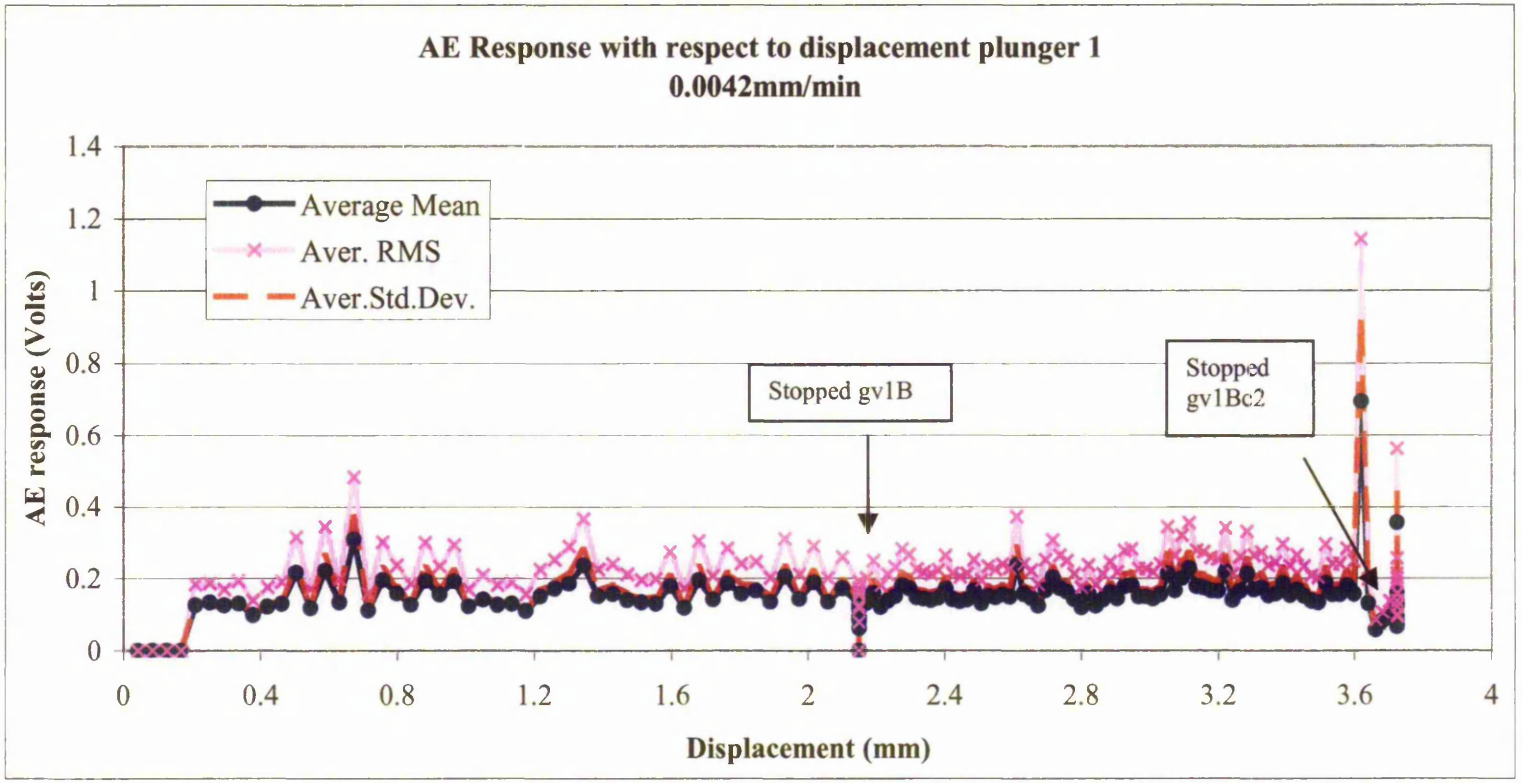


Figure 6.23 AE response with respect to displacement of gravel backfill under Vs: 0.0042mm/min.

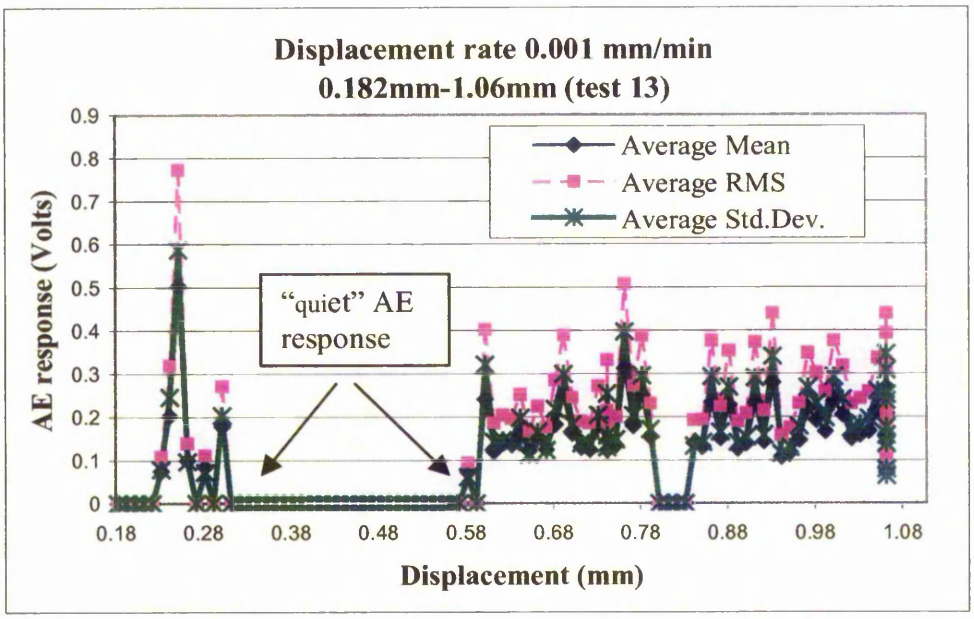


Figure 6.24 AE response with respect to displacement of gravel backfill under Vs: 0.001mm/min test 13 integrated results of 3 files.

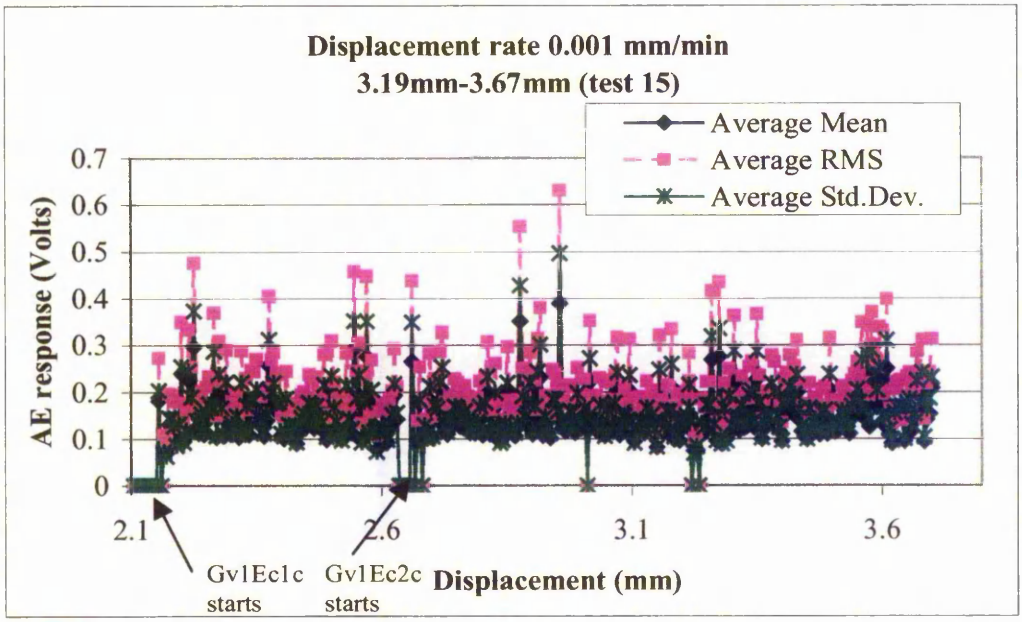


Figure 6.25 AE response with respect to displacement of gravel backfill under Vs: 0.001mm/min test 15 integrated results of 4 files.

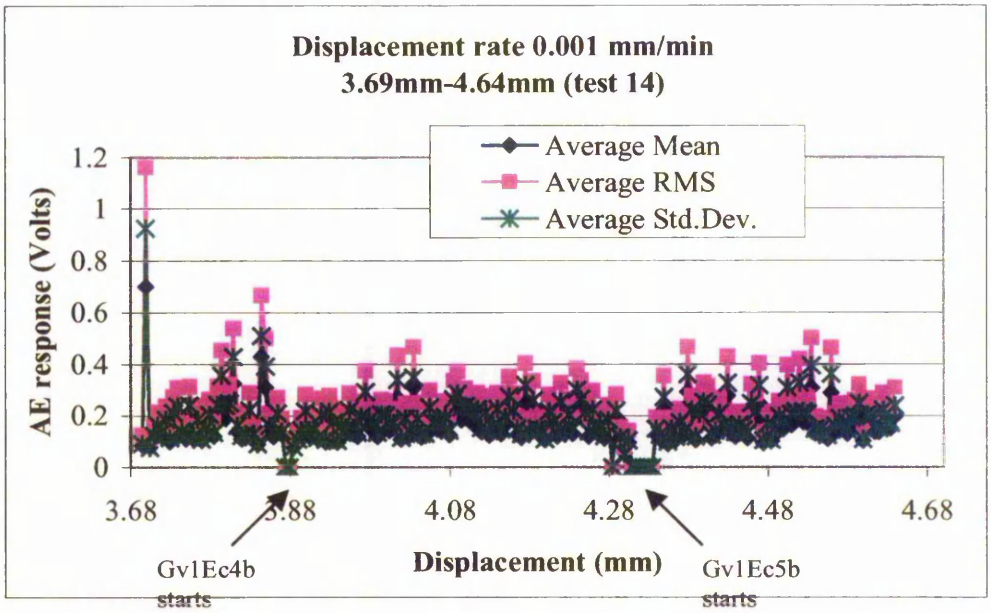


Figure 6.26 AE response with respect to displacement of gravel backfill under Vs: 0.001mm/min test 15 integrated results of 4 files.

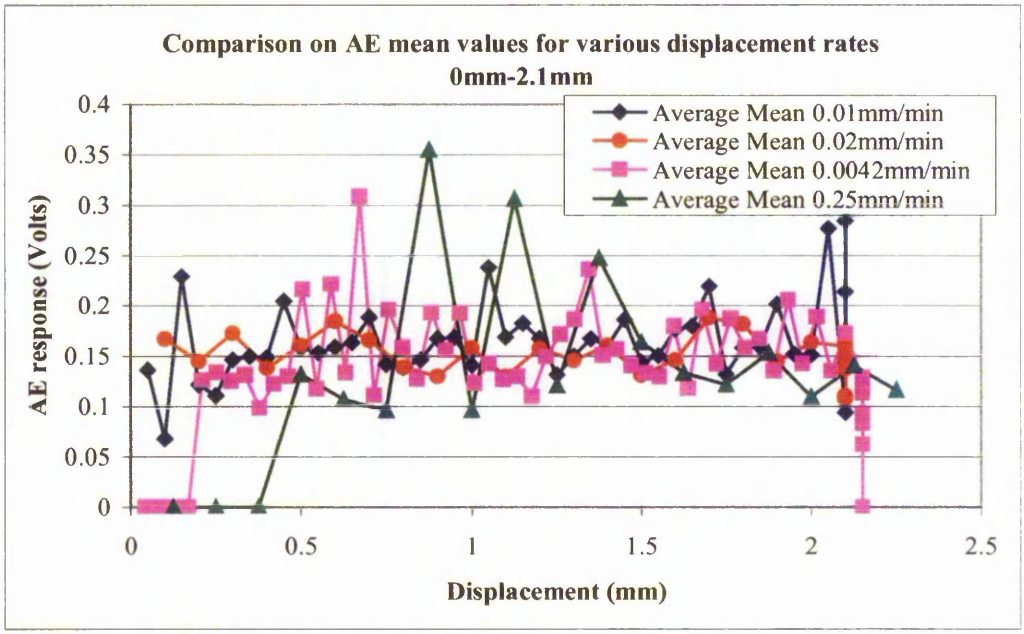


Figure 6.27 Comparison on AE response of gravel backfill under 4 different strain rates for the displacement interval 0mm –2.1 mm.

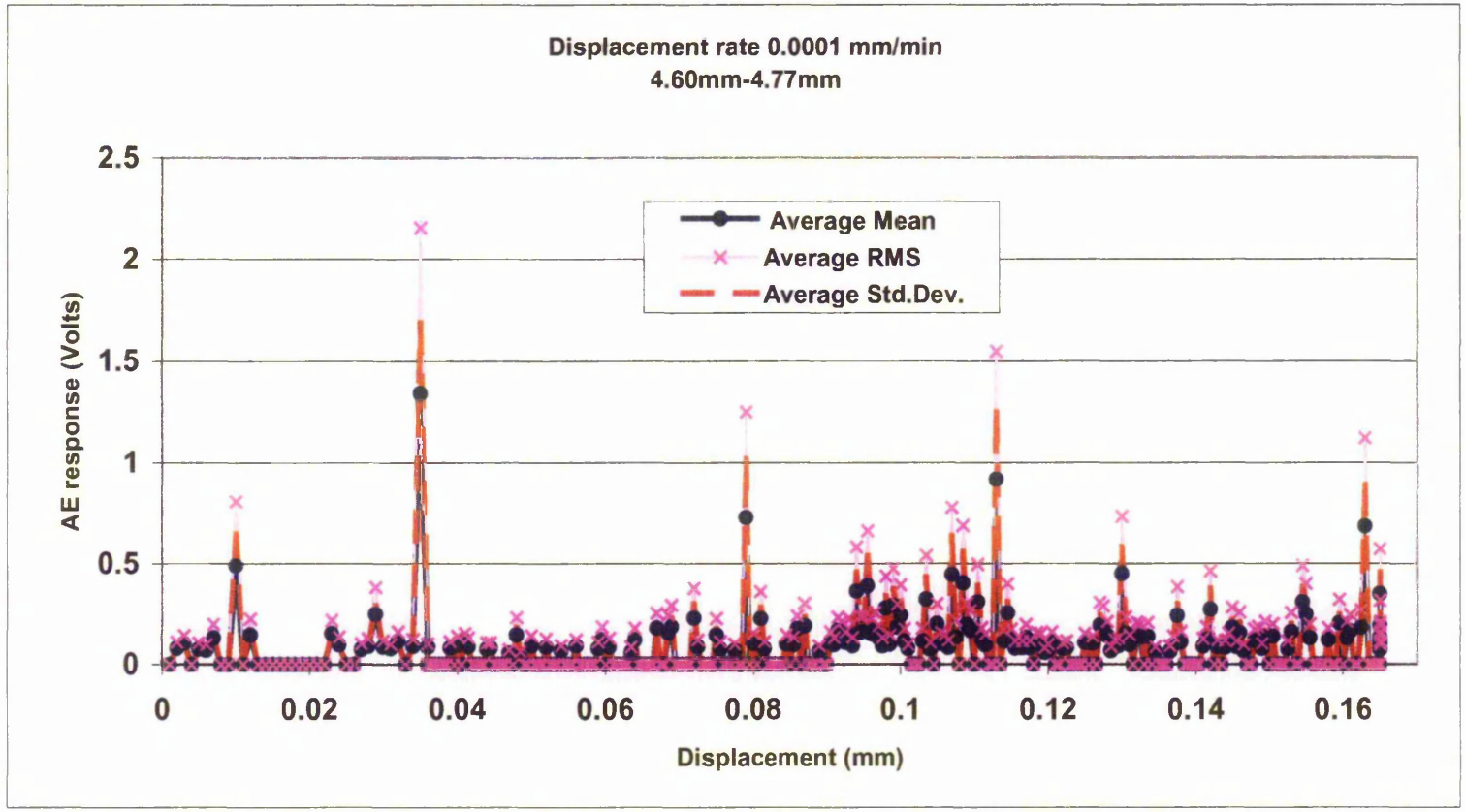


Figure 6.28 AE response with respect to displacement of gravel backfill under Vs: 0.0001mm/min test 14 integrated results of files.

# Chapter 7- Conclusions and Recommendations For Future Work

This research described in this thesis demonstrates performance of an AE monitoring system under laboratory conditions. The investigation was focused on the active wave guide system developed by Kavanagh (1997) and used for field studies of slope instability.

The instrumentation used enabled the capturing of a narrow band high frequency signal. AE signals within the frequency range of 15 kHz to 45 kHz were captured with a resonance frequency of 30 kHz. The signal propagating through at 6 mm wall thickness wave guide was investigated. The two Lamb waves modes studied were:

a) the compressive mode travelling through the steel tube with a velocity of 5500 m/sec; and
b) the shear mode travelling through the steel tube with a velocity of 3040 m/sec.

The existence of these two modes that propagate with different velocities allowed the researcher to estimate AE source location using only one sensor. Source location studies using the Pencil Lead Break (PLB) method, showed a linear relationship of the difference in arrival time between the two modes with respect to propagating distance. As the propagating length increased the difference of the arrival time was increased linearly.

Assessment of two wave guide types of connection (collar and welded) was carried out to investigate the influence on signal attenuation. The collar type of connection resulted in significant signal attenuation and shear wave mode were removed. However, for welded connection the AE signal propagated with insignificant attenuation and both the compression and shear signal modes were present. Therefore, it is suggested to use welded connection in future field studies. Welded connections will aid the engineer locate the forming slip surface in an unstable slope as the shear Lamb wave mode will propagate through connections with minimal modification.

The use of a contact shoe placed between the sensor and the wave guide surface is not recommended. The AE signal is modified by the shoe as the propagating path becomes more complicated. The presence of the contact shoe introduces new boundaries and material type to the AE signal propagation path.

Attenuation of the AE signal propagating along the steel tube wave guide was found to be within the range of 2 to 5dB per meter length. For this type of study a consisted amplitude AE events should be generated so the results could be more accurate. Therefore, this results is only preliminary.

Bending deformation of the steel wave guide emits low levels of AE events that are insignificant compared to the generated events of the soil particle frictional movement. This means that slow pre-failure movements of soil will be more evident and will be captured by the AE operator before any large mass of soil begins to bend the wave guide tube.

The soil column and G-clamp experiments on both gravel and sand backfill showed that sand emits lower amplitude AE events than gravel. It was possible to deform the sand backfill under larger displacement than gravel. The AE response levels gradually increased with cumulative displacements for the sand backfill. The gravel AE response was sporadic without any trend of increase in the AE levels.

Sand backfill when tested under controlled strain rate under the fast rate of 2mm/min demonstrated that AE response amplitude increase with displacement. A clear drop of AE amplitude levels appeared as soon as the displacement stopped. This phenomenon however was not as clear in the slower rates of movement. Under slower rates of movement the AE events emitted are smaller than 0.3 Volts.

The controlled strain rate experimental set-up was not suitable for investigating fast rates of displacement for the gravel backfill. The uplifting of the wave guide/backfill system and the delayed response of gravel did not allow AE response and displacement rates to be related.

In tests conducted at slow displacement rates below the magnitude of 0.0042 mm/min gravel begin to respond well during testing with detectable AE generated. For tests at displacement rates of 0.0042 mm/min AE levels drop as soon as displacement of the plunger stopped.

Gravel backfill generated AE at of displacement rates in the magnitude of 0.0001mm/min. This displacement rate falls in the category of extremely slow slope movements of creep.

Captured AE signals provide a reliable indication of the start and stop of displacement at these small rates. The findings of this research demonstrated that AE monitoring system is sensitive enough to detect pre-failure movements and has the potential to form an early warning system for slope instability.

The laboratory tests and studies presented in this work illustrated that the AE signal is sensitive and is affected by a number of parameters. The future experimental work should be designed to produce consistent conditions and also to represent field AE instrumentation and applications.

The experience gained in conducting this research can be used as basis for further research to develop the AE monitoring technique. A few recommendations are listed below.

It is recommended that similar source studies to those described in sections 4.4 and 4.5 using the Pencil Lead Break (PLB) method to generate a signal, be carried out with longer lengths of wave guide tubes (more than 2 m).

Studies on different type of connections between the tube sections should be extended. It was illustrated in this work, that the welded connection performed much better than the threaded collar connection. However there are difficulties and quality control problems for welding on the site. Other connections types may not perform as good as

the welded type but they may eliminate the signal attenuation and provide an easier and more practical solution for connecting the wave guide sections.

In future laboratory studies it is recommended that the wave guide and the surrounding backfill soil be kept in a vertical orientation. Keeping the active wave guide system vertically the soil will not be disturbed. This might have occurred in the current studies described in chapter 6 where the tube was laid horizontally. This way the backfill soils can also be tested in their loose state.

It is preferable to generate AE events due to a movement of a soil layer against the wave guide system (i.e. rather than a plunger). This will resemble the field conditions of an unstable mass of soil body. It is likely that more AE events will be generated, which will assist in the signal analysis and better representation of field conditions will be achieved.

The uplift problem of the tube when gravel was tested in the controlled rate set up under fast rates of displacement needs to be overcome by designing a different test set up. The backfill container needs to be clamped and held in its original position. It is suggested to make this container from a flexible material (like plastic) and not steel to allow more space for the soil particles to re-arrange similar to as it will on site in a borehole. Using a colourless plastic tube will provide an opportunity to make visual observation of particle deformation during testing.

# REFERENCES

Blystra A.R., (1990) "Using Acoustic Emission Testing in Seepage Investigations" International joint meeting 1st workshop on AE in Civil Engineering & 2nd workshop on AE and Rock Fracture Mechanics, Kumamoto, Japan, Oct. 29-31, S49-S54.

Bray, D.E.and Stanley,R.K. (1989), Nondestructive evaluation: Mc-Graw-Hill Book, Inc., New York.

CEOS/IGOS, "Landslide Hazard Team Report CEOS/IGOS Disaster Management Support Project", http://disaster.ceos.org/lanslide.htm

Chichibu A., Jo K., Nakamura M., Goto T., Kamata M., (1989) "Acoustic emission characteristics of unstable slopes", Journal of Acoustic Emission, Vol. 8, No. 4, pp. 107-112

Dixon N., Kavanagh J. and Hill R., (1997) "Monitoring landslide activity and hazard by acoustic emission", Journal of Geological Society of China, Special Publication of the Proc. 3rd Sino-British Geological Conference, Taiwan, Vol. 39, No. 4, pp. 301-327

Dunegan Engineering consultants Inc., AESMART (2000), Acoustic Emission Signal Model Analysis Real Time, web page www.calypso.com/deci/AEsmart.html

Hardy H.R, (1989) "A Review of International Research Relative to the Geotechnical Field Application of Acoustic Emission/Microseismic Techniques", Journal of Acoustic Emission, Volume 8, Number 4

Hardy H.R, Taioli F and Hager ME (1989) "Use of Mechanical Wave guides and Acoustic Antennae in Geotechnical AE/MS Studies", World Meeting on Acoustic Emission, Special Supplement, Journal of Acoustic Emission, Vol. 8, No. 1-2, S42-S48.

Hardy H.R, (1994) "Geotechnical field applications of AE/MS techniques at the Pennsylvania State University: a historical review", NDT & E International 1994, Vol. 27, No 4, pp. 191-200.

Kavanagh J.G, (1997) "The use of acoustic emission to monitor of a solid body", PhD. Thesis, Nottingham Trent University

Koerner R.M.,.Reif J.S., and Burlingame M.J., (1979) "Detection Methods for Location of Subsurface Water and Seepage", Journal of the Geotechnical Engineering Division, Proc.ASCE, Vol 105, No. GT11, 1301-1316.

Koerner R.M., McCabe W.M., Lord A.E.Jr, (1981) "Acoustic emission behaviour and monitoring soils", Acoustic Emissions Geotechnical Engineering Practice, ASTM STP 750, V.P. Drnevich and R.E. Gray, Eds., American Society for Testing and Materials, 93-141.

Koerner R.M, M, McCabe, W. Martin and Baldivieso, Luis F (1981) "Acoustic Emission Monitoring of Seepage", Journal Geotechnical Eng., ASCE, Vol. 107, No. GT4,521-526.

Lowe M.J.S., Alleyne D.N., Cawley P., (1998) "Defect detection in pipes using guided waves", Ultrasonics, Vol. 36, pp. 147-154

McCauley M.L., (1977) "Monitoring Slope Stability with Acoustic Emission", Proc. 1st Conference on Acoustic Emission/Microseismic Activity in Geologic Structures and Materials, Pennsylvania, June 1975, 257-269.

Maji A.K., Satpathi D., Kratochvil T., (1997) "Acoustic emission source location using lamb wave modes", Journal of Engineering Mechanics, Vol. 123, No. 2, pp. 154-161

Maji A.K, and Kratochvil, T. (1994) "Acoustic emissions, possibilities for monitoring bridges." Scancella and Callahan, eds. Proc. Struct. Mat. Technol., NDT Conf.Technomic Publishing Co., Lanchaster,Pa.,124-130.

Nakajima I., Negilshi M., Ujihara M. and Tanabe T., (1991) "Application of the acoustic emission monitoring rod to the landslide.", Measurement, Pennsylvania State University

Obert L. (1941), "Use of Subaudible Noises for the Prediction of Rockburst", Report Invest. 2555, United States Bureau of Mines.

Obert L. and Duvall W. I., (1946) "Microseismic Method for Predicting Rock Failure in Underground Mining: Part I and Part II, Report Invest. 3897 and 3803, United States Bureau of Mines.

Silk M.G. and Bainton K.F., (1979) "The propagation in metal tubing of ultrasonic wave modes equivalent to Lamb waves, Ultrasonic , Vol. 17, pp.11-19.

Shuster, R.L. and Krizek, R.J. (Eds) (1978) Landslide
Analysis and Control Special Report 176. Transport Research Board, National
Research Council. pp234.

Terzaghi K., (1950) "Mechanism of landslides", Application of Engineering Practice, S. Paige, Ed., Geological Society of America, Berkey, pp. 83-123

Viewdac Users Manual Keithley (1998).

Wood B.R.A and Harris R.W, (1990) "Acoustic Emission Monitoring Activity Caused by Mine Subsidence", The International Joint Meeting, 1st Workshop in Civil Engineering and 2nd Workshop on AE and Rock Fracture Mechanics, Kumoamoto, Japan, October, S29-S34

Yuda S.,Hashimoto Y.,Takahashi K. and Kumagai M., (1984) "Prediction of Slope Failure by Acoustic Emission Technique", Proc 7th International AE Symposium, Japan, 660-667.

Ziola S.M. and Gorman M.R. (1991) "Source location in thin plates using cross correlation." J.Acoust. Soc. Am. Vol.90, No.5 November 1991.

# Appendix 1

## List of published papers

1. Kousteni A, Dixon N., Hill R. "Application of Acoustic Emission Monitoring System for Detecting Slope Instability" Proc. of Young's Geotechnical Engineers Symposium, University of Newcastle, April 1998.

2. Hill R., Dixon N. Kousteni A., Kavanagh J, " Application of Acoustic Emission for Studies of Soil Deformation: Case Studies and New Developments" Proc. Of the World Conference, Hawaii, August 1998.

3. Kousteni A., Hill R., Dixon N., Kavanagh J, "Recent Development in the Application of Acoustic Emission Techniques for Monitoring Soil and Rock Masses".Proc. of International Symposium on Slope Stability, Matsuyama, Shikoku, Japan, November 1999.

**Paper 1**

# LABORATORY INVESTIGATION OF ACOUSTIC EMISSION WAVE GUIDE SYSTEMS FOR DETECTING SLOPE INSTABILITY

BY ANNA KOUSTENI
NOTTINGHAM TRENT UNIVERSITY

## INTRODUCTION

The standard method of assessing the stability of slopes is by measuring ground, deformations. At present using traditional methods such as surface survey markers, or inclinometer tubes installed through the potentially unstable soil/rock, the aim is to detect movements as early as possible. Unfortunately the magnitude of the pre-failure deformations which are of interest are often of the same order as the accuracy of the above methods. This research project is part of an ongoing investigation into the application of acoustic emission (AE) techniques to the geotechnical area for detecting unstable slopes.

## BACKGROUND

Acoustic emission is a relatively recent non-destructive technique which since the 1930's has been used to study rock mass behaviour, and since the 1970's it has been increasingly employed to monitor the stability of soil bodies. The main body of research into AE applications for soil assessment has been carried out in the USA (Koerner el al. 1981), Japan (Chichibu et al. 1989) and more recently at Nottingham Trent University (Dixon el al. 1994, 1997). Solids when deformed generate low level seismic activity at locations of local instability. The associated stress waves propagate from the source of the instability through the surrounding material and can be detected by suitable transducers. Figure 1 illustrates the AE instrumentation set-up applied in the field. The AE detected by a transducer are processed in order to obtain information about the character and location of the source.

## ATTENUATION AND WAVE GUIDES

Soil and rock deformation can be detected by using the AE technique, which in a number of field trials has been shown to provide an early warning of instability. However, the attenuation of AE energy through geological material is high and this has led to the use of wave guides. Wave guides are steel rods or tubes, or any material with low attenuation to increase the sensitivity of the measuring system and to maximise the volume of soil monitored. The wave guide could be in direct contact with the host soil if it is driven in. This is a desirable situation but this method is not feasible especially at large depths. Therefore a borehole is introduced to accommodate the wave guide and which is then filled with a backfill material to improve the contact conditions between wave guide and host soil. Depending on the backfill soil, the wave guide system is classified as active or passive if sand or clay is used respectively.

## DEVELOPMENT ON AE INSTRUMENTATION DESIGN

Field and laboratory studies indicate that: i) the AE monitoring technique can provide an Engineer with an early indication that small deformations are taking place during progressive failure; ii) even in "quiet" material, such as clays, levels of AE can be related to deformation rates and iii) the choice of wave guide system is of fundamental importance (e.g. active (noisy) wave guides are best suited for the study of slopes formed in clay soils). However, quantitative assessment of AE at an early stage is still basic (i.e. qualitative methods such as low AE indicates small movement, moderate AE indicates larger movement and high AE indicates instability are still in use). Therefore, laboratory studies are in progress in order to provide a detail understanding of wave guide systems, as this will lead to a better quantitative assessment of field AE.

## FUTURE WORK

A series of laboratory tests are planned with the aim of examining the AE response of the soil and the factors controlling instrumentation design. These factors include wave guide material type; the type of the backfill soil placed around the wave guide, and the method of wave guide construction. Further research and development is still required on methods of capturing and processing AE data. Such as setting a suitable trigger level which will allows continuous field monitoring and develop methods on analysing the captured signal in order to locate the source. The results of this work could lead to an improved design of wave guide system for field monitoring.

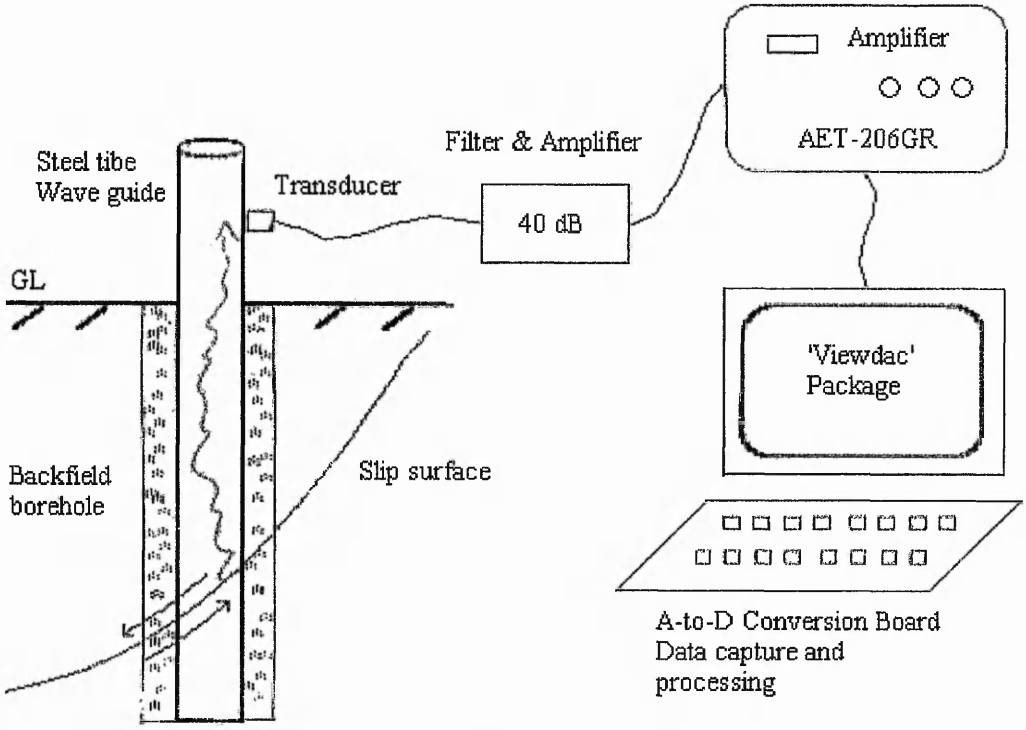


Figure 1: Schematic illustration of an AE instrumentation system for field monitoring

REFERENCES

Chichibu ,A., Nakamura, K.J.M. & Kamata, M.(1989) Acoustic emission characteristics of unstable slopes. *J. of Acoustic Emission*, 8,4, 107-112.

Dixon, N., Hill, R. & Kavanagh, J. (1994) Acoustic emission techniques for assessing deformation of soils. *Proc. Int. Symp, on Prefailure Deformations Characteristics of Geomaterials,* Sapporo, Japan, 1, 253-258.

Dixon, N., Kavanagh, J. & Hill, R. (1997) Monitoring landslide activity and hazard by acoustic emission. J. of *the Geological Society of China*, Special Publication of the Proc. 3rd Sino-British Geological Conference, Taiwan, 39, 4, 301-327.

Koerner, R.M., Lord, A.E. Jr. & McCabe, W.M. (1975) Acoustic emission studies of soil masses in the laboratory and field. *Proc. of the 1st Conf: on Acoustic Emission/Microseismic activity in geologic structures and materials* 243-256.

**Paper 2**

# APPLICATION OF ACOUSTIC EMISSION FOR STUDIES OF SOIL DEFORMATION : CASE STUDIES AND NEW DEVELOPMENTS

ROGER HILL*, NEIL DIXON + , JOHN KAVANAGH +, ANNA KOUSTENI +

*Centre for Research in Materials
+Department of Civil and Structural Engineering
The Nottingham Trent University
Clifton Campus Nottingham, NG11 8NS

## ABSTRACT

Acoustic emission techniques have been developed for field studies of soil deformation and slope failure. Field studies are reported measuring Acoustic Emission generated during cliff failure and the failure of an artificial slope. Measurements demonstrate the AE technique is sensitive to and gives warning of impending failure. The philosophy of measurement is discussed.

Issues relating to the use of active or passive waveguides have arisen. These issues are discussed and recent developments considered.

## INTRODUCTION

Acoustic Emission from soils has been studied over a period approaching four decades with perhaps the earliest work reported by Beard [1] . Work was carried out, notably, by Koerner and Lord over a period of perhaps fifteen years. [2,3,4]

One of the characteristics of Acoustic Emission as a technology is the sensitivity to changes in the material under test and this is no different when testing soils. The characteristic of the soil is the expected high variability since a natural material is being monitored. Acoustic Emission can be used as a laboratory tool to monitor and derive additional information on the deformation of soils, but the aim has usually been to use the technique in the field. This is a goal fraught with difficulty.

Since the work of Koerner and Lord, instrumentation capability has moved on, so the potential of AE to monitor soil deformation effectively and in a sophisticated way is perhaps better than it has been in the past. Having said that, development of AE for soil deformation monitoring, remains a challenging goal.

The initial intention of our work has been to develop instrumentation and apply that in the field to validate AE. Following on from this, work is attempting to consolidate our experience and gain a better understanding of how the technique can be developed.

At present, the standard method for assessing the stability of both natural and man-made slopes is by measuring ground deformations. Whether using surface survey markers, or inclinometer tubes installed through the potentially unstable soil / rock mass, the aim is to detect movements as early as possible. Unfortunately the magnitude of the pre-failure deformations, which could be used to assess the likelihood of catastrophic failure, are often of the same order as the accuracies of the above methods.

In the case of AE, it provides the possibility of orders of magnitude increase in sensitivity. At present the challenge is to transfer AE data into meaningful information on the magnitude of deformation. Even without that, monitoring data accompanied by gathered experience from real life situations will provide the confidence to see AE applied more often for pre-deformation monitoring of soil.

## INSTRUMENTATION

Since effective front end instrumentation was available, our work made use of this. Detection was via an AC30, AET Acoustic Emission sensor, using the AET204GR Acoustic Emission instrument. The sensor had a resonant frequency of 30kHz, which is perhaps higher than that used by some workers. This frequency provides effective immunity from environmental noise.

The AE voltage output was monitored in the form of the AE signal envelope using a Keithley DAS1402 board running at 100kHz sampling rate maximum in a portable computer.

## SITE 1 - COWDEN CLIFF-TOP

The Cowden field test was conducted using a section of coastal cliff situated some 800m from the Building Research Establishment's (BRE) test site at Cowden, in the Holderness Plain on the East Coast of England. The geology consists of a Cretaceous chalk plateau overlain by 20 to 30m of glacial till deposits which are currently considered to consist of three units. From the bottom up, these are the Basement Till, the Skipsea Till and the Withernsea Till.

The site was chosen for a number of reasons.
i) High erosion rates generated by the action of the sea meant that a slope failure was expected to occur in the near future.

ii)The glacial till had a high sand content which would make it acoustically noisy and more amenable to AE measurement. The site was also remote and not subject to man made noise.

## INSTRUMENTATION INSTALLATION AND RESULTS

A total of twelve 50mm diameter steel tube waveguides (WG) were installed during September 1993. Inclinometer tubes were also installed as a measurement reference. The plan of the location of these waveguides is given in figure 1. An illustration of the mode of failure of such a site is given in figure 2.

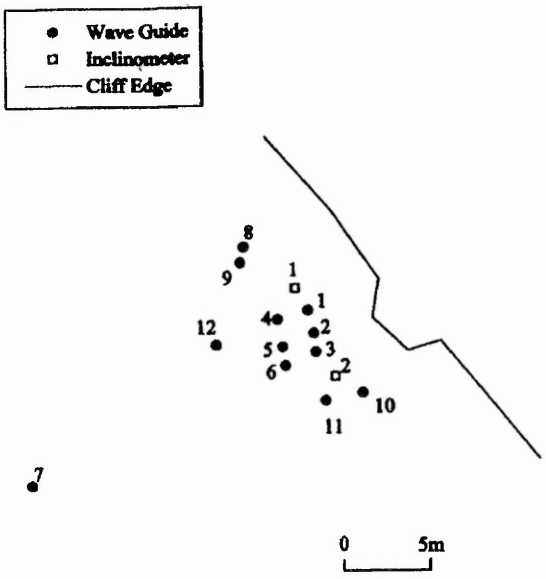


Figure 1 : Waveguide locations at Cowden cliff-top test site (plan view). Cliff edge runs NW to SE.

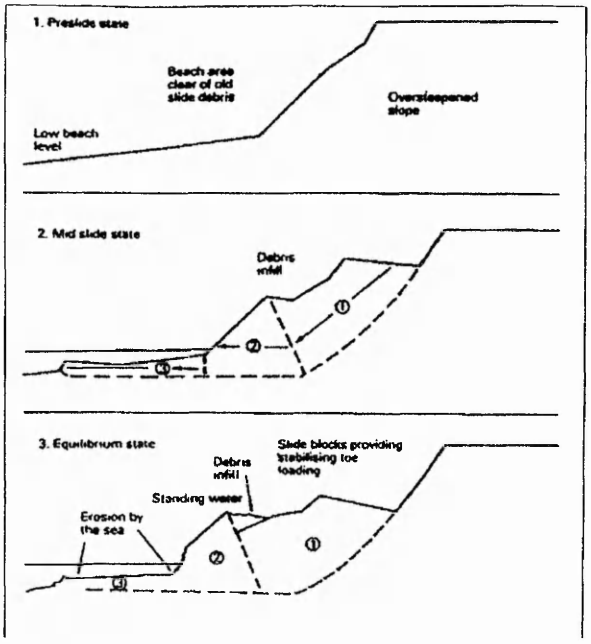


Figure 2 : Typical mode of failure at the Cowden site.

A number of waveguides penetrated 20.5m to intersect the basal shear surfaces. The remainder were installed at depths from 6 to 12 metres. The waveguides were installed in 150m diameter boreholes with the annulus between the borehole and the waveguide filled with either, bentonite grout, medium sand or fine gravel.

Inclinometer readings indicated that pre-failure slope movements were occurring. AE data was accumulated through the winter of 1993/94. A major slope movement (through the middle of the test site!!) occurred in April 1994 which made the site unusable. The trend in AE for three waveguides is shown in figure 3. This rise in the area under the AE signal (monitored for 3 minutes on each occasion) mirror the movement of the inclinometer tubes. Waveguides 1,2 and 3 were in the cliff section which slipped. A number of measurements of AE signal were tried, but area under the AE signal appeared to give the most reliable measure of slope movement.

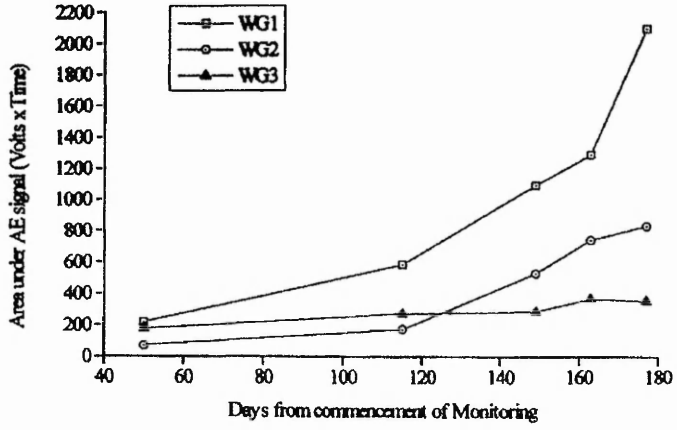


Figure 3 Normalised cumulative area of the AE data in excess of WG12.
WG1- sand backfill. WG2-gravel backfill. WG3-bentonite backfill.

The order of the AE data in figure 3 (sand/ gravel/ bentonite) suggests the backfill has a part to play in effective monitoring of AE.

The Cowden field trial proved that AE waveforms could be recorded using portable instrumentation. A direct relationship was established between AE from an active waveguide system , indicated by the area under the waveguide envelope and the rate of slope movements However, due to the slope starting to deform before the AE monitoring system was fully operational, this trial did not establish whether such a system could detect the onset of failure at an early stage.

## WAVEGUIDES

The design of the waveguides used at the Cowden site was dictated by a number of factors. The likely failure slope could have been up to 20m below the cliff-top and is was desirable that the AE waveguides be very near to or intersect the slip surface. In this case, this meant waveguides of 20m length which had to be installed in boreholes which were then consolidated in position using three kinds of backfill (sand/ gravel/ bentonite).

The tacit assumption is often that the waveguide monitors a volume of material. Where surface monitoring is attempted, then for given level of AE activity, without a waveguide, a detectable hemisphere of material would exist. The radius of this hemisphere would depend on the attenuation coefficient applicable to the sound at a particular frequency. The presence of a waveguide would extend this range down into he soil mass and makes AE monitoring effective down beyond the tip of the waveguide under normal conditions.

The assumption made here is that the emissivity of a particular soil material will generate signals of sufficient amplitude to propagate effectively into the waveguide. The data presented in figure 3 suggests the AE activity is highly dependent on back fill, in this case, with the more emissive back fill generating the AE. Our view is that at 30kHz, the soil mass does not propagate significant amounts of detectable Acoustic Emission to the waveguide wall. If this were the case, then bentonite might be expected to provide the best AE data. Koerner has presented data which suggests saturated clay might have an ultrasound attenuation coefficient of 100dB/m rising to perhaps 1000dB/m at 30kHz for sandy material. Clearly, the safer view is that the AE at 30kHz arises due to interaction of the backfill with the wall of the waveguide. The waveguide appears to be acting as a large sensor responsive to the interaction of the backfill particles with the waveguide wall as the soil mass undergoes complex elastic deformation as it approaches failure.

The ideas discussed above caused us to develop the idea of two possible kinds of waveguide:

i) an "active waveguide" where a feature in the design is responsible for Acoustic Emission generation. In our case this was simply the backfill material. This type of design may be most appropriate where the solid mass (soil) has a low AE emissivity or a high ultrasound attenuation at the measurement frequency

ii) a "passive waveguide", perhaps more suitable for monitoring rock, where it is clear that AE generated in the rock mass does have the ability to propagate to the waveguide, or even a surface transducer and be detected. The intrinsic attenuation in these materials will be orders of magnitude lower.

## SITE 2 - ARLESEY CLAY QUARRY

The village of Arlesey is located in a region famous for the clay used in the making of construction bricks. The site consisted of Gault clay, which is a heavily over consolidated dark-blue grey stiff to very stiff clay with closely spaced fissures (BS 5930).

Seven waveguides and two inclinometers were installed. Details are given in table 1.

| Instrument Type | Instrument Code | Instrument Depth (mbgl) | Instrument Material | Instrument Backfill |
|---|---|---|---|---|
| | | | | |
| Wave Guide | WG1 | 7.09 | Steel Tubing | Gravel |
| Wave Guide | WG2 | 6.63 | Steel Tubing | Sand |
| Wave Guide | WG3 | 7.09 | Steel Tubing | Grout |
| Wave Guide | WG4 | 2.68 | Steel Bar | Driven |
| Wave Guide | WG5 | 2.89 | Steel Tubing | Sand |
| Wave Guide | WG6 | 6.69 | Plastic Tubing | Sand |
| Wave Guide | WG7 | 2.84 | Steel Tubing | Sand |
| Inclinometer | I1 & WGi | 9.00 | Aluminium | Grout |
| Inclinometer | I2 | 9.00 | Aluminium | Grout |

Table 5.1 - Arlesey test site instrumentation (mbgl - metres below ground level). Inclinometer I1 was also utilised as a wave guide for a large part of the test.

Table 1 : Arlesey test site instrumentation. (mbgl - metres below ground level).

The face of the slope in this case was 4.5 to 5.5 metres in height. and approximately 16m in length. Five cuts were made to the clay slope as indicated in figure 4, which shows the plan of the waveguide positions and the cuts.

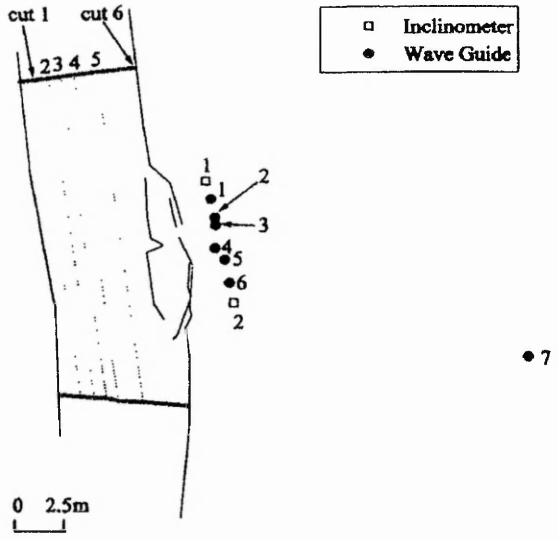


Figure 4 : Arlesey test slope, instrumentation positions and six test cuts. Measurements done October 1994 to February 1995

A sample of Acoustic Emission Data is shown in figure 5, taken from waveguide 1, with the data from waveguide 7, which is well away from the failing slope, acting as "control". The AE response to the cuts into the test slope, is clearly seen, with the response being greater, for the later, more severe cuts.

One issue which causes variability in the data is the time between the taking of AE data. The AE data from each waveguide is sampled separately and if the deformation have a slip stick characteristic, then detectability of AE may be obscured. With a clay of this type, deformation processes are assumed to be slow and the data seems to justify this assumption.

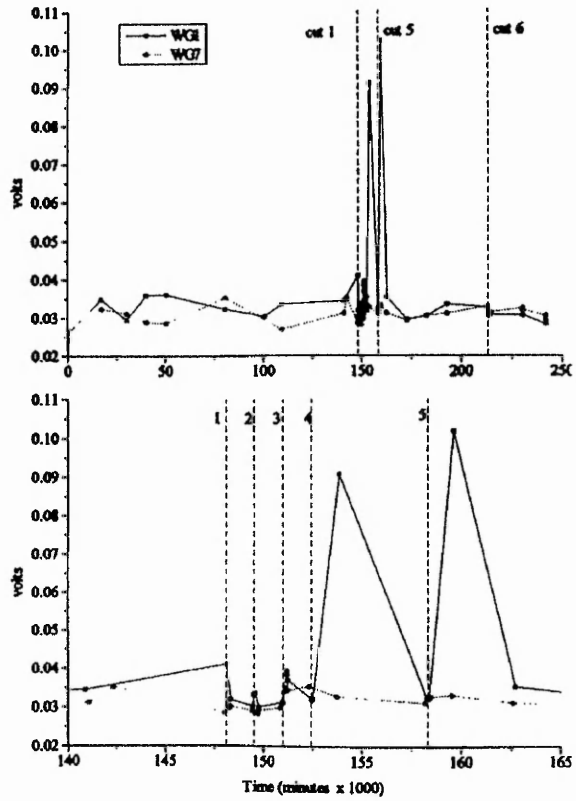


Figure 5 : Arlesey Test site. mean AE signal values for WG1 and WG7 ("control")

## DEVELOPING WAVEGUIDES

Our work suggests that the waveguide may be an important component for effective AE detection from soils. Clearly, some work on developing these devices would enhance the capability of AE. Our work is currently considering wave propagation in a cylindrical steel waveguide.

The point of excitation, when monitoring AE, will be some way down the waveguide and if our model is correct, will consist of a frictional source in contact with the waveguide surface (possibly sand). Movement of the soil mass will result in movement of this particle against the waveguide surface and an AE signal. This frictional source will generate AE in the waveguide wall which will propagate as Lamb wave modes.

It is well known that the wave arrivals and the resulting waveforms are complex

Figure 6 shows waveforms for pencil lead sources on the surface of the waveguide. In case a) the source pencil lead fracture is at 36cm , case b) at 54cm and case c) 72cm from the 30 kHz sensor with the sensor 20 cm from the end of the waveguide. The time scale is 400 data points corresponding to a time of 1.69 ms with the sensor resonance at 30 kHz. The spectra derived from these waveforms are shown in figure 7.

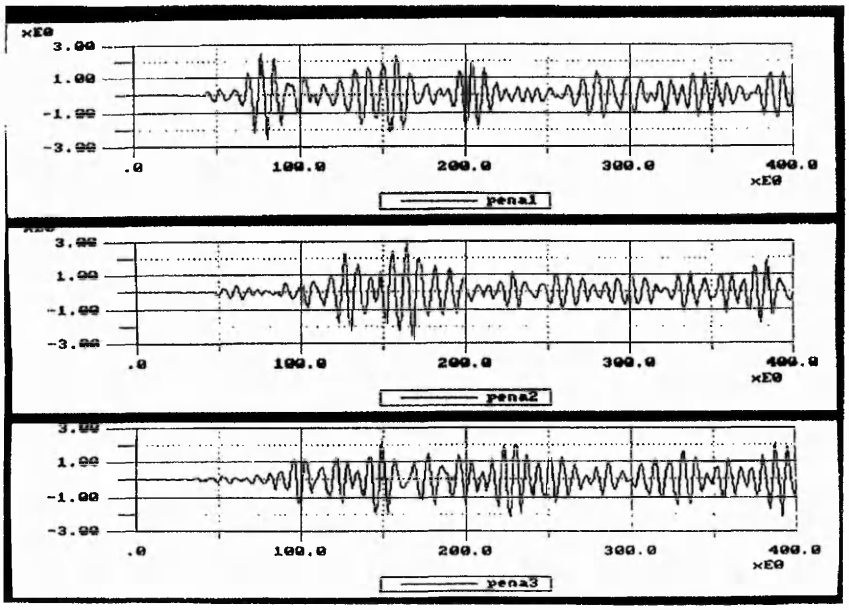


Figure 6 : AE waveforms due to pencil lead fracture on a waveguide. Source at 36, 54, 72 cm from sensor 20 cm from waveguide end.

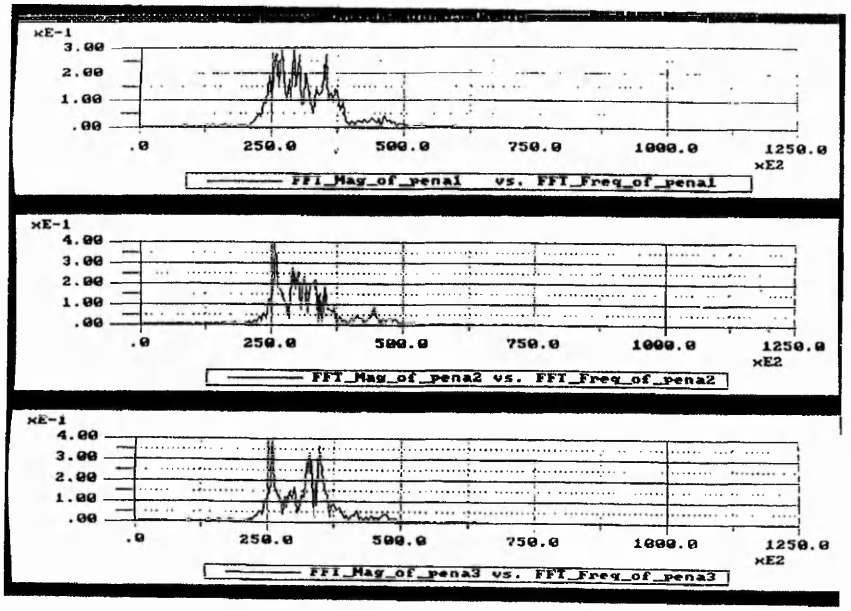


Figure 7 : Spectra of waveforms in figure 6.

Field work reported, has used the envelope of the AE signal to monitor AE. If AE monitoring of soil deformation is to progress, then waveguide technology need to improve. To enable this to occur, the full waveforms ( of the type shown in figure 6 ) need to be captured and processed. In the case of the field work undertaken, a large volume of computer data existed requiring relatively short time samples and storage of the envelope of AE waveforms.

For full wave capture, the data is captured in a configuration which replicates the field situation. The AE source is down the waveguide which is of finite length. The detecting AE sensor is close to one end. Although the wave is complicated by reflection from the end and spiral paths around the pipe, it is necessary to detect the waveforms and extract meaningful data related to the source of AE and not related to waveguide geometry.

## CONCLUSIONS

Acoustic Emission has been monitored in the field from soil deformation, firstly at a coastal site where the deformation of the cliff slope led to confirmation that AE could be effectively monitored and correlates well with inclinometer measurements.

The work led to the conclusion that AE may not arise from the soil body at 30 kHz, but from the back-fill, with the waveguide acting as a giant acoustic antenna, responsive to microscopic ground movement.

Measurements of AE, from an artificial, destabilised slope in a brick quarry confirmed the sensitivity of the technique for monitoring a low emissivity material such as clay, and again confirming the likely model, that the detection occurs by an "active waveguide" detecting microscopic ground motion.

Work on waveguides confirms the complexity of the AE signal from frictional sources on the surface of the waveguide and the need to simulate the actual case of propagation experienced in the field, while extracting data associated with the microscopic deformation of the soil.

The technology continues to leave us with many challenges.

## REFERENCES

[1] Beard F.D. , Western Construction, No. 72
[2] Koerner R.M.,Lord Jr. A.E., Journal Soil Mechanics & Foundations Division, Proc. ASCE, 1972, Vol. 98, No SM1, pp161-165
[3] Lord Jr. A.E., Koerner R.M., Curran J.W., Journal of Testing and Evaluation, 1974, Vol. 2, No.3, pp159-162
[4] Koerner R.M., Land Subsidence, 1986, Vol. 151, Ch. 86, pp225-234

**Paper 3**

**Acoustic emission technique for monitoring soil and rock slope instability**

A.Kousteni *Department of Civil and Structural Engineering, Nottingham Trent University, UK*
R.Hill *Department of Chemistry and Physics, Nottingham Trent University, UK*
N.Dixon *Department of Civil and Structural Engineering, , Nottingham Trent University, UK*
J.Kavanagh-*Transport Research Laboratory, Crowthorne, UK*

ABSTRACT: This paper presents our recent research in Acoustic Emission (AE) monitoring used to assess slope instability and the factors controlling instrumentation design. These factors include wave-guide material type; the type of the backfill soil placed around the wave-guide, and the method of wave-guide construction. Both field and laboratory studies, undertaken by the authors, indicate that, i) the AE monitoring technique provides an early indication that small deformations are taking place during progressive failure; ii) even in "quite" material, such as clays, AE levels can be related to deformation rates and iii) the choice of wave-guide system is of fundamental importance (e.g. active wave-guides are best suited for the study of slopes formed in clay soils). Quantitative assessment of AE at an early stage of slope failure is still basic. Data is provided on the performance of wave-guide systems, and which will lead to a better quantitative assessment of field AE. The results of laboratory and field studies are discussed.

## 1. INTRODUCTION

This type of slope failure, characterised by an unexpected and rapid movement defines a dangerous and fatal landslide, when it occurs in habitant area.

Terzaghi, (1950) stated: "If a landslide comes as a surprise to the eyewitness, it would be more accurate to say that the observers failed to detect the phenomena which proceeded the slide". The implication is that the smallest possible movements should be measured at the earliest possible time.

The standard method for assessing the stability of slopes is by measuring ground deformations. At present, conventional surface survey markers, extensometers, or inclinometer tubes installed through the potentially unstable soil/rock are used to define the area of movement. Unfortunately the magnitude of the pre-failure movements which is of interest, is often of the same order as the accuracy of the above monitoring methods. These methods often require measurements taken many times and over a period of time to obtain trends, thus enabling the certainty of ground movement to be established.

Therefore, there is a need of an instrumentation system which:

1. is sensitive to small pre-failure slope deformations;
2. can detect changes in the rate of movement;
3. provide information about the location of sliding surface; and
4. is portable for monitoring slope stability continuously.

Such a system could provide an early warning of slope instability.

Acoustic emission (AE) monitoring techniques have the potential to meet the above requirements. This paper presents recent developments and considers issues related to instrumentation design. Successful applications on field and laboratory studies are described. The work and results of the current research are discussed with the aim of quantifying the AE response of a wave guide and developing a reliable early warning monitoring system.

### *1.1. Background information*

Acoustic emission is a non-destructive technique which, since the 1970's has been increasingly employed to monitor the stability of soil bodies. The main body of research into AE applications for soil assessment has been carried out in the USA (e.g. Koerner *et al.*, 1981), Japan (e.g. Chichibu *et al.*, 1989, Nakajima *et al.*, 1991) and more recently at Nottingham Trent University (Dixon *et al.*, 1997). When any material is stressed, it generates micro-seismic activity at locations of local instability. When soil is stressed, it responds by reorganising its constituent particles and changing their relative positions with the consequent frictional generation of stress waves. These micro-seismic stress waves, are referred to as acoustic emission. The associated stress waves propagate from the source of instability through the surrounding material and can be detected by suitable high sensitivity transducers.

This is the main principle of the AE monitoring technique, which enables the detection of the occurrence of distress in soil before the development of significant movements. However, monitoring soils by using high frequency AE techniques, is affected by the high attenuation in soils. The attenuation of AE energy in soil is highly frequency dependent. According to Koerner (1981) the attenuation coefficient (in dB/distance) in dry sands varies from 0.09 dB/cm at 500 Hz to 10 dB/cm at 16kHz. Since metals have a three to four orders of magnitude lower attenuation than soils, a metal wave-guide has been found very useful in conducting the signals from within the soil mass to the receiving AE sensor. Therefore, the use wave-guides to monitor AE in soils, has became standard.

## 2. AE MONITORING INSTRUMENTATION

The AE instrumentation components used for field monitoring and laboratory testing at NTU are shown in Figure 1. It is shown as a single channel system, the extension to a multi-channel system can be easily achieved.

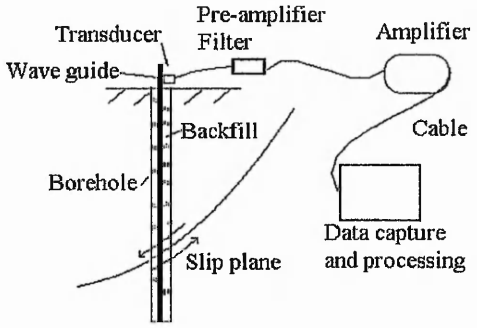


Figure 1. AE field instrumentation

*Sensor:* An AE Technology piezoelectric transducer with a resonant frequency of a 30 kHz has been used. The choice of 30 kHz resonant frequency is due to the need to minimise low frequency environmental noise and at the same time keep the frequency of the system as low as possible, to avoid high levels of attenuation.

*Wave-guide:* Metal wave-guides can take the form of steel reinforcing rods, various metal instrumentation pipes, (e.g. aluminium inclinometer tubes) or construction units (e.g. tiebacks, anchors, piles or soil reinforcement units). It is possible for the length of a wave-guide to be in excess of 30 m when used in field monitoring. In the present study a steel tube of 1.60 m length, 60 mm diameter and 6 mm wall thickness has been used. Steel threaded rings are used for connecting sections of the wave-guide. The choice of the steel tube AE wave-guide has the advantage that it can be easily fabricated to the required cross-section and length, and has a low ultrasonic attenuation coefficient. This wave-guide system transmits the emission generated by the frictional motion of the soil particles which are in contact with or close to the wave-guide.

It is possible to drive the wave-guide into the host soil for short distance. For larger slopes it is necessary to install the wave-guide in pre-drilled boreholes. This method requires a backfill material to improve the contact between the host soil and wave-guide. Depending on the backfill material two possible systems are formed: *Passive* and *Active* wave-guide systems.

For passive systems the annulus around the wave-guide has to be backfilled with low AE activity material (i.e. clay), so the installation does not introduce additional sources of AE into the wave-guide. Any recorded AE signal is assumed to emanate from the deforming host soil. Driven systems can also be defined as passive, as a result of the wave-guide being in direct contact with the in-situ material.

Active wave-guide systems are installed when the monitoring site consists of cohesive material. As the emission levels generated are low, it is difficult to obtain quality AE data. Therefore, the annulus can be backfilled with granular soils such as sand or gravel which produce high AE levels. Although the recorded AE data will not relate directly to the stress state of the host soil, it may be possible to calibrate the system, such that the recorded AE signal can be related to the magnitude of the general ground deformations. It is this type of system which has been studied by the authors.

*Preamplifier and Filter*: A preamplifier is used to amplify the low level signals from the sensor by 40 dB. The signal is filtered by a band pass filter with a bandwidth of 15 - 45 kHz. Hence the output signal consisted of waves with frequencies between 15 kHz and 45 kHz. This ensured that any low frequency background noise is not included in the recorded signal.

*Main Amplifier*: The system can amplify the signal between 50 and 108dB.

*Data capture*: An A-to-D board converts the analogue voltage to a digital value. The maximum sampling rate used is 1 MHz. By directly writing to the board, via the digital ports, it is possible to set the default to capture a stream of data including data points before any trigger time or voltage set by the operator.

*Data processing:* A high-level programming language for data acquisition and processing was used. AE captured data are saved into binary files which can then be analysed.

## 3. FIELD AE MONITORING

Results from recent field studies are reported by Dixon *et.al.* and Kavanagh (1996, 1997). One of the case study areas was located on the north eastern coast of England at Cowden. At this location 20 meters high cliffs are formed of stiff cohesive glacial till. The failure mechanism of the cliffs was a rotational sliding which is triggered by marine erosion of the toe. Twelve steel tubing wave-guides and two inclinometer casings were installed into the coastal cliff section. Figure 2 shows the instrumentation array arrangement at November 1993.

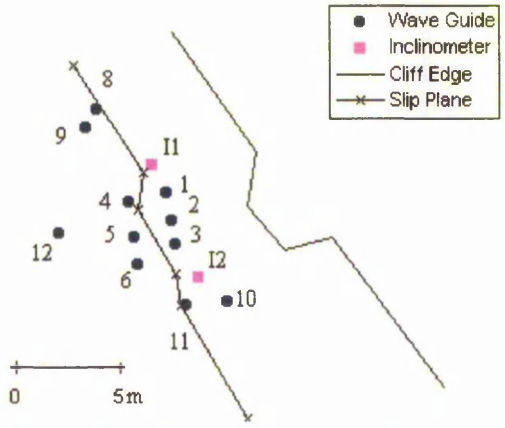


Figure 2. Cowden instrumentation array

Part of the results that were obtained from a monitoring period of almost one year are shown in Figure 3. In this figure a comparison of the AE recorded data from 4 different wave-guides is made with displacement rates recorded by inclinometer I1.

It can be seen that there is a reduction in AE mean signal value between days 149 and 163 recorded by all wave-guides, which is accompanied by a reduction in the rate of increase of displacement recorded by the inclinometer. Correlation of displacement rates with AE was encouraging, and proved the good qualitative status of the AE monitoring technique. However, the signal could not be quantified to provide an independent measure of slope instability.

One of the wave-guide design parameters was backfill type. Wave-guides 1, 5 and 12 were backfilled with sand, wave-guides 2, 6 with gravel and the rest of them with grout. The grout backfill produced the least AE, gravel appeared to be the next active and the sand backfill clearly produced the highest levels of AE (Figure 3b). The poor response of gravel backfilled wave-guides was a result of the gravel particles requiring greater displacements of the host soil to cause them slip. In addition, slippage would occur over a shorter period of time, but AE would be of much greater amplitude than for sand particles.

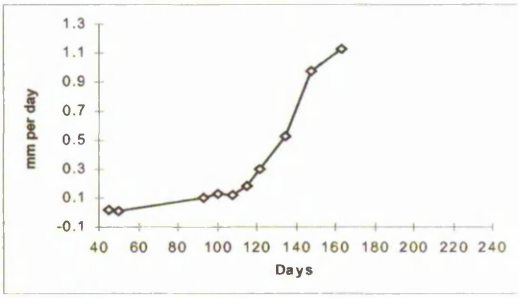


(a)

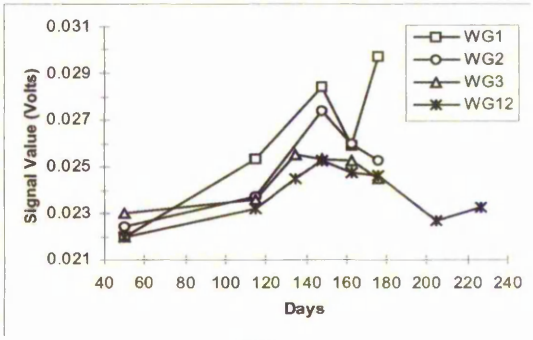


(b)

Figure 3 Displacement rate inclinometer 1 and AE mean signal value of four WG's.

## 4. CURRENT LABORATORY STUDIES

The aim of recent laboratory work has been to investigate the AE wave-guide response and quantify the AE levels with displacement. For the first stage of this work, the waveforms of the AE signals, propagating through a free surface wave-guide were investigated to locate the AE source. For the second part the AE investigation of two granular backfills (gravel and sand) surrounding the wave-guide were investigated.

### *4.1. AE source location*

Two sections of 1.63 m length (6 mm wall thickness) steel tubes connected by a steel collar were used. The whole wave-guide body (two sections with the collar) was lifted from the ground and supported by three wooden supports (Figure 4). This was to provide a free surface around the wave-guide.

The signal was generated in the form of a transient step force function by carrying out pencil lead breaks. This method was used because the generated signal mainly consisted of one event with short duration and was reproducible and consistent.

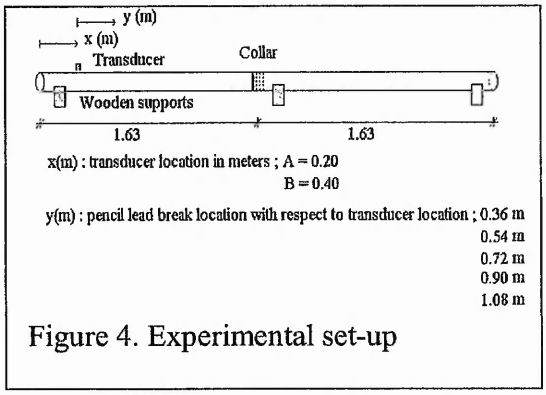


Figure 4. Experimental set-up

The 0.3 mm pencil lead, of 3 mm length (Nielson/Hsu source), was broken at a constant angle, multiple times, at five different locations, with distances of 0.36 m, 0.54 m, 0.72 m, 0.90 m, and 1.08 m away from the sensor. The signals were sensed and processed by the instrumentation described in section 2. The main amplifier (AET 204GR) was set to 50 dB and the total ring down counts of the signal were measured. The DAS50 board was set to capture a stream of 400 data points including 50 pre-trigger points at a frequency of 237 kHz.

Analysis was focused only on the first part of each captured event. The reason being to identify the first two fastest modes, and not to complicate the study with other flexural modes or reflections. The arrival time of the first peak was plotted on a graph with respect to the distance between source and sensor. At each distance ten values of arrival time for the first peak from different pencil lead break records were plotted. Figure 5 shows a linear relationship between propagating distance and arrival times of the first peak. This is an indication of a constant velocity difference between the fastest mode, which triggers the DAS-board, and the flexural mode which arrives with

The pencil breaks were repeated when the transducer was moved further away from the edge of the wave-guide to position B (0.40 m). This was to investigate whether reflections from the edge of the wave-guide would be included in the waveform. It was found that the slope of the line was similar to the above plot. This indicates that there is no interference of reflections in the first part of the waveform section that is under investigation, and that the results are consistent.higher amplitude.

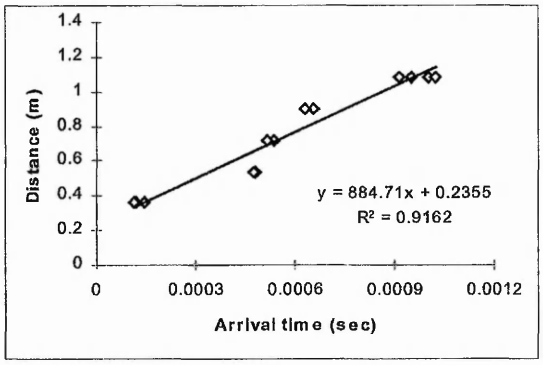


Figure 5. Arrival time of the 1st peak versus distance between source and sensor

The results of these tests show that it is possible to locate the AE source without using a second transducer. The recognition of the two fastest wave modes can be achieved, and hence the difference in their arrival times and the location of the source can be measured. It has to be noted that the above findings are at present only applicable for propagating distances of up to 1.6 m.

### *4.2. Active wave-guide system*

Two types of backfill soil were investigated:

i) well graded sand and ii) medium size rounded gravel.

A thick polythene sleeve (D=195mm, L=1650mm) was used to contain the backfill material. The soil column was supported vertically by a steel frame. Before filling the sleeve with the soil, one section of 1.65 m (steel tube) wave-guide was inserted in the centre of the polythene sleeve (i.e. representing a wave-guide in a borehole filled with the backfill soil). The backfill soil then was poured between the wave-guide and sleeve, 5 kilograms at a time and was compacted by a rod to distribute the soil evenly and achieve uniform density. The transducer was fixed using elastic bands on an exposed top section of the tube. The AE instrumentation components were the same as in the previous experiment. The only difference was that A-to-D frequency was reduced to 150 kHz, and 1000 data were captured including the 100 pre-trigger points when a threshold of 0.11 Volts was exceeded. The AE events were generated by a compression action, on the soil surrounding the wave-guide, achieved by using a G-clamp. The compression was applied at two different heights. The clamp was calibrated to produce controlled displacements of the soil cylinder surrounding the wave-guide (i.e. changes in diameter).

The recorded AE events were assessed, by carrying out statistical analysis. The recorded signal consisted of positive and negative values, so prior the statistical analysis the absolute values of the recorded signal were obtained. The mean and the standard deviation of the AE voltage response were plotted against cumulative displacements. This is shown in Figure 6(a), (b) for gravel backfill and 7(a), (b) for sand backfill. It is obvious that the deformation of the gravel emits higher AE levels than the sand. There is a

general trend of increase in the AE mean amplitude with displacement. The sand backfill behaviour seems to consists of sporadic releases of energy which results in the AE level dropping temporarily and then rising again to a new maximum value with increasing displacement. This phenomenon seems to be the "Kaiser effect" in which AE levels are low until the material is stressed beyond that which it has experienced in the past. Kavanagh (1977) demonstrated this effect on Leighton Buzzard sand in a compression tests.

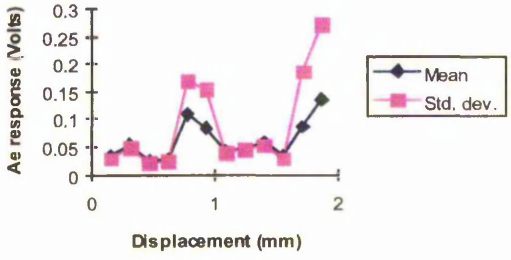


(a)

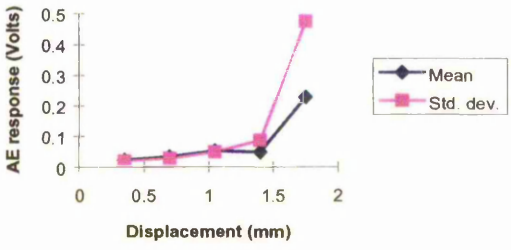


(b)

Figure 6 Cumulative displacement of gravel backfill at propagating distance of (a) 565 mm (b) 1170 mm

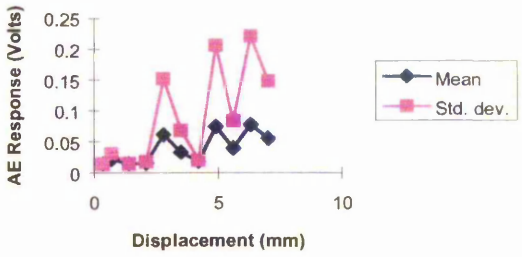


(a)

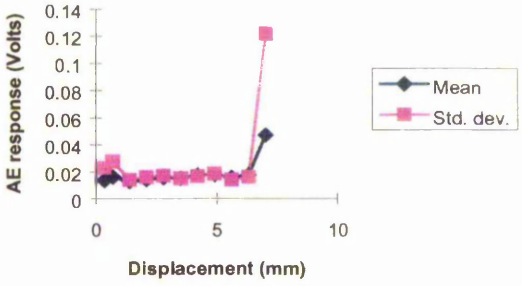


(b)

Figure 7 Cumulative displacement of sand backfill at propagating distance of (a) 565 mm (b) 1170 mm

Measurements indicate that exact AE repeatability is difficult to obtain. This remains a topic for further research.

## 5. CONCLUSIONS

Results from field studies suggest that the AE technique can be used to detect and monitor the pre-failure deformations. The most promising area of research relates to the use of active wave-guide systems with the assessment of AE signal characteristics.

The pencil lead break studies suggest that is possible to locate the AE source using only one transducer. The two fastest guided-wave modes in the first

part of the captured signal can be identified, and therefore the difference in their arrival times could be seen in the recorded histogram and the propagating distance of the signal could be estimated, since the mode velocities are known.

The study of the two backfill types, gravel and sand, showed that the former backfill was "noisier" under small displacements than the latter. This behaviour was shown in previous studies by Kavanagh where sand backfill appears to generate low magnitude emission over a long time scale whereas gravel backfill generates high magnitude emission over a short time scale.

The relationship between displacement and statistical mean and standard deviation values of AE was as expected (the statistical values increase with displacement). However, more studies are required in the future where the displacement rate is also related to the AE response.

REFERENCES

Chichibu A., Jo K., Nakamura M., Goto T., Kamata M., 1989. "Acoustic emission characteristics of unstable slopes". Journal of Acoustic Emission, Vol. 8, No. 4, pp. 107-112

Dixon N., Kavanagh J., Hill R., 1997. "Monitoring landslide activity and hazard by acoustic emission". Journal of Geological Society of China, Special Publication of the Proc. 3rd Sino-British Geological Conference, Taiwan, Vol. 39, No. 4, pp. 301-327

Kavanagh J.G, 1997. "The use of acoustic emission to monitor of a solid body". PhD. Thesis, Nottingham Trent University

Koerner R.M., McCabe W.M., Lord A.E.Jr, 1981. "Acoustic emission behaviour and monitoring soils". Acoustic Emissions Geotechnical Engineering Practice, ASTM STP 750, V.P. Drnevich and R.E. Gray, Eds., American Society for Testing and Materials, 93-141.

Nakajima I., Negilshi M., Ujihara M., Tanabe T., 1991. "Application of the acoustic emission monitoring rod to the landslide". Measurement, Pennsylvania State University

Terzaghi K., 1950. "Mechanism of landslides". Application of Engineering Practice, S. Paige, Ed., Geological Society of America, Berkey, pp. 83- 123

# Appendix 2

## FORTRAN 77 PROGRAM

"GROUPING"
Grouping AE statistical values with respect
c to real time monitoring

```
c   Analysis for good events statistics
    DIMENSION ITRDX(3000)
    DIMENSION JCUMEV(80)
    DIMENSION A(3000)
    DIMENSION B(3000)
    DIMENSION C(3000)
    DIMENSION CONT(3000)
    OPEN (unit=11, file= 'gv3f.ndc', status='old')
    OPEN (unit=12, file='gv3f.cm', status='old')
    OPEN (unit=13, file='gv3f.stc',status='old')
    OPEN (unit=14, file='rg3f.dat', status='NEW')
    OPEN (UNIT=15, FILE='CNT3f.DAT', STATUS='NEW')

    WRITE(*,*) 'GIVE THE NUMBER OF GOOD EVENTS GE='
    READ(*,*) GE
    WRITE(*,*) 'SIZE OF CUM. EVENTS MATRIX CM='
    READ(*,*) CM
    DO 50 K=1,GE
    READ(11,*) ITRDX(K)
 50 CONTINUE
    DO 60 L=1,CM
    READ(12,*) JCUMEV(L)

 60 CONTINUE

    IN=1
    DO 100 J=1,CM+1
    IN=ICOUNT+1

    WRITE(*,*)'COUNTER', COUNTER
    WRITE (15,*) COUNTER
    IF (COUNTER.EQ.0) THEN
        GOTO 10
    ELSE
    SM=0
    SS=0
    SR=0
     DO 110 K=1,COUNTER
```

```
      READ(13,*) A(K),B(K),C(K)
C       WRITE(*,*) 'AK ',A(K)
          SM=A(K)+SM
          SS=B(K)+SS
          SR=C(K)+SR
C       WRITE(*,*)'SM',SM
  110 CONTINUE
      AM=SM/COUNTER
      AS=SS/COUNTER
      AR=SR/COUNTER
C       WRITE(*,*) AM
      WRITE(14,*) AM,AS,AR

      ENDIF
   10   COUNTER = 0
            DO 150 I=IN,GE

            IF (JCUMEV(J).LT.ITRDX(I)) THEN
            GOTO 100
            ELSE
            COUNTER=COUNTER+1
            ICOUNT=ICOUNT+1
            ENDIF

  150   CONTINUE
  100 CONTINUE


            END
```